QUANTUM THEORY OF CHERENKOV RADIATION AT FINITE TEMPERATURE WITH MASSIVE PHOTONS

Kamol Janngun

A Thesis Submitted to the Graduate School of Naresuan University
in Partial Fulfillment of the Requirements
for the Doctor of Philosophy Program in Physics
May 2024

Thesis entitled "Quantum theory of Cherenkov radiation at finite temperature with massive photons"

by Kamol Janngun

has been approved by the Graduate School as partial fulfillment of the requirements

for the Doctor of Philosophy Degree in Physics of Naresuan University

Oral Defense Committee

.....Chair

(Associate Professor Chaiyapoj Muthapon, Ph.D.)

.....Advisor

(Associate Professor Pornrad Srisawad, Ph.D.)

.....Co–Advisor

(Associate Professor Anucha Kaewpoonsuk, Ph.D.)

.....Internal Examiner

(Associate Professor Attapon Amthong, Ph.D.)

.....Internal Examiner

(Associate Professor Aek Jantayod, Ph.D.)

Approved

.....

(Associate Professor Krongkarn Chootip, Ph.D.)

Dean of the Graduate School

23 MAY 2024

Title	QUANTUM THEORY OF CHERENKOV RADIATION AT FINITE TEMPERATURE WITH MASSIVE PHONSONS
Author	Kamol Janngun
Advisor	Associate Professor Pornrad Srisawad, Ph.D.
Co-Advisor	Associate Professor Anucha Kaewpoonsuk, Ph.D.
Academic Paper	Ph.D. Dissertation in Physics, Naresuan University, 2023.
Keywords	Cherenkov radiation, Quantum theory, Power spectrum, Source theory

ABSTRACT

The theoretical study of the power spectrum of Cherenkov radiation is mostly based on electrodynamics theory. However, quantum theory has been slightly applied in the radiation investigation, especially source theory. Thus, this dissertation aims to apply source theory to calculate the power spectrum of Cherenkov radiation in two cases. First is the power spectrum of massive photons at a finite temperature caused by a charged electron moving through a dielectric medium. Second, the power spectrum of massless and massive photons at a finite temperature is caused by a two-charge electron system moving through the medium. For calculation, we start with finding the propagator of massive photons at finite temperatures in the medium. Then, we calculate the action of the massive electromagnetic field. Finally, we can derive the power spectrum from the action. The results found that the power spectrum in water at 0 and 20 °C has almost no difference, while the power spectrum at 50, 80, and 100 °C has decreased slightly, respectively. We also found that the photon mass, the velocity, and the distance between two charges affect the power spectrum. The results illustrate the potential of source theory in calculating the power spectrum of Cherenkov radiation.

ACKNOWLEDGEMENTS

Throughout the long journey of hard work on my thesis, I have learned and received valuable experience from many supporters, the advisor team, the thesis examination committee, fund grantors, NU staff, and especially my family.

I would like to thank you Assoc. Prof. Dr. Pornrad Srisawad and Assoc. Prof. Dr. Anucha Kaewpoonsuk for being my thesis advisor. I feel deeply grateful to Assoc. Prof. Dr. Pornrad for kindness and support when I confronted hard times during my studies. She was dedicated to guiding me in working on my thesis.

I am very thankful to the thesis committee, Assoc. Prof. Dr. Chaiyapoj Muthapon, Assoc. Prof. Dr. Attapon Amthong, and Assoc. Prof. Dr. Aek Jantayod for their great suggestion and guidance during and after the defense thesis in order to make the thesis more comprehensive and academic.

Special thanks to Assoc. Prof. Dr. Chaiyapoj Muthapon for kindly taking private time to advise on making my thesis more accurate and complete.

I would like to gratitude to the Science Achievement Scholarship of Thailand for supporting the scholarship during the period of study. Thank you very much to the staff of the Graduate School and Faculty of Science at Naresuan University for generously providing the facilities and documents to carry out this thesis.

Finally, I gratitude thankfulness to my family, father, mother, and older sister who are available every time to support and cheer up me whenever I need it.

Kamol Janngun

LIST OF CONTENTS

Chapter Page

LIST OF CONTENTS (CONT.)

Chapter Page

LIST OF TABLES

Table **Page**

LIST OF FIGURES

Figure **Page**

LIST OF FIGURES (CONT.)

Figure **Page**

CHAPTER I

INTRODUCTION

1.1 Historical Background

Cherenkov radiation is the radiation phenomenon that occurs when a charged particle moves through in a transparent medium, any liquid or solid, with a speed faster than light in that medium (L'Annunziata, 2020). The origin of this radiation was observed by many scientists before it was discovered and understood this phenomenon. The first appearance of this radiation dates back to 1910 when Marie Curie observed a soft blue light emanating from a concentrated solution of radium in a dark room. Unfortunately, she did not investigate the cause of this luminescence (Curie, 1941). Later in the 1920s, Mallet was the first to conduct deliberate experiments on the phenomenon. He found that various transparent materials would emit light when exposed to a radioactive source. He also observed that it was distinct from other types of luminescence. Nevertheless, Mallet did not propose any theory to explain the origin of that light (Mallet, 1926, 1928, 1929). Afterward, Pavel Cherenkov began a series of thorough experiments in 1934 on the luminescence of solutions under gamma rays (Cerenkov, 1934). This was his doctoral research under the supervision of Vavilov, the world's leading luminescence expert physicist. Cherenkov initiated the experiment to examine what he assumed was luminescence. However, he discovered that the light emission was not fluorescence, but a new radiation that was unknown to humankind.

The new radiation that has the characteristics of faint blue light was discovered by Cherenkov through his experiments. It was later revealed by further investigations by Cerenkov in 1936-1938 (Cerenkov, 1936, 1937, 1938) and theoretical interpretation by Frank and Tamm in 1937, it was eventually known that this radiation arose from charged particles moving at a speed faster than light in a transparent medium (Frank, & Tamm, 1937). Cherenkov, Frank, and Tamm were

CHAPTER I

INTRODUCTION

1.1 Historical Background

Cherenkov radiation is the radiation phenomenon that occurs when a charged particle moves through in a transparent medium, any liquid or solid, with a speed faster than light in that medium (L'Annunziata, 2020). The origin of this radiation was observed by many scientists before it was discovered and understood this phenomenon. The first appearance of this radiation dates back to 1910 when Marie Curie observed a soft blue light emanating from a concentrated solution of radium in a dark room. Unfortunately, she did not investigate the cause of this luminescence (Curie, 1941). Later in the 1920s, Mallet was the first to conduct deliberate experiments on the phenomenon. He found that various transparent materials would emit light when exposed to a radioactive source. He also observed that it was distinct from other types of luminescence. Nevertheless, Mallet did not propose any theory to explain the origin of that light (Mallet, 1926, 1928, 1929). Afterward, Pavel Cherenkov began a series of thorough experiments in 1934 on the luminescence of solutions under gamma rays (Cerenkov, 1934). This was his doctoral research under the supervision of Vavilov, the world's leading luminescence expert physicist. Cherenkov initiated the experiment to examine what he assumed was luminescence. However, he discovered that the light emission was not fluorescence, but a new radiation that was unknown to humankind.

The new radiation that has the characteristics of faint blue light was discovered by Cherenkov through his experiments. It was later revealed by further investigations by Cerenkov in 1936-1938 (Cerenkov, 1936, 1937, 1938) and theoretical interpretation by Frank and Tamm in 1937, it was eventually known that this radiation arose from charged particles moving at a speed faster than light in a transparent medium (Frank, & Tamm, 1937). Cherenkov, Frank, and Tamm were

awarded the Nobel Prize in Physics for their discovery and theoretical interpretation of this phenomenon in 1958. This radiation is called Cherenkov radiation in honor of Cherenkov who discovered a new type of radiation that has unique characteristics. This discovery and theoretical interpretation have influenced physicists to later uncover the application of Cherenkov radiation.

A few years later, the principle of Cherenkov radiation was applied to develop particle detectors. In the early 1960s, the first Cherenkov detector of large size was constructed by the Russian Academy of Sciences. They used it for several years to study the multiple production of muons in high-energy nuclear interactions (Vavilov et al., 1963). It was the largest Cherenkov detector in the world at the time. In addition, another massive Cherenkov detector was installed in Japan in 1996, it was called Super-Kamiokande. With these Cherenkov detectors, neutrinos from distant cosmic sources could be observed. In the year 1987, neutrinos from an explosion of supernova in the Large Magellanic Cloud were detected. (Koshiba, 2003; Bolotovskii, 2009). This marked the birth of neutrino astronomy. A few decades passed until 2020, the principle of Cherenkov radiation was applied to many fields. This radiation has many applications in science and technology, such as detecting nuclear reactors, measuring the energy and direction of cosmic rays, and imaging tumors in radiotherapy. Nowadays, Cherenkov radiation continues to develop in both practical applications and theoretical studies.

1.2 Theoretical Development and Knowledge Gap

As mentioned above, in 1937 Frank and Tamm were pioneers in the theoretical interpretation of the Cherenkov radiation which was based on classical theory. They employ the principles of classical electrodynamics theory and successfully derive the formula to calculate the main properties of the radiation by using the Poynting vector (Frank, & Tamm, 1937). As a consequence, this theory has been extensively employed by physicists to investigate the properties of Cherenkov radiation, such as power spectrum, number of photons, velocity, and

frequency in diverse conditions and mediums, both in homogeneous and inhomogeneous mediums (Ginzburg, & Frank, 1945; Garibian, 1958; Ginzburg, & Tsytovich, 1979; Ginzburg, 1982, 1996, 2005). However, the theoretical studies of Cherenkov radiation in the framework of classical electrodynamics theory still have limitations. Some conditions have been simplified to reduce complexity. By assuming that charged particles have uniform motion within a medium at a constant velocity including neglecting the effects of radiation reactions and others. It appears that the investigation of Cherenkov radiation through the framework of classical electrodynamics theory appears to contravene the principle of conservation (Kobzev, 2010, 2014). So, it can be seen that the theoretical study of this phenomenon by using the concepts of classical theory is still incomplete in investigating the real condition of the phenomenon.

Later, quantum theory started to play a role in studying Cherenkov radiation. In 1940 Ginzburg presented the approach of quantum theory for the study of Cherenkov radiation (Ginzburg, 1940). He applies the principle of quantum theory investigation and considers conditions more correspond with the reality of the phenomenon. Ginzburg has implemented the requisite modifications by permitting the reaction of the particle while it emits the radiation. The modifications are inherently anticipated to be small given that the energy of the emitted quanta is negligible in comparison to the kinetic energy of the particle (Jelley, 1958). In 1975, Schwinger developed the source theory approach, which formulated quantum theory by applying the quantum vacuum persistence amplitude to calculate the power spectrum and the number of photons of Cherenkov radiation in a medium (Schwinger et al., 1976). Thereafter, the source theory was used to calculate the power spectrum and the intensity spectrum of Cherenkov radiation in various mediums and conditions (DeRaad et al., 1978; Drimal, 1984; Pardy, 1989). Since the 1990s, the source theory approach has rarely been used to study Cherenkov radiation. It is mostly found only in Pardy's article that uses the source theory approach to study this radiation. He utilizes the source theory to calculate the power spec-

trum of Cherenkov radiation in different conditions such as finite temperature, massive photons, and gravitational (Pardy, 1995, 2002, 2015). The current state of theoretical development on Cherenkov radiation demonstrates the advancements in theoretical investigations of this phenomenon by utilizing classical and quantum theories. This radiation remains an interesting and significant research topic, specifically using quantum theory such as the source theory. For the approach of the source theory in studying Cherenkov radiation, I will present and discuss it in Chapter II.

Although the current theoretical study on the power spectrum of Cherenkov radiation has been extensively studied in various conditions (Alfimov, 2010; Kheirandish, & Amooghorban, 2010; Roques-Carmes et al., 2018). Most theoretical investigations of this radiation are based on classical electrodynamics theory (Tuchin, 2018; Macleod et al., 2019). However, a theoretical study of Cherenkov radiation from the viewpoint of quantum theory especially the source theory has not yet been investigated in numerous. Quantum theory based on quantum mechanics has a better potential to describe phenomena at the quantum level, whereas classical electrodynamics has some limitations (Feynman, 2010, 2011). We believe that quantum theory is powerful in calculating the properties of Cherenkov radiation. Thus, this dissertation will apply the quantum theory and focus on the source theory to calculate the power spectrum of Cherenkov radiation in conditions of finite temperature and massive photon combination in one and two-charge systems. We also perform numerical calculations of the power spectrum in each condition. This study will contribute knowledge for the theoretical physics of quantum theory that can be applied to investigate this radiation phenomenon in the future.

1.3 Objectives of Research

This dissertation aims to study Cherenkov radiation by applying source theory. The first case is to calculate the power spectrum of massive photons at a finite temperature from a charged electron moving through a dielectric medium. In the second case, to calculate the power spectrum of massless and massive photons at a finite temperature from a two-charge electron system moving through the medium.

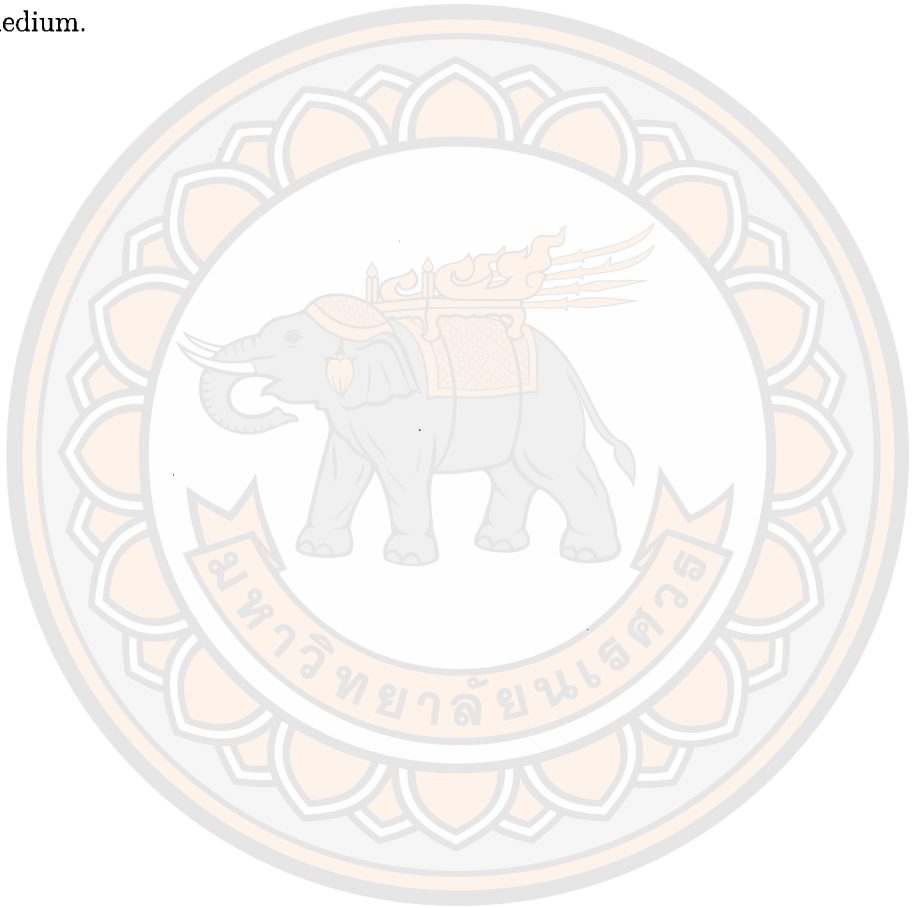

CHAPTER II

FUNDAMEMTAL THEORY

RELATED TO CHERENKOV RADIATION

In this chapter, we will introduce the basic concepts and theories essential for studying Cherenkov radiation. In order to understand the theory applied to study Cherenkov radiation, especially source theory, we review and present the previous knowledge relating to the Cherenkov radiation phenomena. It is composed of three main sections. First section 2.1 focuses on the basic concept of Cherenkov radiation. It consisted of 1) Cherenkov radiation and dielectric medium 2) the Mechanism of Cherenkov radiation and 3) a previous study of Cherenkov radiation with source theory. The second section 2.2 emphasizes the electrodynamics theory of Cherenkov radiation, comprised of 1) the fundamentals of electrodynamics theory and 2) the approach of electrodynamics theory. The third section 2.3 presents the quantum theory of Cherenkov radiation. This section is composed of 1) the approach of source theory and 2) the approach of field theory. The detail of each section is shown as follows.

2.1 Basic Concept of Cherenkov Radiation

2.1.1 Cherenkov Radiation and Dielectric Medium

1) Cherenkov Radiation

Radiation is the process of the emission or transmission of energy as waves or particles through a medium or space. There exist a variety of radiation forms, depending on their origin, energy, and interaction with substances. A few prevalent forms of radiation include electromagnetic radiation, nuclear radiation, and cosmic radiation. Electromagnetic radiation is the radiation that consists of oscillating electric and magnetic fields, so as radio waves, microwaves, infrared, visible light, Cherenkov radiation, ultraviolet, X-rays, and gamma rays. Nuclear radiation is the

radiation that results from the decay of unstable atomic nuclei or nuclear reactions such as fission or fusion. Cosmic radiation is the radiation that originates from outer space, such as from the sun, stars, supernovae, black holes, or cosmic rays.

Cherenkov radiation is a radiation phenomenon that occurs when charged particles, such as electrons, travel through a dielectric medium at speeds greater than the phase velocity of light within that medium. Interesting about the phenomenon of Cherenkov radiation is its unique mechanism. The mechanism of Cherenkov radiation is unique because it involves charged particles exceeding the speed of light in a medium, such as when charged particles move through water at a speed faster than light in water. This creates a shockwave of light that manifests as a blue glow. This results in a characteristic blue glow, often observed in nuclear reactors, which is actually electromagnetic radiation emitted by the particles as they pass through the medium (Bolotovskii, 2009; L'Annunziata, 2020).

The applications of Cherenkov radiation are extensive and impactful across various fields such as particle physics, astrophysics, and biomedical sciences. In particle physics, Cherenkov radiation enables the measurement of the energy and velocity of particles. For instance, the Cherenkov detector was a crucial instrument in the detection of fundamental particles like antiprotons and neutrinos (Chamberlain, 1955; Bolotovskii, 2009). In astrophysics, Cherenkov radiation facilitates the observation of cosmic rays and high-energy gamma rays in the Earth's atmosphere (Mirzoyan, 2022). Moreover, Cherenkov radiation has recently been applied to biomedical sciences, especially in novel imaging techniques such as Cherenkov luminescence imaging. These techniques have demonstrated their usefulness in medical evaluations involving tissue, such as tumor diagnosis and treatment (Tanha et al., 2015; Ciarrocchi, & Belcari, 2017; Wang et al., 2022).

2) Dielectric Medium

A medium is a substance that transfers energy or light from one location to another. The types of medium include transparent, translucent, and opaque. Classifications according to composition are homogeneous and inhomogeneous (hetero-

geneous) or, according to the properties of the medium, categorized into isotropic and anisotropic, detailed in Table 1 (Helbig, 2015).

Table 1 Types of mediums, definitions, and examples.

Medium	Definition	Example
Homogeneous	Medium has a uniform composition throughout its material.	Water, glass, vacuum
Inhomogeneous	Medium has different compositions at different points.	Air, fog, smoke
Isotropic	Medium has the same properties in all directions.	Pure water, clear glass, diamond
Anisotropic	Medium has different properties in different directions.	Composite materials, all crystal

A dielectric (or dielectric medium) is essentially an electrical insulator that can be polarized when subjected to an electric field. Unlike conductors, where electric charges flow freely due to the presence of free electrons, dielectric materials do not allow electric charges to flow through. Instead, when placed within an electric field, the charges in a dielectric are displaced minutely from their normal positions. This slight shift from equilibrium is known as dielectric polarization. Most common substances or materials can be classified into two broad categories: conductors and insulators (or dielectrics). Conductors are materials that have an abundance of charges that can freely move within the material. Usually, this implies that many electrons are not bound to any specific nucleus, but wander around randomly. In contrast, in dielectrics, all charges are linked to certain atoms or molecules that are constrained, and they can only shift slightly within the atom or molecule. There are two main mechanisms by which electric fields can distort the charge distribution of a dielectric atom or molecule: induced dipoles and polarization. In the next sections, we will discuss these processes (Griffiths, 2013).

2.1) Induced Dipoles

A neutral atom experiences a polarization effect when it is exposed to an electric field. The atom is comprised of a nucleus that is positively charged and an electron cloud with a negative charge, which are both affected by the field. The nucleus is attracted to the field direction, while the electrons are repelled by it.

A strong enough field can potentially ionize the atom by separating the charges completely, making the substance a conductor. However, for weaker fields, the atom reaches a stable state, where the nucleus and the electron cloud are slightly shifted from each other, creating an internal attraction force. The atom becomes polarized, with a small dipole moment that aligns with the field direction.

2.2) Polarization

We have considered how an individual atom or molecule responds to an external electric field in the preceding sections. Now can answer how a dielectric material behaves when it is exposed to an electric field. The field will induce a small dipole moment in each neutral atom (or nonpolar molecule) that aligns with the field direction. The field will also exert a torque on each permanent dipole in a polar molecule, which will tend to orient it along the field direction. The result of these two mechanisms is essentially the same: a large number of small dipoles point in the direction of the field causing the material to become polarized.

2.3) Permittivity and Dielectric Constant

In previous sections, we have qualitatively known that an electric field can induce the polarization of a dielectric by aligning its atomic or molecular dipoles. For numerous substances, the polarization is directly proportional to the field:

$$\mathbf{P} = \epsilon_0 \chi_e \mathbf{E}. \tag{2.1.1}$$

The proportionality constant, χ_e, is the electric susceptibility of the medium. The value of χ_e is determined by the microscopic structure of the substance. Griffiths will refer to materials that satisfy Eq.(2.1.1) as linear dielectrics.

He denotes the total field by $\mathbf{E}$ in Eq.(2.1.1), which may consist of contributions from both free charges and the polarization itself. Starting with displacement is the easiest way, especially since $\mathbf{D}$ can be directly calculated from the free charge distribution.

In linear medium

$$\mathbf{D} = \epsilon_0 \mathbf{E} + \mathbf{P} = \epsilon_0 \mathbf{E} + \epsilon_0 \chi_e \mathbf{E} = \epsilon_0 \left(1 + \chi_e\right) \mathbf{E} \tag{2.1.2}$$

so $\mathbf{D}$ is also directly proportional to $\mathbf{E}$:

$$\mathbf{D} = \epsilon \mathbf{E} \tag{2.1.3}$$

where

$$\epsilon \equiv \epsilon_0 (1 + \chi_e) \tag{2.1.4}$$

called constant ϵ that the permittivity of the material. (There is no matter to polarization in a vacuum, resulting in the susceptibility being zero, the permittivity is ϵ_0. Thus ϵ_0 is called the permittivity of free space, in which the permittivity has the value $8.85\times\ 10^{-12}C^2/Nm^2$.) Removing a factor of ϵ_0 remain as,

$$\epsilon_r \equiv 1 + \chi_e = \frac{\epsilon}{\epsilon_0} \tag{2.1.5}$$

where the material's relative permittivity, or dielectric constant, is denoted by ϵ_r. Table 2 shows the dielectric constants of some common substances. (He observe that ϵ_r is always larger than 1 for ordinary materials; this indicates that the polarization is usually in the same direction as the field.)

Table 2 The dielectric constants of various substances at standard conditions.

Material	Dielectric Constant	Material	Dielectric Constant
Vacuum	1	Benzene	2.28
Helium	1.000065	Diamond	5.7-5.9
Neon	1.00013	Salt	5.9
Hydrogen (H_2)	1.000254	Silicon	11.7
Argon	1.000517	Methanol	33.0
Air (dry)	1.000536	Water	80.1
Nitrogen (N_2)	1.000548	Ice (-30° C)	104
Water vapor (100° C)	1.00589	$KTaNbO_3$ (0° C)	34,000

Source: The Handbook of Chemistry and Physics, 91st edition.

2.1.2 Mechanism of Cherenkov Radiation

Frank and Tamm proposed a theoretical interpretation of Cherenkov radiation. They explained that it occurs when an electron moves faster than the light

speed in that medium (Frank, & Tamm, 1937). Although, Einstein's theory of relativity states that matter cannot exceed the light velocity in a vacuum. However, the light speed in a vacuum is different from the speed of light in a gas, liquid, or solid medium, where it is lower. Therefore, an electron with enough energy can move faster than the light speed in such media, producing Cherenkov radiation.

Cherenkov radiation (Figure 1) is a phenomenon that involves the local polarization of the medium by a charged particle, creating electric dipoles along its trajectory. These dipoles oscillate and emit electromagnetic radiation. However, this emission only occurs when the particle velocity exceeds c/n, where c is the speed of light and n is the refractive index of the medium. Below this threshold, the dipoles interfere destructively and no photons are produced. Above this threshold, the dipoles form a coherent electromagnetic shock wave behind the particle.

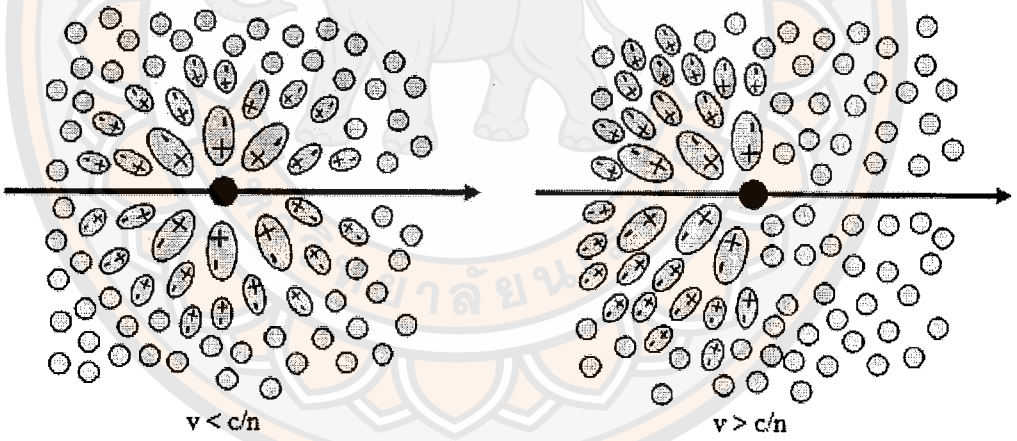

Figure 1 Polarization of the medium induced by a charged particle. Adapted from Naurois and Mazin (2015).

This electromagnetic shock wave is similar to the sonic boom created by an aircraft that moves faster than the speed of sound can be observed in the electromagnetic domain, as shown in Figure 2.

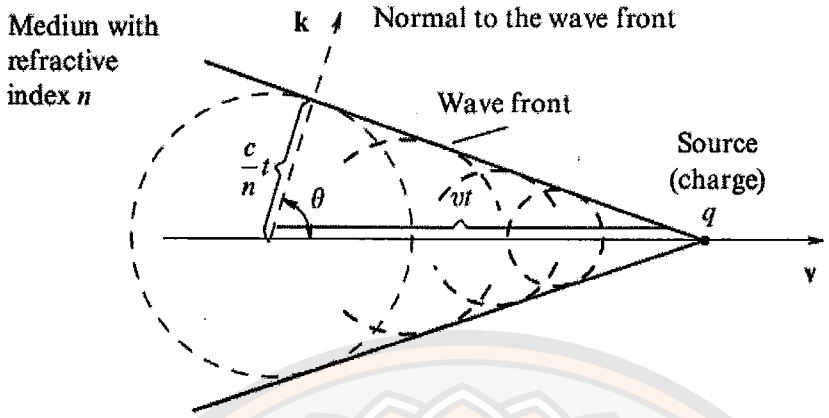

Figure 2 The Cherenkov cone is formed when a charged particle moves faster than the velocity of light in the medium. From Ginzburg (2005).

This can be deduced from Figure 2 that the distance moved by the electromagnetic wave of the atoms in a medium during a certain time interval is ct/n, while the particle covers a distance of $vt = \beta ct$, where $\beta = v/c$. Therefore, the angle of emission of the Cherenkov radiation relation with the direction of motion of the electrons is determined by (Frank, & Tamm, 1937)

$$\cos\theta = \frac{ct/n}{\beta ct} = \frac{1}{\beta n} \tag{2.1.6}$$

where θ is the angle of emission, n is the refractive index of the medium, $\beta = v/c$, v is the charge velocity, and c is the velocity of light in a vacuum. Frank and Tamm demonstrated that the above equation is valid only when $\beta n > 1$. When the electron velocity approaches the light speed in a vacuum, where $\beta = 1$, the emission angle of the Cherenkov radiation reaches a maximum value given by $\theta_{max} = \cos^{-1}(1/n)$.

Frank and Tamm derived the total energy of Cherenkov radiation by passing an electron through the surface of a cylinder of length l, with the cylinder's axis aligned with the electron's line of travel, and obtained the equation as

$$W = \frac{e^2 l}{c^2} \int_{\beta n > 1} \left(1 - \frac{1}{\beta^2 n^2}\right) \omega d\omega \tag{2.1.7}$$

where W is the total radiated energy, e is the electron charge, ω is the Cherenkov radiation frequency. The lower limit of the integral, $\beta n > 1$, corresponds to the condition for Cherenkov radiation to occur in a given medium. The equation is only valid if l is large compared to the wavelength of the emitted Cherenkov radiation.

Using equation (2.1.7), Frank and Tamm derived an expression for the photon emission rate of an electron within a specified spectral range. The spectral range is bounded by the wavelengths λ_1 and λ_2 is equal to

$$N = 2\pi\alpha l \left(\frac{1}{\lambda_2} - \frac{1}{\lambda_1}\right)\left(1 - \frac{1}{\beta^2 n^2}\right) \tag{2.1.8}$$

where N is the number of photons emitted, α is the fine structure constant $= 1/137$ and n is the medium's average refractive index.

These above formulas agree with the experiment of Cherenkov. The experimental evidence confirmed that the emission angle and the total energy including the number of photons emitted consistent with the theoretical calculations of Frank and Tamm that apply electrodynamics theory (Frank, & Tamm, 1937).

2.1.3 Previous Study of Cherenkov Radiation with Source Theory

As mentioned above, Cherenkov radiation has unique characteristics that are emitted by charged particles. Its intensity depended on the energy of the particles and the properties of the solution. It only appeared in the same direction as the charged particles were moving. Moreover, the radiation had specific angles of emission relative to the charged particles' direction (Cerenkov, 1936, 1937, 1938). The discovery of the unique Cherenkov radiation yielded many physicists' interest in studying the properties of this radiation in various mediums. In quantum theory, many academics have investigated properties. Power spectrum is the most studied, followed by the number of photons and the velocity. In addition, intellectuals tend to study by applying various theories in order to validate and compare the results of each theory.

In terms of source theory, there are a few scholars who apply this theory to study Cherenkov radiation. After Schwinger et al. (1976) explained the Cherenkov radiation by applying quantum theory, Pardy is a scholar who extended the idea of source theory to investigate the Cherenkov radiation. His result contributes to the knowledge of applying source theory to calculate the power spectrum. Table 3 shows that, from 1980s to 2023, he have been various research articles related to Cherenkov radiation. Before 2000, he applied source theory to calculate the power spectrum with radiative corrections and gravitation at a finite-temperature. After 2000 he expands and integrates the idea of the Cherenkov effect with various conditions and methods to calculate the power spectrum such as massive and massless photons, two-three dimensions, Lorentz contraction and, etc. Now Pardy applied source theory to study the Cherenkov power spectrum in the system of two opposite charges with Lorentz contraction, which published in 2023. Therefore, it can be said that he is the one expert who applied source theory to calculate Cherenkov radiation.

In this section, we have introduced the basic concepts of Cherenkov radiation, which is a phenomenon that occurs when a charged particle travels faster than the speed of light in a medium. We have described the properties of radiation, medium, and material, including the properties of Cherenkov radiation and the physical mechanism behind it. This will provide the necessary background for understanding the phenomenon of Cherenkov radiation in the later chapters.

In summary, section 2.1 describes a basic idea that relates to radiation phenomena. Radiation is the transmission of energy as waves or particles through a medium or space. Cherenkov radiation is a type of radiation that is classified in the form of electromagnetic radiation. This radiation study focuses on the calculation of many properties: power spectrum, velocity, frequency, wavelength, and energy. Radiation transmission through a different material or medium, that is directed affects the mechanism of inducing dipoles and polarization because the medium has a different constant value. Not only that but the radiation is also affected

Table 3 Previous study of Cherenkov radiation with source theory.

Author/Year	Title	Condition	Property
1. Schwinger, J. et al. (1976)	Classical and Quantum Theory of Synergic Synchrotron-Cerenkov Radiation	-	Power spectrum
2. Pardy, M. (1989)	Finite-Temperature Cerenkov Radiation	Finite temperature	Power spectrum
3. Pardy, M. (1994)	The Cerenkov effect with radiative corrections	Modify photon propagator with radiative corrections	Power spectrum
4. Pardy, M. (1995)	Finite-Temperature Gravitational Cerenkov Radiation	Constant gravitational index of refraction, zero and nonzero temperature	Power spectrum
5. Pardy, M. (1997)	Cerenkov effect and the Lorentz contraction	The system with two equal charges, the radiative corrections	Power spectrum
6. Pardy, M. (1999)	The Cerenkov effect with massive photons	Massive photon, one and two charge system	Power spectrum
7. Pardy, M. (2002)	Cerenkov Effect with Massive Photons	Massive photon	Power spectrum
8. Pardy, M. (2015)	The two-dimensional Vavilov-Cerenkov radiation in LED	2D sheet, graphene-like structures	Power spectrum
9. Pardy, M. (2022)	The 3D and 2D Cerenkov effect with massive photons	3D and 2D Cerenkov effect with massless and massive photon	Power spectrum
10. Pardy, M. (2023)	The Cerenkov Radiation from Dipole and the Lorentz Contraction	The system of two opposite charges	Power spectrum

by other factors. In calculating methods, Frank and Tamm are the pioneers in formulating the equation to derive the total energy of Cherenkov radiation and the number of photons. Understanding of these concepts that support the author in terms of working on my dissertation successfully.

2.2 Electrodynamics Theory of Cherenkov Radiation

2.2.1 The Fundamentals of Electrodynamics Theory

In this section, we will introduce the basic theory of electrodynamics for the study of Cherenkov radiation. These theories were compiled from the textbook classical electrodynamics by Jackson (1999) and Schwinger et al. (2018).

1) Maxwell Equations in Vacuum, Sources and Fields

The equations of Maxwell govern the phenomenon of electromagnetic

$$\begin{aligned} \nabla \cdot \mathbf{D} &= \rho \\ \nabla \times \mathbf{H} - \tfrac{\partial \mathbf{D}}{\partial t} &= \mathbf{J} \\ \nabla \times \mathbf{E} + \tfrac{\partial \mathbf{B}}{\partial t} &= 0 \\ \nabla \cdot \mathbf{B} &= 0 \end{aligned} \tag{2.2.1}$$

where the external sources in a vacuum, $\mathbf{D} = \epsilon_0 \mathbf{E}$ and $\mathbf{B} = \mu_0 \mathbf{H}$. The first two equations be

$$\begin{aligned} \nabla \cdot \mathbf{E} &= \rho/\epsilon_0 \\ \nabla \times \mathbf{B} - \tfrac{\partial \mathbf{E}}{c^2 \partial t} &= \mu_0 \mathbf{J} \end{aligned} \tag{2.2.2}$$

The equations of Maxwell implicitly are the continuing equation for charge density and current density,

$$\frac{\partial \rho}{\partial t} + \nabla \cdot \mathbf{J} = 0 \tag{2.2.3}$$

The equations presented here are written in SI units. A fundamental concept of electrodynamics is the speed of light in a vacuum, given in SI units by $c = (\mu_0 \epsilon_0)^{-1/2}$. The SI unit for length, the meter, is established based on the second (a unit of time derived from a hyperfine transition in cesium-133) and the exact value of $c = 299792458$ m/s. This definition signifies that the velocity of light remains constant universally, which aligns with experimental observations indicating that the velocity of light in a vacuum is independent of frequency, ranging from extremely low frequencies to at least $\nu = 10^{24}$ Hz. For practical intention, it is acceptable to use the approximation $c = 3 \times 10^8$ m/s or a more precise value, $c = 2.998 \times 10^8$ m/s.

In classical electromagnetism, they use $\rho(x,t)$ and $J(x,t)$ to represent the electric charge density and the electric current density, respectively. These are continuous functions of x, the spatial variable, and t, the temporal variable. However, sometimes they encounter localized distributions that can be modeled by point charges. These point charges have arbitrary values in theory, but in reality they are quantized (Jackson, 1999).

Maxwell's Displacement Current

The fundamental laws of electricity and magnetism studied thus far may be expressed in differential form by the four equations below:

$$\begin{aligned} \text{Coulomb's law; } & \nabla \cdot \mathbf{D} = \rho \\ \text{Ampere's law; } & \nabla \times \mathbf{H} = \mathbf{J} \\ \text{Faraday's law; } & \nabla \times \mathbf{E} + \frac{\partial \mathbf{B}}{\partial t} = 0 \\ \text{Absence of free magnetic poles; } & \nabla \cdot \mathbf{B} = 0 \end{aligned} \tag{2.2.4}$$

The derivation of all the equations in set (2.2.4) except for Faraday's law was based on steady-state observations. Therefore, logically, there is no guarantee that the static equations will remain valid for fields that vary with time. In fact, the equations in set (2.2.4) are not compatible with each other. It was Maxwell, inspired by Faraday's observations, who noticed the incompatibility in equations (2.2.4) and corrected them into a consistent set that predicted new physical phenomena, which were later confirmed by experiments in every detail. The corrected set of equations is rightfully called the Maxwell equations, in honor of his remarkable achievement in 1865. The equation that needed correction was Ampere's law. It was derived for current phenomena that were steady-state with $\nabla \cdot \mathbf{J} = 0$. This condition on the divergence of $\mathbf{J}$ is implicit in Ampere's law, as can be shown by taking the divergence of both sides:

$$\nabla \cdot \mathbf{J} = \nabla \cdot (\nabla \times \mathbf{H}) = 0 \tag{2.2.5}$$

While $\nabla \cdot \mathbf{J} = 0$ is valid for steady-state problems, the common relation is

provided from the continuity equation of charge and current:

$$\nabla \cdot \mathbf{J} + \frac{\partial \rho}{\partial t} = 0 \tag{2.2.6}$$

Maxwell observed that the continuity equation may be turned into a vanishing divergence by applying Coulomb's law (2.2.4). Hence

$$\nabla \cdot \mathbf{J} + \frac{\partial \rho}{\partial t} = \nabla \cdot \left(\mathbf{J} + \frac{\partial \mathbf{D}}{\partial t} \right) = 0 \tag{2.2.7}$$

Then Maxwell replaced $\mathbf{J}$ in Ampere's law by its generalization

$$\mathbf{J} \rightarrow \mathbf{J} + \frac{\partial \mathbf{D}}{\partial t}$$

for time-dependent fields. Thus Ampere's law became

$$\nabla \times \mathbf{H} = \mathbf{J} + \frac{\partial \mathbf{D}}{\partial t} \tag{2.2.8}$$

The same law, which has been confirmed by experiments, applies to both steady-state and time-dependent phenomena. It is compatible with the continuity equation (2.2.6) that describes the variation of fields over time.Maxwell designated the additional term in equation (2.2.8) as the displacement current. This indicates that a varying electric field has the capability to induce a magnetic field, even in the absence of an electric current. This concept stands in contrast to Faraday's law. The modification to Ampere's law is crucial when dealing with rapidly changing fields. In the absence of this modification, the existence of electromagnetic radiation would be negated. Maxwell postulated that light was a manifestation of electromagnetic wave phenomena and that electromagnetic waves with varying frequencies could be generated, attracted the interest of all physicists and inspired a lot of theoretical and experimental work on electromagnetism in the late nineteenth century. The four equations that summarize these laws are:

$$\begin{aligned} \nabla \cdot \mathbf{D} = \rho, \quad & \nabla \times \mathbf{H} = \mathbf{J} + \tfrac{\partial \mathbf{D}}{\partial t} \\ \nabla \cdot \mathbf{B} = 0, \quad & \nabla \times \mathbf{E} + \tfrac{\partial \mathbf{B}}{\partial t} = 0 \end{aligned} \tag{2.2.9}$$

well-known the Maxwell equations which form the foundation for all phenomenon classical electromagnetic.

2) Vector and Scalar Potentials

The electric and magnetic fields are interrelated by a set of first-order partial differential equations, known as the Maxwell equations. These equations can be directly applied to simple cases, but sometimes it is useful to introduce potentials, which reduce the number of equations to second-order ones, and automatically satisfy some of the Maxwell equations. This idea is not new to us, as it have already used the scalar potential Φ and the vector potential $\mathbf{A}$ in electrostatics and magnetostatics.

Since $\nabla \cdot \mathbf{B} = 0$ still holds, can define $\mathbf{B}$ in terms of a vector potential:

$$\mathbf{B} = \boldsymbol{\nabla} \times \mathbf{A} \tag{2.2.10}$$

Then the other homogeneous equation in (2.2.9), Faraday's law, can be written

$$\boldsymbol{\nabla} \times \left(\mathbf{E} + \frac{\partial \mathbf{A}}{\partial t} \right) = 0 \tag{2.2.11}$$

It implies that a value with vanishing curl in (2.2.11) may be expressed as the gradient of a scalar potential Φ.

$$\mathbf{E} + \frac{\partial \mathbf{A}}{\partial t} = -\mathbf{v}\Phi \tag{2.2.12a}$$

or

$$\mathbf{E} = -\boldsymbol{\nabla}\Phi - \frac{\partial \mathbf{A}}{\partial t} \tag{2.2.12b}$$

Using the potentials $\mathbf{A}$ and Φ, can express $\mathbf{B}$ and $\mathbf{E}$ as in equations (2.2.10) and (2.2.12), which automatically satisfy the two homogeneous Maxwell equations. To find the dynamics of $\mathbf{A}$ and Φ, It needs to solve the two non-homogeneous equations in (2.2.9). For simplicity, focus on the vacuum case of the Maxwell equations. Then, the non-homogeneous equations in (2.2.9) can be rewritten in terms of the potentials as

$$\begin{aligned} \nabla^2\Phi + \frac{\partial}{\partial t}(\boldsymbol{\nabla} \cdot \mathbf{A}) &= -\rho'\epsilon_0 \\ \nabla^2\mathbf{A} - \frac{1}{c^2}\frac{\partial^2 \mathbf{A}}{\partial r^2} - \nabla\left(\boldsymbol{\nabla} \cdot \mathbf{A} + \frac{1}{c^2}\frac{\partial \Phi}{\partial t} \right) &= -\mu_0 \mathbf{J} \end{aligned} \tag{2.2.12}$$

The two equations that remain after simplifying the four Maxwell equations are still interdependent. To separate them, can use the freedom in choosing the potentials. Since (2.2.10) defines **B** in terms of **A**, can add the gradient of any scalar function to the vector potential without changing B. This is called a gauge transformation.

$$\mathbf{A} \rightarrow \mathbf{A}' = \mathbf{A} + \nabla \mathbf{A} \tag{2.2.13}$$

For the electric field (2.2.12) to be unchanged as well, the scalar potential must be simultaneously transformed.

$$\Phi \rightarrow \Phi' = \Phi - \frac{\partial \Lambda}{\partial t} \tag{2.2.14}$$

The independence implicit by (2.2.13) and (2.2.14) implies that can select the set of potentials $(\mathbf{A}, \Phi)$ for satisfying the Lorenz condition.

$$\boldsymbol{\nabla} \cdot \mathbf{A} + \frac{1}{c^2} \frac{\partial \Phi}{\partial t} = 0 \tag{2.2.15}$$

This will uncouple the pair of equations (2.2.12) and leave two inhomogeneous wave equations, one for Φ and one for $\mathbf{A}$:

$$\begin{aligned} \nabla^2 \Phi - \frac{1}{c^2} \frac{\partial^2 \Phi}{\partial t^2} &= -\rho/\epsilon_0 \\ \nabla^2 \mathbf{A} - \frac{1}{c^2} \frac{\partial^2 \mathbf{A}}{\partial \mathrm{r}^2} &= -\mu_0 \mathbf{J} \end{aligned} \tag{2.2.16}$$

Equations (2.2.16) along with equation (2.2.15) constitute a set of equations that are equivalent to the Maxwell equations in a vacuum as Lorenz and others observed.

3) Green's Functions

The differential equation regulating the scalar potential of a given charge distribution in a dielectric medium, which is the result of the combination of

$$\begin{aligned} \boldsymbol{\nabla} \cdot \mathbf{D} &= 4\pi\rho, \\ \mathbf{D} = \epsilon \mathbf{E}, \quad \mathbf{E} &= -\boldsymbol{\nabla}\phi, \end{aligned} \tag{2.2.17}$$

is

$$-\nabla \cdot (\epsilon \nabla \phi) = 4\pi\rho \tag{2.2.18}$$

In the special situation of the vacuum, $\epsilon = 1$ (or, effectively, for a spatially homogeneous dielectric constant), this becomes

$$-\nabla^2\phi = 4\pi\rho \tag{2.2.19}$$

the equation of Siméon Denis Poisson (1781-1840); in regions devoid of charge, it reduces to the equation of Pierre Simon Laplace (1749-1827),

$$\nabla^2\phi = 0 \tag{2.2.20}$$

Our task is to find the solution of (2.2.18) for ϕ, for a given charge distribution. Since (2.2.18) is a linear differential equation relating ρ and ϕ, the potential at a point $\mathbf{r}$ is the additive contribution of all individual charge elements $(d\mathbf{r}')\,\rho(\mathbf{r}')$:

$$\phi(\mathbf{r}) = \int (d\mathbf{r}')\, G(\mathbf{r}, \mathbf{r}')\, \rho(\mathbf{r}')\,. \tag{2.2.21}$$

It is evident that $G(\mathbf{r}, \mathbf{r}')$ is the potential at $\mathbf{r}$ arising from a unit point charge at $\mathbf{r}'$, so that it satisfies the differential equation

$$-\nabla \cdot [\epsilon(\mathbf{r})\nabla G(\mathbf{r}, \mathbf{r}')] = 4\pi\delta(\mathbf{r} - \mathbf{r}') \tag{2.2.22}$$

Equation (2.2.21) expresses the fact that the potential due to a charge distribution is simply the sum of the contributions of each of the charges. $G(\mathbf{r}, \mathbf{r}')$ is an example of a class of functions introduced by George Green (1793-1841). Once we have Green's function, the solution for any charge distribution in a given dielectric arrangement is a matter of integration (Schwinger et al., 2018).

Retarded Green's Function

3.1) Potentials and Gauges

In a vacuum, the Maxwell's equations are

$$\begin{aligned} \boldsymbol{\nabla} \times \mathbf{B} &= \frac{1}{c}\frac{\partial}{\partial t}\mathbf{E} + \frac{4\pi}{c}\mathbf{j}, \\ \boldsymbol{\nabla} \cdot \mathbf{E} &= 4\pi\rho, \\ -\boldsymbol{\nabla} \times \mathbf{E} &= \frac{1}{c}\frac{\partial}{\partial t}\mathbf{B}, \\ \boldsymbol{\nabla} \cdot \mathbf{B} &= 0, \end{aligned} \tag{2.2.23}$$

where ρ is the charge, and $\mathbf{j}$ is the current density, and assumed that no magnetic charge is present. Notice that the local conservation law

$$\nabla \cdot \mathrm{j} + \frac{\partial}{\partial t}\rho = 0, \tag{2.2.24}$$

is not an independent statement, but is derivable from (2.2.23a) and (2.2.23b).

To solve Maxwell's equations, first recognize that the last two equations, (2.2.23c) and (2.2.23d), not referral to charge or current, which be able to similarly satisfying by potentials via the definition

$$\begin{aligned} \mathbf{B} &= \boldsymbol{\nabla} \times \mathbf{A}, \\ \mathbf{E} &= -\frac{1}{c}\frac{\partial}{\partial t}\mathbf{A} - \boldsymbol{\nabla}\phi. \end{aligned} \tag{2.2.25}$$

the potentials A and ϕ are not uniquely defined. Since the magnetic field is the curl of $\mathbf{A}$, it is unchanged when a gradient is added to $\mathbf{A}$,

$$\mathbf{A} \to \mathbf{A} + \boldsymbol{\nabla}\lambda \tag{2.2.26}$$

where λ is an arbitrary function. In order that this new choice of vector potential not alter the electric field, (2.2.25b), it is necessary to simultaneously replace the scalar potential by

$$\phi \to \phi - \frac{1}{c}\frac{\partial}{\partial t}\lambda. \tag{2.2.27}$$

The original set of potentials is not unique, can choose another set that satisfies equations (2.2.26) and (2.2.27) and leads to the same observable fields $\mathbf{B}$ and $\mathbf{E}$. This ambiguity in the selection of potentials is known as the gauge freedom of the theory, and the transformations that preserve it are called gauge transformations. This freedom will be used to simplify the solution of the differential equations for the potentials in the next section.

Upon substituting the constructions of $\mathbf{B}$ and $\mathbf{E}$ in terms of potentials, (2.2.25), into the first set of Maxwell's equations, from (2.2.23a),

$$\boldsymbol{\nabla} \times (\boldsymbol{\nabla} \times \mathbf{A}) = \frac{1}{c}\frac{\partial}{\partial t}\left(-\boldsymbol{\nabla}\phi - \frac{1}{c}\frac{\partial}{\partial t}\mathbf{A}\right) + \frac{4\pi}{c}\mathbf{j} \tag{2.2.28}$$

or

$$-\left(\nabla^2-\frac{1}{c^2}\frac{\partial^2}{\partial t^2}\right)\mathbf{A}=-\boldsymbol{\nabla}\left(\boldsymbol{\nabla}\cdot\mathbf{A}+\frac{1}{c}\frac{\partial}{\partial t}\phi\right)+\frac{4\pi}{c}\mathbf{j} \tag{2.2.29}$$

and, from (2.2.23b),

$$-\nabla^2\phi-\frac{1}{c}\frac{\partial}{\partial t}(\boldsymbol{\nabla}\cdot\mathbf{A})=4\pi\rho. \tag{2.2.30}$$

The potentials $\mathbf{A}$ and ϕ are defined by a system of two second order differential equations, which depend on the choice of gauge. It can simplify the equations by selecting a suitable gauge. Below, discuss the most common and convenient gauges for this purpose.

1. The radiation gauge (or Coulomb gauge) is defined by the condition

$$\boldsymbol{\nabla}\cdot\mathbf{A}=0 \tag{2.2.31}$$

In this gauge, (2.2.29) and (2.2.30) reduce to

$$-\nabla^2\phi=4\pi\rho, \tag{2.2.32}$$

$$-\Box^2\mathbf{A}=\frac{4\pi}{c}\mathrm{j}-\frac{1}{c}\frac{\partial}{\partial t}(\nabla\phi), \tag{2.2.33}$$

where

$$\Box^2=\nabla^2-\frac{1}{c^2}\frac{\partial^2}{\partial t^2} \tag{2.2.34}$$

is the d'Alembertian. (Jean d'Alembert's Traité de Dynamique was published in 1758.) The equation for ϕ, (2.2.32), is just the same as that in electrostatics (hence the origin of the term "Coulomb gauge") so that ϕ is, in principle, known. The structure on the right hand side of (2.2.33) is proportional to an effective current, the second term of which is present in order that it be divergenceless:

$$\boldsymbol{\nabla}\cdot\left[\mathbf{j}-\nabla\left(\frac{1}{4\pi}\frac{\partial}{\partial t}\phi\right)\right]=\boldsymbol{\nabla}\cdot\mathbf{j}-\frac{1}{4\pi}\frac{\partial}{\partial t}\left(\nabla^2\phi\right)=\boldsymbol{\nabla}\cdot\mathbf{j}+\frac{\partial}{\partial t}\rho=0 \tag{2.2.35}$$

where the last equality follows from charge conservation, (2.2.24). This relation also entails the consistency of the choice of the radiation gauge in that if set $\boldsymbol{\nabla}\cdot\mathbf{A}$ equal to zero at one time, it remains zero for all time, since

$$-\Box^2(\boldsymbol{\nabla}\cdot\mathbf{A})=\frac{4\pi}{c}\nabla\cdot\left[\mathbf{j}-\nabla\left(\frac{1}{4\pi}\frac{\partial}{\partial t}\phi\right)\right]=0. \tag{2.2.36}$$

2. The Lorentz gauge condition is a relation between vector and scalar potentials,

$$\nabla \cdot \mathbf{A} + \frac{1}{c}\frac{\partial}{\partial t}\phi = 0. \tag{2.2.37}$$

In this gauge, the equations for $\mathbf{A}$ and ϕ have the symmetrical form,

$$-\Box^2 \mathbf{A} = \frac{4\pi}{c}\mathbf{j} \tag{2.2.38}$$

$$-\Box^2 \phi = 4\pi\rho. \tag{2.2.39}$$

The consistency of this gauge choice again follows from the fact that charge is conserved,

$$-\Box^2\left(\nabla \cdot \mathbf{A} + \frac{1}{c}\frac{\partial}{\partial t}\phi\right) = \frac{4\pi}{c}\left(\nabla \cdot \mathbf{j} + \frac{\partial \rho}{\partial t}\right) = 0 \tag{2.2.40}$$

3.2) Green's Function in the Lorentz Gauge

The following paragraphs will present a solution to the differential equations (2.2.38) and (2.2.39) for potentials in the Lorentz gauge. The potentials have a linear relationship with their sources, which allows us to express them in terms of a Green's function.

$$\begin{aligned} \phi(\mathbf{r},t) &= \int (d\mathbf{r}')\, dt' G\left(\mathbf{r}-\mathbf{r}', t-t'\right) \rho\left(\mathbf{r}', t'\right) \\ \mathbf{A}(\mathbf{r},t) &= \int (d\mathbf{r}')\, dt' G\left(\mathbf{r}-\mathbf{r}', t-t'\right) \frac{1}{c}\mathbf{j}\left(\mathbf{r}', t'\right) \end{aligned} \tag{2.2.41}$$

The Green's function, $G\left(\mathbf{r}-\mathbf{r}', t-t'\right)$, depends only on the relative positions and times due to the translational invariance in unbounded space. Since ϕ satisfies (2.2.39), the Green's function also satisfies the differential equation.

$$-\Box^2 G\left(\mathbf{r}-\mathbf{r}', t-t'\right) = 4\pi\delta\left(\mathbf{r}-\mathbf{r}'\right)\delta\left(t-t'\right), \tag{2.2.42}$$

which is a four-dimensional generalization of the three-dimensional Green's function equation studied in electrostatics,

$$-\nabla^2 G\left(\mathbf{r}-\mathbf{r}'\right) = 4\pi\delta\left(\mathbf{r}-\mathbf{r}'\right) \tag{2.2.43}$$

To solve (2.2.42), will analyze its time dependence by making use of the exponential representations (Fourier transforms in time)

$$\begin{aligned} \delta\left(t-t'\right) &= \int_{-\infty}^{\infty} \frac{d\omega}{2\pi} e^{-i\omega(t-t')}, \\ G\left(\mathbf{r}-\mathbf{r}', t-t'\right) &= \int_{-\infty}^{\infty} \frac{d\omega}{2\pi} e^{-i\omega(t-t')} G_\omega\left(\mathbf{r}-\mathbf{r}'\right), \end{aligned} \tag{2.2.44}$$

where G_ω satisfies the three-dimensional differential equation,

$$-\left(\nabla^2+\frac{\omega^2}{c^2}\right)G_\omega\left(\mathbf{r}-\mathbf{r}'\right)=4\pi\delta\left(\mathbf{r}-\mathbf{r}'\right). \tag{2.2.45}$$

In the static limit, $\omega \to 0$, (2.2.45) reduces to (2.2.43), the solution of which is Coulomb's potential:

$$G_{\omega=0}\left(\mathbf{r}-\mathbf{r}'\right)=\frac{1}{|\mathbf{r}-\mathbf{r}'|}. \tag{2.2.46}$$

Since G_ω depends only on $\mathbf{r}-\mathbf{r}'$, set $\mathbf{r}'=\mathbf{0}$, without loss of generality in the following discussion. Also, since now looking for a spherically symmetrical solution for G_ω, it is natural to use a spherical coordinate system in which the Laplacian here reduces to

$$\nabla^2 \to \frac{1}{r^2}\frac{d}{dr}\left(r^2\frac{d}{dr}\right) \tag{2.2.47}$$

Therefore, for $r>0$, to solve the homogeneous equation

$$\left[\frac{1}{r^2}\frac{d}{dr}\left(r^2\frac{d}{dr}\right)+\frac{\omega^2}{c^2}\right]G_\omega(\mathbf{r})=0 \tag{2.2.48}$$

subject to the boundary condition that there is a point charge at the origin. The consequence of this requirement is most conveniently extracted by integrating (2.2.45) over a sphere S of vanishing radius r_0 about the origin,

$$4\pi=-\int(d\mathbf{r})\nabla\cdot(\nabla G_\omega)=-\oint_S dS\nabla_r G_\omega=-4\pi r^2\frac{d}{dr}G_\omega\Big|_{r_0\to 0} \tag{2.2.49}$$

or

$$-r^2\frac{d}{dr}G_\omega(\mathbf{r})\Big|_{r_0\to 0}=1. \tag{2.2.50}$$

Noted that the ω^2/c^2 term in the differential equation does not contribute to the integral since

$$\frac{\omega^2}{c^2}G_\omega\sim\frac{1}{r},\qquad \text{as}\qquad r\to 0, \tag{2.2.51}$$

which has vanishing volume integral as $r_0\to 0$. To solve (2.2.48), introduce g_ω, defined by

$$G_\omega=\frac{1}{r}g_\omega, \tag{2.2.52}$$

which satisfies the differential equation

$$\left(\frac{d^2}{dr^2}+\frac{\omega^2}{c^2}\right)g_\omega(r)=0, \quad \text{for} \quad r>0, \tag{2.2.53}$$

where

$$\begin{aligned} r^2\frac{d}{dr}G_\omega &= r\frac{d}{dr}g_\omega - g_\omega \\ \frac{1}{r^2}\frac{d}{dr}\left(r^2\frac{d}{dr}G_\omega\right) &= \frac{1}{r}\frac{d^2}{dr^2}g_\omega \end{aligned} \tag{2.2.54}$$

The independent solutions of (2.2.53) have the form

$$g_\omega \sim e^{\pm i\omega r/c}, \tag{2.2.55}$$

and the corresponding forms for G_ω are

$$G_\omega(r)=\frac{C}{r}e^{\pm i\omega r/c}, \text{ for } r>0. \tag{2.2.56}$$

For either choice of $+$ or $-$ sign, the constant C is determined by the boundary condition (2.2.50) to be

$$C=1. \tag{2.2.57}$$

Therefore, will have two fundamental solutions to (2.2.45),

$$G_\omega\left(\mathbf{r}-\mathbf{r}'\right)=\frac{1}{|\mathbf{r}-\mathbf{r}'|}e^{\pm i\omega|\mathbf{r}-\mathbf{r}'|/c}, \tag{2.2.58}$$

while from (2.2.44b) now obtain the space-time form of the Green's functions,

$$\begin{aligned} G\left(\mathbf{r}-\mathbf{r}',t-t'\right) &= \int_{-\infty}^{\infty}\frac{d\omega}{2\pi}\frac{1}{|\mathbf{r}-\mathbf{r}'|}e^{i\omega[\pm|\mathbf{r}-\mathbf{r}'|/c-(t-t')]} \\ &= \frac{1}{|\mathbf{r}-\mathbf{r}'|}\delta\left(\pm\frac{1}{c}|\mathbf{r}-\mathbf{r}'|-(t-t')\right) \end{aligned} \tag{2.2.59}$$

What is implied by the use of the $+$ or - sign in (2.2.59)? The choice of the $+$ sign leads to the retarded Green's function,

$$G_{\text{ret}}\ \left(\mathbf{r}-\mathbf{r}',t-t'\right)=\frac{1}{|\mathbf{r}-\mathbf{r}'|}\delta\left(\frac{1}{c}|\mathbf{r}-\mathbf{r}'|-(t-t')\right) \tag{2.2.60}$$

which is nonvanishing when

$$t=t'+\frac{1}{c}|\mathbf{r}-\mathbf{r}'| \tag{2.2.61}$$

This implies that the sign propagates at the velocity of light c from the source (at time t') to the spectator (at time t); the effect happens after the cause. If pick the - sign, will obtain the advanced Green's function

$$G_{\text{adv}}(\mathbf{r}-\mathbf{r}', t-t') = \frac{1}{|\mathbf{r}-\mathbf{r}'|}\delta\left(\frac{1}{c}|\mathbf{r}-\mathbf{r}'| + (t-t')\right) \tag{2.2.62}$$

which is nonzero when

$$t = t' - \frac{1}{c}|\mathbf{r}-\mathbf{r}'| \tag{2.2.63}$$

To avoid the violation of causality, which implies that the observer receives the signal before the source emits it, choose the retarded Green's function as the solution that meets the appropriate temporal boundary condition. (However, both retarded and advanced Green's functions have applications in physics.) By inserting (2.2.60) into (2.2.41a) and (2.2.41b), will can derive explicit formulas for the potentials.

$$\begin{aligned}\phi(\mathbf{r},t) &= \int (d\mathbf{r}')\, dt' \frac{\delta\left(\frac{1}{c}|\mathbf{r}-\mathbf{r}'| - (t-t')\right)}{|\mathbf{r}-\mathbf{r}'|}\rho(\mathbf{r}',t') \\ \mathbf{A}(\mathbf{r},t) &= \int (d\mathbf{r}')\, dt' \frac{\delta\left(\frac{1}{c}|\mathbf{r}-\mathbf{r}'| - (t-t')\right)}{|\mathbf{r}-\mathbf{r}'|}\frac{1}{c}\mathbf{j}(\mathbf{r}',t').\end{aligned} \tag{2.2.64}$$

Integrating over t', will obtain the so-called retarded or Lienard-Wiechert potentials (published in 1898 and 1900 , respectively),

$$\begin{aligned}\phi(\mathbf{r},t) &= \int (d\mathbf{r}')\frac{1}{|\mathbf{r}-\mathbf{r}'|}\rho\left(\mathbf{r}', t-\frac{1}{c}|\mathbf{r}-\mathbf{r}'|\right) \\ \mathbf{A}(\mathbf{r},t) &= \int (d\mathbf{r}')\frac{1}{|\mathbf{r}-\mathbf{r}'|}\frac{1}{c}\mathbf{j}\left(\mathbf{r}', t-\frac{1}{c}|\mathbf{r}-\mathbf{r}'|\right)\end{aligned} \tag{2.2.65}$$

These results are elementary generalizations of the potentials for electrostatics and magnetostatics, but now reflecting the finite propagation speed of light.

2.2.2 The Approach of Electrodynamics Theory

In this section, we will present the approach of electrodynamics theory for the calculation of the power spectrum of Cherenkov radiation. The method in this section is from the textbook classical electrodynamics by Schwinger et al.(2018).

1) Spectral and Angular Distribution

Let's focus on the spectrum characteristic of this radiation, that is, its dependence on frequency, or wavelength. To investigate this dependence, return to

our starting point, the potentials in the Lorentz gauge, given by (2.2.64a) and (2.2.64b)

$$\begin{aligned}\phi(\mathbf{r},t) &= \int (d\mathbf{r}')\, dt' \frac{\delta\left(\frac{1}{c}|\mathbf{r}-\mathbf{r}'| - (t-t')\right)}{|\mathbf{r}-\mathbf{r}'|}\rho(\mathbf{r}',t'),\\ \mathbf{A}(\mathbf{r},t) &= \int (d\mathbf{r}')\, dt' \frac{\delta\left(\frac{1}{c}|\mathbf{r}-\mathbf{r}'| - (t-t')\right)}{|\mathbf{r}-\mathbf{r}'|}\frac{1}{c}\mathbf{j}(\mathbf{r}',t').\end{aligned} \tag{2.2.66}$$

In deriving these results, will use the spectral representation [cf. (2.2.62)]

$$\delta\left(\frac{1}{c}|\mathbf{r}-\mathbf{r}'| - (t-t')\right) = \int_{-\infty}^{\infty}\frac{d\omega}{2\pi}e^{i\omega[|\mathbf{r}-\mathbf{r}'|/c-(t-t')]}. \tag{2.2.67}$$

If now reinsert (2.2.67) into (2.2.66a) and (2.2.66b), and carry out the t' integration by introducing the temporal Fourier transform

$$\begin{aligned}\int_{-\infty}^{\infty} dt' e^{i\omega t'} f(t') &= f(\omega),\\ \int_{-\infty}^{\infty}\frac{d\omega}{2\pi}e^{-i\omega t'} f(\omega) &= f(t'),\end{aligned} \tag{2.2.68}$$

will obtain the Fourier transformed versions of (2.2.66a) and (2.2.66b):

$$\phi(\mathbf{r},\omega) = \int (d\mathbf{r}')\frac{e^{i\omega|\mathbf{r}-\mathbf{r}'|/c}}{|\mathbf{r}-\mathbf{r}'|}\rho(\mathbf{r}',\omega), \tag{2.2.69}$$

$$\mathbf{A}(\mathbf{r},\omega) = \int (d\mathbf{r}')\frac{e^{i\omega|\mathbf{r}-\mathbf{r}'|/c}}{|\mathbf{r}-\mathbf{r}'|}\frac{1}{c}\mathbf{j}(\mathbf{r}',\omega). \tag{2.2.70}$$

Observe that if $f(t')$ is a real function of t', its Fourier transform, $f(\omega)$, satisfies the condition

$$f(\omega)^* = f(-\omega) \tag{2.2.71}$$

consequently,

$$f(\omega)^* f(\omega) = |f(\omega)|^2 = f(-\omega)f(\omega) \tag{2.2.72}$$

is a real positive number, symmetric under the interchange $\omega \to -\omega$. This implies that the algebraic sign of ω is not significant, since only its magnitude enters into physical quantities.

Let us focus our attention on the radiation fields, far from the sources. Using the expansion for $|\mathbf{r}-\mathbf{r}'|$ in (2.2.69) and (2.2.70), will obtain the asymptotic

expression for the potentials, in terms of spatial Fourier transforms,

$$\begin{aligned}\phi(\mathbf{r},\omega) &\sim \frac{e^{i\omega r/c}}{r}\int (d\mathbf{r}')\, e^{-i\omega \mathbf{n}\cdot\mathbf{r}'/c}\rho(\mathbf{r}',\omega)\,,\\ \mathbf{A}(\mathbf{r},\omega) &\sim \frac{e^{i\omega r/c}}{r}\int (d\mathbf{r}')\, e^{-i\omega \mathbf{n}\cdot\mathbf{r}'/c}\frac{1}{c}\mathrm{j}(\mathbf{r}',\omega)\,,\end{aligned} \tag{2.2.73}$$

where $\mathbf{n} = \mathbf{r}/r$. Evidently, the effectiveness of radiation with a given wavelength and direction of propagation depends upon the Fourier analysis of the time and spatial dependences of the charges and currents. In the exponential, the term $\omega\mathbf{n}\cdot\mathbf{r}'/c$, which is of the order of the ratio of the size of the system to the wavelength of the radiation, is significant for all but small systems.

$$\mathbf{k} = \frac{\omega}{c}\mathbf{n} \tag{2.2.74}$$

the propagation vector, in terms of which the potentials are written as Fourier transforms in space and time,

$$\begin{Bmatrix}\phi\\ \mathbf{A}\end{Bmatrix}(\mathbf{r},\omega) \sim \frac{e^{i\omega r/c}}{r}\begin{Bmatrix}\rho\\ \frac{1}{c}\mathbf{j}\end{Bmatrix}(\mathbf{k},\omega), \tag{2.2.75}$$

where, for example,

$$\rho(\mathbf{k},\omega) = \int (d\mathbf{r}')\, e^{-i\mathbf{k}\cdot\mathbf{r}'}\rho(\mathbf{r}',\omega)\,. \tag{2.2.76}$$

The corresponding field strengths can now be computed from the time Fourier transforms of (2.2.69) and (2.2.70):

$$\begin{aligned}\mathbf{E}(\mathbf{r},\omega) &= i\frac{\omega}{c}\mathbf{A}(\mathbf{r},\omega) - \nabla\phi(\mathbf{r},\omega),\\ \mathbf{B}(\mathbf{r},\omega) &= \boldsymbol{\nabla}\times\mathbf{A}(\mathbf{r},\omega)\end{aligned} \tag{2.2.77}$$

where use the effective replacement

$$\frac{\partial}{\partial t} \to -i\omega, \tag{2.2.78}$$

because

$$\int_{-\infty}^{\infty} dt e^{i\omega t}\frac{\partial}{\partial t}F(\mathbf{r},t) = -i\omega F(\mathbf{r},\omega), \tag{2.2.79}$$

provided that $F(\mathbf{r},t) \to 0$ as $t \to \pm\infty$. Physically, the time boundary conditions state that in the infinite past and the infinite future, nothing is happening: what

is significant for our observation takes place in a finite time interval only. The measure of significant variation in r is the wavelength, $\lambda = 2\pi c/\omega$, as indicated by the effective replacement for the gradients in (2.2.77a) and (2.2.77b),

$$\boldsymbol{\nabla} \to i\mathbf{k} \tag{2.2.80}$$

Consequently, the asymptotic forms of the electric and magnetic fields are

$$\begin{aligned} \mathbf{E}(\mathbf{r},\omega) &\sim i\frac{\omega}{c}\frac{e^{i\omega r/c}}{r}\frac{1}{c}\mathbf{j}(\mathbf{k},\omega) - i\frac{\omega}{c}\frac{e^{i\omega r/c}}{r}\mathbf{n}\rho(\mathbf{k},\omega), \\ \mathbf{B}(\mathbf{r},\omega) &\sim i\frac{\omega}{c}\frac{e^{i\omega r/c}}{r}\mathbf{n}\times\frac{1}{c}\mathbf{j}(\mathbf{k},\omega). \end{aligned} \tag{2.2.81}$$

By using the Fourier transformed version of the local charge conservation condition,

$$\omega\rho(\mathbf{k},\omega) = \mathbf{k}\cdot\mathbf{j}(\mathbf{k},\omega), \tag{2.2.82}$$

rewrite the second term of (2.2.81a) as

$$-\frac{i}{c}\frac{e^{i\omega r/c}}{r}\mathbf{n}\mathbf{k}\cdot\mathbf{j}(\mathbf{k},\omega) = -\frac{i\omega}{c}\frac{e^{i\omega r/c}}{r}\mathbf{n}\mathbf{n}\cdot\frac{1}{c}\mathbf{j}(\mathbf{k},\omega). \tag{2.2.83}$$

The electric field now becomes

$$\begin{aligned} \mathbf{E}(\mathbf{r},\omega) &\sim \frac{e^{i\omega r/c}}{r}i\frac{\omega}{c}(1-\mathbf{n}\mathbf{n})\cdot\frac{1}{c}\mathbf{j}(\mathbf{k},\omega) \\ &= -\frac{e^{i\omega r/c}}{r}i\frac{\omega}{c}\mathbf{n}\times\left[\mathbf{n}\times\frac{1}{c}\mathbf{j}(\mathbf{k},\omega)\right] \\ &\sim -\mathbf{n}\times\mathbf{B}(\mathbf{r},\omega) \end{aligned} \tag{2.2.84}$$

Before proceeding, remark that the relation between the two terms in (2.2.81a) can also be obtained by using the Lorentz gauge condition; this is not surprising since the consistency of the Lorentz gauge depends upon current conservation. The Fourier transform of (2.2.37) reads

$$\nabla\cdot\mathbf{A}(\mathbf{r},\omega) - i\frac{\omega}{c}\phi(\mathbf{r},\omega) = 0, \tag{2.2.85}$$

which becomes, upon using the asymptotic replacement (2.2.80),

$$ik[\mathbf{n}\cdot\mathbf{A}(\mathbf{r},\omega) - \phi(\mathbf{r},\omega)] = 0, \tag{2.2.86}$$

or

$$\phi(\mathbf{r},\omega) \sim \mathbf{n}\cdot\mathbf{A}(\mathbf{r},\omega), \tag{2.2.87}$$

so from (2.2.77a) the reduction (2.2.84) follows.

The instantaneous flux of energy, at a particular time t, is given by Poynting's vector

$$\mathbf{S}(\mathbf{r},t) = \frac{c}{4\pi}\mathbf{E}(\mathbf{r},t)\times\mathbf{B}(\mathbf{r},t), \tag{2.2.88}$$

so the total radiated energy crossing a unit area of surface normal to $\mathbf{S}$ is

$$\begin{aligned}\int_{-\infty}^{\infty} dt\mathbf{S}(\mathbf{r},t) &= \frac{c}{4\pi}\int_{-\infty}^{\infty} dt\int_{-\infty}^{\infty}\frac{d\omega}{2\pi}\mathbf{E}(\mathbf{r},\omega)^* e^{i\omega t}\times\mathbf{B}(\mathbf{r},t)\\ &= \frac{c}{4\pi}\int_{-\infty}^{\infty}\frac{d\omega}{2\pi}\mathbf{E}(\mathbf{r},\omega)^*\times\mathbf{B}(\mathbf{r},\omega)\\ &= \mathbf{n}\frac{c}{4\pi}\int_{-\infty}^{\infty}\frac{d\omega}{2\pi}|\mathbf{B}(\mathbf{r},\omega)|^2\end{aligned} \tag{2.2.89}$$

using (2.2.84), and the fact that $\mathbf{n}\cdot\mathbf{B}=0$. The energy flows in the direction of $\mathbf{n}$ and the energy radiated per unit area perpendicular to this direction is

$$\int_{-\infty}^{\infty} dt\mathbf{n}\cdot\mathbf{S}(\mathbf{r},t) = \frac{c}{4\pi^2}\int_0^{\infty} d\omega|\mathbf{B}(\mathbf{r},\omega)|^2 \tag{2.2.90}$$

where use the symmetry property (2.2.72). It is more useful to consider the total energy radiated into the solid angle $d\Omega$,

$$\begin{aligned}\int_{-\infty}^{\infty} dt(\mathbf{n}\cdot\mathbf{S})r^2 d\Omega &= d\Omega r^2\frac{c}{4\pi^2}\int_0^{\infty} d\omega|\mathbf{B}(\mathbf{r},\omega)|^2\\ &\equiv d\Omega\frac{dE}{d\Omega}\equiv d\Omega\int_0^{\infty} d\omega\frac{d^2E}{d\omega d\Omega}\end{aligned} \tag{2.2.91}$$

where

$$\begin{aligned}\frac{d^2E}{d\omega d\Omega} &= \frac{\omega^2}{4\pi^2c^3}|\mathbf{n}\times\mathbf{j}(\mathbf{k},\omega)|^2\\ &= \frac{\omega^2}{4\pi^2c}\left\{\left|\frac{1}{c}\mathbf{j}(\mathbf{k},\omega)\right|^2 - |\rho(\mathbf{k},\omega)|^2\right\}\end{aligned} \tag{2.2.92}$$

is the general expression for the spectral distribution, the energy radiated per unit frequency per unit solid angle in the direction of observation $\mathbf{n}$.

2) Power Spectrum of Cherenkov Radiation

In the previous section, a general expression for the spectral distribution is obtained, (2.2.92), which accounts for the radiation from all times, $t\to-\infty$ to

$t \to +\infty$. To obtain a generalization applicable to a limited epoch. In so doing, must note that time and frequency are complementary; that is, a time interval of many periods is required in order to identify a corresponding frequency. First rewrite (2.2.92) in the space-time form:

$$\frac{d^2E}{d\omega d\Omega} = \frac{\omega^2}{4\pi^2 c^3}\left[\mathbf{n}\times\int dt e^{i\omega t}\mathbf{j}(\mathbf{k},t)\right]^*\cdot\left[\mathbf{n}\times\int dt' e^{i\omega t'}\mathbf{j}\left(\mathbf{k},t'\right)\right], \tag{2.2.93}$$

and focus our attention on the part involving time integrations:

$$\begin{aligned}&\int dt dt' e^{-i\omega(t-t')}\mathbf{j}(\mathbf{k},t)^*\mathbf{j}\left(\mathbf{k},t'\right)\\ &=\int dT d\tau e^{-i\omega\tau}\mathbf{j}(\mathbf{k},T+\tau/2)^*\mathbf{j}(\mathbf{k},T-\tau/2)\end{aligned} \tag{2.2.94}$$

where introduce the average time and the time difference,

$$T=\frac{1}{2}\left(t+t'\right),\quad \tau=t-t',\quad dtdt'=dTd\tau \tag{2.2.95}$$

The integral in (2.2.94) is dominated by the values of τ that are approximately $1/\omega$, which determines the time scale for the radiation emission. This microscopic time scale may be much shorter than macroscopic time intervals; for example, for visible light, $\tau\sim 10^{-15}$sec. The time T is then understood as the mean (macroscopic) time of emission, which can only be defined within a time of order τ.

Substituting (2.2.94) into (2.2.93), will write

$$\frac{d^2E}{d\omega d\Omega}=\int dT\frac{d^2P(T)}{d\omega d\Omega}, \tag{2.2.96}$$

from which infer the power spectrum at time T,

$$\frac{d^2P(T)}{d\omega d\Omega}=\frac{\omega^2}{4\pi^2 c}\int_{-\infty}^{\infty}d\tau e^{-i\omega\tau}\left[\mathbf{n}\times\frac{1}{c}\mathbf{j}(\mathbf{k},T+\tau/2)^*\right]\cdot\left[\mathbf{n}\times\frac{1}{c}\mathbf{j}(\mathbf{k},T-\tau/2)\right], \tag{2.2.97}$$

or, alternatively, using the second form of (2.2.92),

$$\begin{aligned}\frac{d^2P(T)}{d\omega d\Omega}=\frac{\omega^2}{4\pi^2 c}\int_{-\infty}^{\infty}d\tau e^{-i\omega\tau}\Big\{&\frac{1}{c}\mathbf{j}(\mathbf{k},T+\tau/2)^*\cdot\frac{1}{c}\mathbf{j}(\mathbf{k},T-\tau/2)\\ &-\rho(\mathbf{k},T+\tau/2)^*\rho(\mathbf{k},T-\tau/2)\Big\}\end{aligned} \tag{2.2.98}$$

To apply (2.2.98), will examine the radiation generated by a charged particle traveling with constant velocity $\mathbf{v}$, where the charge and current density are

$$\begin{aligned} \rho(\mathbf{r},t) &= e\delta(\mathbf{r}-\mathbf{v}t), \\ \mathbf{j}(\mathbf{r},t) &= e\mathbf{v}\delta(\mathbf{r}-\mathbf{v}t). \end{aligned} \tag{2.2.99}$$

The Fourier transforms in (2.2.98) are trivially evaluated:

$$\int (d\mathbf{r}) e^{\pm i\omega\mathbf{n}\cdot\mathbf{r}/c} \begin{Bmatrix} \rho(\mathbf{r}, T\pm\tau/2) \\ \frac{1}{c}\mathbf{j}(\mathbf{r}, T\pm\tau/2) \end{Bmatrix} = e^{\pm i\omega\mathbf{n}\cdot\mathbf{v}(T\pm\tau/2)/c} \begin{Bmatrix} e \\ \frac{e}{c}\mathbf{v} \end{Bmatrix} \tag{2.2.100}$$

When these are substituted into (2.2.98), the T dependence disappears, as expected, and obtain

$$\begin{aligned} \frac{d^2P}{d\omega d\Omega} &= \frac{\omega^2}{4\pi^2 c}\int_{-\infty}^{\infty} d\tau e^{-i\omega\tau} e^2 \left(\frac{v^2}{c^2}-1\right) e^{i\omega\mathbf{n}\cdot\mathbf{v}\tau/c} \\ &= \frac{\omega^2}{4\pi^2 c} e^2 \left(\frac{v^2}{c^2}-1\right) \int_{-\infty}^{\infty} d\tau e^{-i\omega\tau(1-\mathbf{n}\cdot\mathbf{v}/c)} \\ &= \frac{\omega^2 e^2}{4\pi^2 c}\left(\frac{v^2}{c^2}-1\right) 2\pi\delta\left(\omega\left(1-\frac{v}{c}\cos\theta\right)\right) \end{aligned} \tag{2.2.101}$$

where θ is the angle between the direction of observation, $\mathbf{n}$, and the velocity of the particle, $\mathbf{v}$. The δ function implies that there is no radiation, since

$$\frac{v}{c}\cos\theta < 1. \tag{2.2.102}$$

This is the familiar result that a charged particle moving with a constant velocity in vacuum does not radiate. However, if it were possible that

$$\frac{v}{c} > 1, \tag{2.2.103}$$

the argument of the delta function could vanish, and radiation would be emitted by the charged particle. Is there any way of effectively satisfying (2.2.103)? In a medium, light can move with a speed, c', less than c, and correspondingly the speed of a particle can be greater than c'. Now does the particle radiate? Recall that the macroscopic Maxwell's equations, for a medium with dielectric constant ϵ and magnetic permeability μ, can be put into vacuum form, by the redefinitions

$$\mathbf{E}' = \sqrt{\epsilon}\mathbf{E}, \quad \mathbf{H}' = \sqrt{\mu}\mathbf{H}, \quad c' = \frac{c}{\sqrt{\epsilon\mu}}, \quad \rho' = \frac{1}{\sqrt{\epsilon}}\rho, \quad \mathbf{J}' = \frac{1}{\sqrt{\epsilon}}\mathbf{J}. \tag{2.2.104}$$

Therefore, the power radiated when a charged particle is moving with constant velocity in a nonmagnetic medium ($\mu = 1$) of index of refraction $n = \sqrt{\epsilon}$ can be obtained immediately from (2.2.101) by the substitutions $e \to e/n$ and $c \to c/n$:

$$\frac{d^2P}{d\omega d\Omega} = \frac{\omega^2}{4\pi^2(c/n)}\left(\frac{e}{n}\right)^2\left(\frac{v^2}{(c/n)^2} - 1\right)2\pi\delta\left(\omega\left(1 - \frac{v}{(c/n)}\cos\theta\right)\right). \quad (2.2.105)$$

Thus, indeed there is radiation if the condition

$$\frac{nv}{c}\cos\theta = 1, \quad (2.2.106)$$

or

$$\cos\theta = \frac{c}{nv} < 1, \quad (2.2.107)$$

is satisfied. Here will see that, for a charged particle traveling with a constant velocity inside a medium characterized by an index of refraction $n > 1$, electromagnetic radiation can be emitted if the criterion

$$v > \frac{c}{n} \quad (2.2.108)$$

is satisfied. Such a medium can be easily found for fast particles. The radiation is emitted on a cone described by (2.2.107), and because of its unique characteristics, is especially suited for determining the velocities of relativistic charged particles. This phenomenon is called Cherenkov radiation. Emphasize that the condition (2.2.107) can only be satisfied when $n > 1$. Because the index of refraction depends on frequency, that is, media are dispersive, this means that the condition (2.2.108) can only hold for a finite range of frequencies (typically, in the optical region). Moreover, this dispersion implies that different frequencies are emitted at different angles. Cherenkov radiation is commonly seen in watermoderated nuclear reactors as blue light surrounding the core.

The frequency spectrum of the radiated power can be obtained by integrat-

ing (2.2.105) over all angles,

$$\begin{aligned}\frac{dP}{d\omega} &= \int d\Omega \frac{d^2P}{d\omega d\Omega} \\ &= \omega^2 \frac{e^2}{nc}\frac{n^2v^2}{c^2}\left(1-\frac{c^2}{n^2v^2}\right)\int_{-1}^{1} d(\cos\theta)\delta\left(\omega\left(1-\frac{nv}{c}\cos\theta\right)\right) \\ &= \omega\frac{e^2v}{c^2}\left(1-\frac{c^2}{n^2(\omega)v^2}\right), \quad \text{if } n(\omega) > \frac{c}{v}\end{aligned} \tag{2.2.109}$$

and the total radiated power is

$$\begin{aligned}-\frac{dE}{dt} = P &= \int_0^\infty d\omega \frac{dP}{d\omega} \\ &= \int d\omega\omega\frac{e^2v}{c^2}\left(1-\frac{c^2}{n^2(\omega)v^2}\right) \\ P &= \omega\frac{e^2v}{c^2}\left(1-\frac{c^2}{n^2(\omega)v^2}\right)\end{aligned} \tag{2.2.110}$$

where E is the energy of the particle. In practice, it is more convenient to consider the energy lost per unit distance traveled by the particle, since this is what can be directly measured by a Cherenkov counter:

$$-\frac{dE}{dz} = \int d\omega\omega\frac{e^2}{c^2}\left(1-\frac{c^2}{n^2(\omega)v^2}\right). \tag{2.2.111}$$

In (2.2.110) and (2.2.111) it is understood that the ω integration extends only over the range where $n(\omega) > c/v$. Finally, note that detection is a quantum process, involving photons. The energy of a photon of frequency $\nu = \omega/2\pi$ is $h\nu = \hbar\omega$, where $h = 2\pi\hbar$ is Planck's constant (Schwinger et al., 2018).

2.3 Quantum Theory of Cherenkov Radiation

2.3.1 The Approach of Source Theory

In this section, we will introduce the approach of source theory in the calculation of the power spectrum of Cherenkov radiation. This theoretical approach uses quantum mechanical language, which is a very compact formula developed by Schwinger et al. (1976).

1) Propagator of Photon in a Medium

A key concept in the theory of radiation is the propagator of photon, $D_+^{\mu v}(x-x')$, which describes how photons travel in a given medium. In this section, will present a simple method to compute $D_+^{\mu v}$ for a medium that has both polarization and permeability properties. Our starting point is the set of Maxwell equations in the rationalized cgs system, which govern the electromagnetic fields in such a medium (Schwinger et al. 1976)

$$\begin{aligned} \nabla \cdot \mathbf{D} = \rho, \quad \nabla \times \mathbf{H} = \tfrac{1}{c}\mathbf{J} + \tfrac{1}{c}\tfrac{\partial \mathbf{D}}{\partial t}, \\ \nabla \cdot \mathbf{B} = 0, \quad \nabla \times \mathbf{E} = -\tfrac{1}{c}\tfrac{\partial \mathbf{B}}{\partial t}, \end{aligned} \tag{2.3.1}$$

for an isotropic medium

$$\mathbf{D} = \epsilon \mathbf{E}, \quad \mathbf{B} = \mu \mathbf{H}, \quad n^2 = \epsilon\mu. \tag{2.3.2}$$

Equation (2.3.1b) means that could express the potentials $\mathbf{A}$ and φ as

$$\mathbf{B} = \nabla \times \mathbf{A}, \quad \mathbf{E} = -\frac{1}{c}\frac{\partial \mathbf{A}}{\partial t} - \nabla\varphi; \tag{2.3.3}$$

or in covariant form

$$F^{\mu v} = \partial^\mu A^v - \partial^v A^\mu \tag{2.3.4}$$

with

$$F^{0i} = E^i, \quad F^{ij} = \epsilon^{ijk} B_k, \quad A^\mu = (\varphi, \mathbf{A}). \tag{2.3.5}$$

In terms of potentials, equation (2.3.1a) may be rewritten in the form

$$\begin{aligned} \nabla^2\varphi - \frac{\mu\epsilon}{c^2}\frac{\partial^2\varphi}{\partial t^2} = -\frac{1}{\epsilon}\rho, \\ \nabla^2\mathbf{A} - \frac{\mu\epsilon}{c^2}\frac{\partial^2\mathbf{A}}{\partial t^2} = -\frac{\mu}{c}\mathbf{J}. \end{aligned} \tag{2.3.6}$$

In the Lorentz gauge

$$\partial_\mu A^\mu = (\mu\epsilon - 1)(\eta\partial)(\eta A) = 0, \tag{2.3.7}$$

where $\eta^\mu = (1, 0)$ is the unit timelike vector in the rest frame of the medium.

By utilizing the four vectors

$$J^\mu = (c\rho, \mathbf{J}), \quad \chi^\mu = (ct, \mathbf{r}), \quad k^\mu = (k^\circ, \mathbf{k}); \tag{2.3.8}$$

and the momentum representation

$$\begin{aligned} A^\mu(x) &= \int \frac{(dk)}{(2\pi)^4} e^{ikx} A^\mu(k), \\ J^\mu(x) &= \int \frac{(dk)}{(2\pi)^4} e^{ikx} J^\mu(k), \end{aligned} \tag{2.3.9}$$

then can combine equation (2.3.6) in the covariant form (letting $n^2 = \epsilon\mu$)

$$\left(\mathbf{k}^2 - n^2 (k^\circ)^2\right) A^\mu(k) = \frac{\mu}{c}\left(g^{\mu v} + \frac{n^2 - 1}{n^2}\eta^\mu\eta^v\right) J_v(k). \tag{2.3.10}$$

In virtue of the definition of $D_+^{\mu v}(k)$[Eq.(2.3.19)] this implies

$$D_+^{\mu v}(k) = \frac{\mu}{c}\left(g^{\mu v} + \frac{n^2 - 1}{n^2}\eta^\mu\eta^v\right)\frac{1}{|\mathbf{k}|^2 - n^2 (k^\circ)^2}. \tag{2.3.11}$$

In coordinate space, will get (Schwinger et al. 1976)

$$D_+^{\mu v}(x - x') = \frac{\mu}{c}\left(g^{\mu v} + \frac{n^2 - 1}{n^2}\eta^\mu\eta^\nu\right) D(x - x'), \tag{2.3.12}$$

where

$$\begin{aligned} D(x - x') &= \int \frac{(dk)}{(2\pi)^4} e^{ik(x - x')} \frac{1}{|\mathbf{k}|^2 - n^2 (k^\circ)^2 - i\epsilon} \\ &= \frac{i}{c}\frac{1}{4\pi^2}\int_0^\infty d\omega \frac{\sin(n\omega/c\,|\mathbf{r} - \mathbf{r}'|)}{|\mathbf{r} - \mathbf{r}'|} e^{-im|t - t'|}. \end{aligned} \tag{2.3.13}$$

by the standard contour integral method.

2) The Power Spectrum of Cherenkov Radiation

The expression for the vacuum persistence amplitude (Schwinger et al. 1976)

$$\langle 0_+ \mid 0_- \rangle^J = \exp\left\{\frac{i}{\hbar} W\right\} \tag{2.3.14}$$

where

$$W = \frac{1}{2c^2}\int (dx)\,(dx')\,J^{\mu}(x)D_{+\mu\nu}\,(x-x')\,J^{\nu}\,(x') \tag{2.3.15}$$

$J^{\mu} = (c\rho, \mathbf{J})$ is the source current, and $D_{+\mu\nu}$ denotes the propagator of photon. The vacuum persistence probability can identify the decay rate $\gamma(t)$ (Schwinger et al. 1976)

$$\left|\langle 0_+ \mid 0_-\rangle^{J}\right|^2 = \exp\left\{-\frac{2}{\hbar}\operatorname{Im} W\right\} = \exp\left\{-\int dt\gamma(t)\right\} \tag{2.3.16}$$

to be

$$\int \gamma(t)dt = \frac{2}{\hbar}\operatorname{Im} W \tag{2.3.17}$$

and this is linked to the power spectrum $P(\omega, t)$ by

$$\gamma(t) = \int d\omega \frac{P(\omega,t)}{\hbar\omega} \tag{2.3.18}$$

All of the major results be able to derived from these fundamental relations.

The behavior of radiation in a medium that surrounds it is the topic of this paper. The assumption that the medium has uniform and isotropic properties, and that its interaction with the electromagnetic field is characterized by a dielectric permittivity $\epsilon(\omega, H)$ and a magnetic permeability $\mu(\omega, H)$ that may vary with the frequency and the (multivalued) magnetic field. The refractive index is defined as usual by $n(\omega, H) = (\epsilon\mu)^{1/2}$, and assume that this is a real number. By neglect absorption, anisotropy, spatial dispersion, and other effects, since they can be accounted for in extensions of the theory that are analogous to the generalizations of ordinary Cherenkov radiation. The information about the medium may be integrated in (2.3.15) via the propagator of photon, which can be obtained from Maxwell equations using the relation in the medium's frame of reference.

$$A^{\mu}(x) = \int (dx')\,D_{+}^{\mu v}\,(x-x')\,J_{v}\,(x') \tag{2.3.19}$$

The essential result is that [compare (2.3.12)]

$$D_{+}^{\mu v}\,(x-x') = (\mu/c)\left(g^{\mu v} + \left[1-n^{-2}\right]\eta^{\mu}\eta^{v}\right) D\,(x-x') \tag{2.3.20}$$

where $\eta^{\mu} = (1, \mathbf{0})$ is the unit timelike vector, and

$$D(x - x') = \frac{i}{4\pi^2 c} \int_0^{\infty} d\omega \frac{\sin\left((n\omega/c)\left|\mathbf{r} - \mathbf{r}'\right|\right)}{\left|\mathbf{r} - \mathbf{r}'\right|} \exp\left\{-i\omega\left|t - t'\right|\right\} \tag{2.3.21}$$

By inserting (2.3.20,21) into (2.3.15) and separating the imaginary part, will get

$$\begin{aligned} \operatorname{Im} W = &- \frac{1}{8\pi^2} \int d\omega dt dt' d\mathbf{r} d\mathbf{r}' \frac{\mu \sin\left((n\omega/c)\left|\mathbf{r} - \mathbf{r}'\right|\right)}{n^2\left|\mathbf{r} - \mathbf{r}'\right|} \cos\left[\omega\left(t - t'\right)\right] \\ &\times \left\{\rho(\mathbf{r}, t)\rho\left(\mathbf{r}', t'\right) - \frac{n^2}{c^2}\mathbf{J}(\mathbf{r}, t) \cdot \mathbf{J}\left(\mathbf{r}', t'\right)\right\} \end{aligned} \tag{2.3.22}$$

The power spectrum could then be identified from the equation (2.3.17) and (2.3.18)

$$\begin{aligned} P(\omega, t) = &- \frac{\omega}{4\pi^2}\frac{\mu}{n^2} \int d\mathbf{r} d\mathbf{r}' dt' \frac{\sin\left((n\omega/c)\left|\mathbf{r} - \mathbf{r}'\right|\right)}{\left|\mathbf{r} - \mathbf{r}'\right|} \cos\left[\omega\left(t - t'\right)\right] \\ &\times \left\{\rho(\mathbf{r}, t)\rho\left(\mathbf{r}', t'\right) - \frac{n^2}{c^2}\mathbf{J}(\mathbf{r}, t) \cdot \mathbf{J}'\left(\mathbf{r}', t'\right)\right\} \end{aligned} \tag{2.3.23}$$

These methods can be applied to derive the other relevant quantities.

Here, will show how simply Cherenkov radiation can be derived from equation (2.3.23). By consider a charged particle e, which moves with a constant speed represented by $\mathbf{v}$, the source functions to be

$$\rho = e\delta(\mathbf{r} - \mathbf{v}t), \quad \mathbf{J} = e\mathbf{v}\delta(\mathbf{r} - \mathbf{v}t) \tag{2.3.24}$$

By inserting (2.3.24) in (2.3.23) and taking some fundamental reduction, will get (letting $\tau = t' - t, \beta = v/c$) (Schwinger et al. 1976)

$$\begin{aligned} P(\omega, t) &= \frac{e^2}{4\pi^2}\frac{\mu\omega v}{c^2}\left(1 - \frac{1}{n^2\beta^2}\right) \int_{-\infty}^{\infty} \frac{d\tau}{\tau} \sin(n\beta\omega\tau)\cos\omega\tau \\ &= \begin{cases} 0, & n\beta < 1, \\ \frac{e^2}{4\pi}\frac{\mu\omega}{c^2} v\left(1 - \frac{1}{n^2\beta^2}\right), & n\beta > 1. \end{cases} \end{aligned} \tag{2.3.25}$$

This is the power spectrum of Cherenkov radiation, which has the threshold $n\beta > 1$ for the radiation to occur.

2.3.2 The Approach of Field Theory

The investigation of the phenomenon of Cherenkov radiation through the concepts of quantum field theory. In the process of calculation, the power spectrum and the minimum velocity threshold of Cherenkov radiation in the dielectric medium. We have applied the ideas and methods of Edouard B. Manoukian, in the article titled "Vacuum-to-vacuum transition probability and radiation in a medium". The calculation process consists of 3 steps as follows: 1. Calculation of the average number of photons 2. Calculation of the current distribution and the photon propagator and 3. Substitute the value in the average number of photons. Each step is shown as follows:

1. Calculation of the average number of photons

In the first step, we utilize the Poisson distribution and transition probability to obtain the average number of photons. The Poisson distribution is applied to provide an equation for the relation between the average number of photons and the vacuum-to-vacuum transition probability. Schwinger and Manoukian employ the Poisson distribution to describe the probability distribution of the photon number N generated by the current (Schwinger 1970; Manoukian, 2012), that is

$$\text{Prob}(N=n)=\frac{(\lambda)^n}{n!}\mathrm{e}^{-\lambda}, \quad n=0,1,2,... \tag{2.3.26}$$

where $\lambda=\langle N\rangle$ represents the average number of photons generated by the current source and and from equation (2.3.26), we could get the equation for the relation between the average number of photons and the vacuum-to-vacuum transition probability as follows (Manoukian, 2015)

$$\exp[-\langle N\rangle]=|\langle 0_+\mid 0_-\rangle|^2, \tag{2.3.27}$$

The vacuum-to-vacuum transition amplitude given by Manoukian (2015)

$$\langle 0_+\mid 0_-\rangle=\exp\left[\frac{\mathrm{i}}{2\hbar c^3}\int(\mathrm{d}\underline{x})\,(\mathrm{d}\underline{x}')\,\underline{J}_\mu(x)D_+^{\mu\nu}\,(\underline{x}'\underline{x}')\,\underline{J}_\nu\,(x')\right], \tag{2.3.28}$$

where $D^{\mu\nu}\,(x,x')$ is the propagator of photon.

To calculate the average number of photons, will express the vacuum-to-vacuum

transition probability as function integrals (Manoukian, 2015)

$$|\langle 0_+ \mid 0_- \rangle|^2 = \exp\left[-\frac{1}{\hbar c^3}\int (\mathrm{d}\underline{x})\,(\mathrm{d}\underline{x}')\,\underline{J}_\mu(x)\,(\mathrm{Im}\,D_+^{\mu\nu}(\underline{x},\underline{x}'))\,\underline{J}_\nu(x')\right], \quad (2.3.29)$$

where $(\mathrm{d}x) \equiv \mathrm{d}x^0\,\mathrm{d}x^1\,\mathrm{d}x^2\,\mathrm{d}x^3$, From the average number of photons in equation (2.3.27) and the vacuum-to-vacuum transition probability in equation (2.3.29) could derive the average number of photons emitted by the arbitrary current distribution to be

$$\langle N\rangle = \frac{1}{\hbar c^3}\int (\mathrm{d}\underline{x})\,(\mathrm{d}\underline{x}')\,\underline{J}_\mu(x)\,(\mathrm{Im}\,D_+^{\mu\nu}(\underline{x},\underline{x}'))\,\underline{J}_\nu(x')\,. \quad (2.3.30)$$

In the case of the dielectric medium permittivity ε and permeability $\mu = 1$, may rewrite the equation (2.3.30) according to Manoukian (2015) as follows

$$\langle N\rangle = \frac{1}{\varepsilon\hbar c^3}\int (\mathrm{d}\underline{x})\,(\mathrm{d}\underline{x}')\,\underline{J}_\mu(x)\,(\mathrm{Im}\,D_+^{\mu\nu}(\underline{x},\underline{x}'))\,\underline{J}_\nu(x')\,. \quad (2.3.31)$$

The above equation will be applied further to calculate the average number of photons in the dielectric medium.

2. Calculation of the current distribution and the photon propagator

This step involves calculating the current distribution and the photon propagator in the dielectric medium to substitute values and calculate the average number of photons.

The current distribution from electrons e moving in the medium with velocity v along the x^1-axis can be calculated as follows

$$J^i(x) = ev\delta^{i1}\delta\left(x^2\right)\delta\left(x^3\right)\delta\left(x^1 - \frac{v}{c}x^0\right), \quad (2.3.32)$$

$$J^0(x) = \mathrm{e}c\,\delta\left(x^2\right)\delta\left(x^3\right)\delta\left(x^1 - \frac{v}{c}x^0\right). \quad (2.3.33)$$

For calculating the Photon propagator, can find from the Lifshitz and Pitaevskii (1984) ($v = 0, 1, 2, 3$, and $i, j = 1, 2, 3$) that is

$$\left[-\partial_\nu\partial^\nu\delta^{ij} + \partial^i\partial^j\right] D_+^{jk}(x, x') = \delta^{ik}\delta^{(4)}(x, x')\,. \quad (2.3.34)$$

From equation (2.3.34), will can calculate the relevant component of the photon propagator in a dielectric medium moving along the x^1-axis and can be expressed

according to Manoukian (2015) as follows

$$D_{+}^{11}(\underline{x},\underline{x}') = \int \frac{(\mathrm{d}Q)}{(2\pi)^4} \frac{\mathrm{e}^{\mathrm{i}\mathbf{Q}\cdot(\mathbf{x}-\mathbf{x}')}\mathrm{e}^{-\mathrm{i}Q^0\left(x^0-x'^0\right)/\sqrt{\varepsilon}}}{\left[\mathbf{Q}^2 - Q^{0^2} - \mathrm{i}\delta\right]}, \quad \delta \to 0. \tag{2.3.35}$$

3. Substitute the value in the average number of photons

The last step involves substituting the current distribution and the photon propagator into the average number of photons in equation (2.3.31) will get for $\langle N \rangle$ as in the following equation (Manoukian, 2015)

$$\begin{aligned}\langle N \rangle =& \frac{1}{\varepsilon^{1/2}\hbar \mathrm{c}^3} \int (\mathrm{d}x)\,(\mathrm{d}x') \left(\mathbf{J}(x)\cdot\mathbf{J}\,(x') - \frac{1}{\mu\varepsilon} J^0(x) J^0\,(x')\right) \\ &\times \int \frac{\mathrm{d}^3\mathbf{Q}}{(2\pi)^3 2|\mathbf{Q}|} \mathrm{e}^{\mathrm{i}\mathbf{Q}\cdot(\mathbf{x}-\mathbf{x}')}\mathrm{e}^{-\mathrm{i}|\mathbf{Q}|\left(x^0-x'^0\right)/\sqrt{\varepsilon}},\end{aligned} \tag{2.3.36}$$

Additionally, to be able to determine the photon number density, use the principle of symmetry under the interchange $(x - x') \leftrightarrow (x' - x)$ and insertion of the identity

$$1 = \int_0^\infty \mathrm{d}\omega \delta\left(\omega - \frac{|\mathbf{Q}|\mathrm{c}}{\sqrt{\varepsilon}}\right) \tag{2.3.37}$$

Then substitute the identity in equation (2.3.37) into the integrand equation of the average number of photons (2.3.36), and could obtain $\langle N \rangle = \int_0^\infty \mathrm{d}\omega N(\omega)$, with $\mathbf{Q} = |\mathbf{Q}|\mathbf{n}, |\mathbf{Q}| = \left((Q^1)^2 + \left|\mathbf{Q}_{\|}\right|^2\right)^{1/2}$. After substituting the current distribution equation (2.3.32) and (2.3.33) into equation (2.3.36) will obtained the photon number density to be (Manoukian, 2015)

$$\begin{aligned}N(\omega) =& \frac{e^2 v^2}{\varepsilon\hbar c^2}\left(1 - \frac{c^2}{\varepsilon v^2}\right) \int dx^0\, \mathrm{d}x'^0 \frac{\mathrm{d}Q^1\left(\pi \mathrm{d}\left|\mathbf{Q}_{\|}\right|^2\right)}{16\pi^3\omega} \\ &\times \delta\left(\omega - \frac{|\mathbf{Q}|\mathrm{c}}{\sqrt{\varepsilon}}\right) \exp\left[\mathrm{i}\left(\frac{Q^1 v}{c} - \frac{\omega}{c}\right)\left(x^0 - x'^0\right)\right]\end{aligned} \tag{2.3.38}$$

In order to get the power spectrum, first calculate the energy by $E = \hbar\omega N(\omega)$. After that, execute the integrals over $Q^1, \left|\mathbf{Q}_{\|}\right|^2, \tau$, following Manoukian (2015) then can obtain the power spectrum in the dielectric medium as follows

$$P(\omega) = \frac{e^2}{4\pi}\frac{\omega v}{c^2}\left(1 - \frac{c^2}{\varepsilon v^2}\right) \tag{2.3.39}$$

the power spectrum in the dielectric medium occurred only for $v > c/\sqrt{\varepsilon}$.

To calculate the minimum velocity threshold of CR in the dielectric medium, we consider the power spectrum must be greater than 0 as follows:

$$P(\omega) > 0 \tag{2.3.40}$$

Therefore, imply that

$$\left(1 - \frac{c^2}{\varepsilon v^2}\right) > 0 \tag{2.3.41}$$

Then we obtained the minimum threshold velocity is

$$v_{th} > \frac{c}{\sqrt{\varepsilon}} \tag{2.3.42}$$

Numerical calculations

Numerical calculations are methods that rely on numerical values to model mathematical procedures, that reflect real-world circumstances (Hamming, 2012). This capability permits an improved comprehension of the Cherenkov phenomena. For the numerical computations, the result of the quantum field theory takes into account a charged electron traversing through water. In order to visualize data and functions in both 2D and 3D, we utilize Wolfram Mathematica for numerical calculations and plotting functions, resulting in Figures 3 and 4.

1) The Minimum Velocity Threshold

Considering the value of the dielectric permittivity of water $\varepsilon \approx 1.8$. The computation of the minimum velocity threshold for generating Cherenkov radiation $v > c/\sqrt{\varepsilon}$ leads to the determination that the minimum threshold velocity of a moving charged electron in water is $v_{th} > 0.74c$. Thus, it can be inferred that the minimum velocity threshold required for generating Cherenkov radiation in water must be at least approximately 0.75c, where c represents the speed of light.

The depiction of the power spectrum can be observed in Figures 3 and 4, which showcase the correlation of the power spectrum at discrete velocities of three distinct values in a two dimensional graph and the correlation of the power spectrum at continuous velocities from zero to the speed of light in a three dimensional graph respectively. In Figure 3, the correlation of the power spectrum

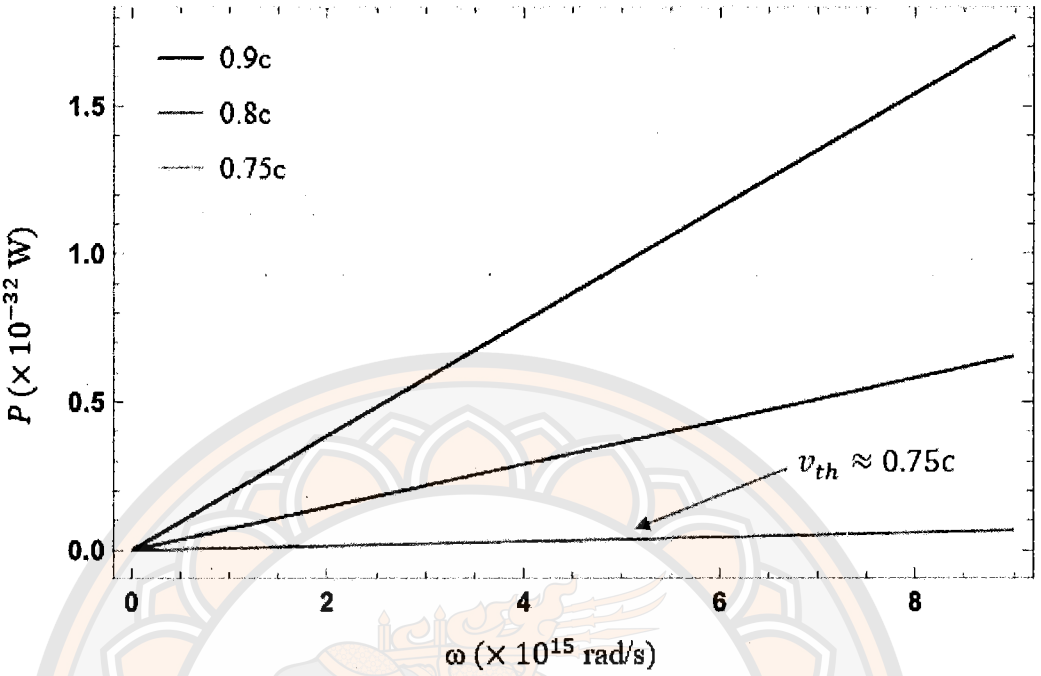

Figure 3 The correlation 2D of the power spectrum of a moving electron in water P with angular frequency ω at velocities of $v = 0.75c$, $v = 0.8c$, and $v = 0.9c$.

P with angular frequency ω for visible light in the range of 10^{15} rad/s at various velocities of v=0.75c, v=0.8c, and v=0.9c is illustrated in two dimensions, thereby signifying that the threshold velocity for Cherenkov radiation generation in water is approximately 0.75c. This leads to the surpassing of the power spectrum beyond 0. It is notable that the aforementioned figure elucidates that the power spectrum is directly proportional to the angular frequency and velocity. Whereas Figure 4 portrays the correlation in three dimensions of the power spectrum P with angular frequency ω at velocities ranging from $v = 2 \times 10^8$ to 3×10^8 m/s. In this regard, it can be inferred that the power spectrum remains below 0 at velocities less than 0.75c. This result highlights the significance of velocity in influencing the power spectrum of Cherenkov radiation. These figures provide an understanding of the power spectrum of Cherenkov radiation at various velocities and angular frequencies.

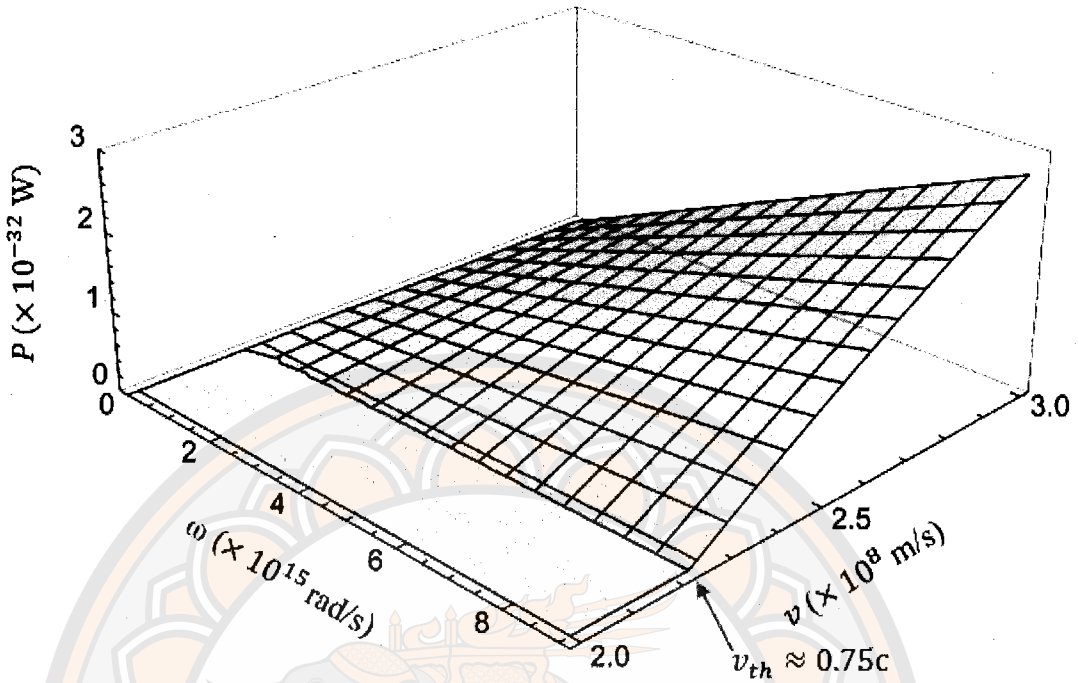

Figure 4 The correlation 3D of the power spectrum of a moving electron in water P with angular frequency ω at velocities $v = 2 \times 10^8$ to 3×10^8 m/s.

2) The Power Spectrum Comparison

order to verify the result of the power spectrum at a minimum velocity threshold as predicted by both quantum field theory and electrodynamics theory. Figures 5 presented the comparison of the correlation in two dimensions of the power spectrum P at a range angular frequency of ω rad/s. Upon analyzing the graph illustrated in Figure 5 it has been found that the power spectrum P, as derived by both electrodynamic theory and quantum field theory, demonstrates values that are either similar or comparable when the range of angular frequency ω is lower than 1×10^{15} rad/s. It is shown that the power spectrum of both theories has similar results at low angular frequencies. Conversely, the results reveal that

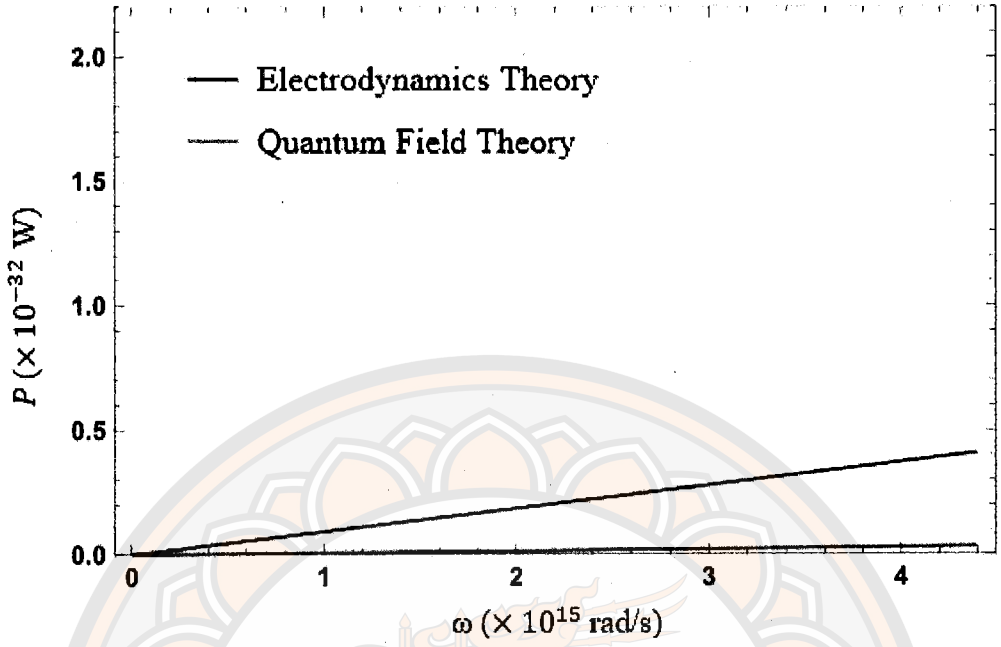

Figure 5 The power spectrum of an electron in water at a minimum velocity threshold P at range angular frequency ω.

the power spectrum P exhibits significant divergence in value when the range of angular frequency ω is higher than 1×10^{15} rad/s. Remarkable that the power spectrum of both theories began to have significantly different results at higher angular frequencies.

CHAPTER III

CHERENKOV RADIATION OF MASSIVE PHOTONS AT FINITE TEMPERATURE

In studying the phenomenon of Cherenkov radiation that occurs from a charged electron moving through a dielectric medium Figure 6, we will utilize the concepts of quantum theory by applying source theory to calculate the power spectrum of massive photons at a finite temperature from a charged electron moving through a dielectric medium. This chapter includes three sections. Section 3.1 Propagator of Massive Photons at Finite Temperature, we will present an approach to calculating the propagator of massive photons at finite temperatures in a dielectric medium. Section 3.2 Power Spectrum of Massive Photons at Finite Temperature, we will show steps to calculate the power spectrum of massive photons at finite temperatures in the medium. In section 3.3 Numerical Calculation of the Power Spectrum at Finite Temperature, we will numerically calculate the results of the power spectrum obtained and display the results as a graph.

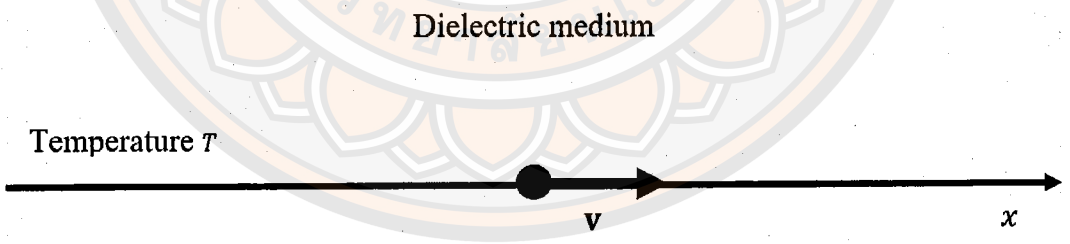

Figure 6 A charge electron e moves through a dielectric medium with velocity v at finite temperatures T.

3.1 Propagator of Massive Photons at Finite Temperature

In the calculation of the propagator of massive photons at finite temperatures in the medium. We have applied the methods following the paper of Pardy (1989, 2002), which have been studied within the framework of the source theory. In order to obtain the propagator, we begin by considering the massive spin 0 field then the massive spin 1 field, and finally the massive photon in electrodynamics.

3.1.1 The Massive Spin 0 Fields

To illustrate the fundamentals of source theory, start with the massive spin 0 field, which is the simplest example (Schwinger, 1970). According to source theory, the action of spin 0 particles is composed of the scalar source $K(x)$ and the propagator Δ_+. Here, the action is

$$W(K) = \frac{1}{2}\int (dx)\,(dx')\,K(x)\Delta_+\,(x-x')\,K\,(x') \tag{3.1.1}$$

where provides the correct condition for probability $|\langle 0_+ \mid 0_-\rangle|^2 \leq 1$ (Schwinger, 1970; Schwinger et al., 1976), and ($\hbar = 1$)

$$\langle 0_+ \mid 0_-\rangle^K = e^{iW(K)} \tag{3.1.2}$$

is the fundamental formula of Schwinger's source theory is represented by the term, where the expression $\langle 0_+ \mid 0_-\rangle$ denotes the amplitude from one vacuum state to another. This core concept is pivotal in understanding the intricacies of quantum theory and the behavior of particles at quantum levels.

To demonstrate that the quantity $\langle 0_+ \mid 0_-\rangle$ truly represents the amplitude from vacuum to vacuum, it's essential to know the explicit form of Green's function $\Delta_+\,(x-x')$, which satisfies the given equation (Pardy, 2002)

$$\left(-\partial^2 + m^2\right)\Delta_+\,(x-x') = \delta\,(x-x') \tag{3.1.3}$$

From the last equation, it indicates that

$$\Delta_+\,(x-x') = \frac{1}{(-\partial^2+m^2)}\int \frac{(dp)}{(2\pi)^4} e^{ip(x-x')}. \tag{3.1.4}$$

The formula (3.1.4) is not unambiguous and it is necessary to specify it by the ε-term, or

$$\Delta_+(x-x') = \int \frac{(dp)}{(2\pi)^4} \frac{e^{ip(x-x')}}{p^2+m^2-i\varepsilon}; \quad \varepsilon \to 0_+. \tag{3.1.5}$$

Next, will show that $|\langle 0_+ \mid 0_- \rangle|^2$ is the probability of the persistence of vacuum. According to the definition (Pardy, 2002)

$$\langle 0_+ \mid 0_- \rangle = \exp\left\{ \frac{i}{2} \int (dx)\,(dx')\, K(x) \Delta_+(x-x')\, K(x') \right\} \tag{3.1.6}$$

will get (Pardy, 2002)

$$\begin{aligned} \langle 0_+ \mid 0_- \rangle &= \exp\left\{ \frac{i}{2} \int (dx)\,(dx') \int \frac{(dp)}{(2\pi)^4} K(x) \frac{e^{ip(x-x')}}{p^2+m^2-i\varepsilon} K(x') \right\} \\ &= \exp\left\{ \frac{i}{2} \int \frac{(dp)}{(2\pi)^4} \frac{K(p)K(-p)}{p^2+m^2-i\varepsilon} \right\} \\ &= \exp\left\{ \frac{i}{2} \int \frac{(dp)}{(2\pi)^4} \frac{|K(p)|^2}{p^2+m^2-i\varepsilon} \right\} \end{aligned} \tag{3.1.7}$$

a result of Equation (3.1.5) and $K^*(p) = K(-p)$. Using the well-known theorem

$$\frac{1}{x-i\varepsilon} = P\left(\frac{1}{x}\right) + i\pi\delta(x); \quad \varepsilon \to 0 \tag{3.1.8}$$

where P represents the principal value of integral, will obtain the follows formula for the vacuum persistence (Pardy, 2002):

$$|\langle 0_+ \mid 0_- \rangle|^2 = e^{-2\,\mathrm{Im}\,W} = \exp\left\{ -2 \int \frac{(dp)}{(2\pi)^4} \pi |K(p)|^2 \delta\left(p^2+m^2\right) \right\} \tag{3.1.9}$$

By using

$$\begin{aligned} \delta\left(p^2+m^2\right) =& \frac{1}{2\left(\mathbf{p}^2+m^2\right)^{1/2}} \left\{ \delta\left(p^0 - \left(\mathbf{p}^2+m^2\right)^{1/2}\right) \right. \\ & \left. + \delta\left(p^0 + \left(\mathbf{p}^2+m^2\right)^{1/2}\right) \right\}, \end{aligned} \tag{3.1.10}$$

will obtain (Pardy, 2002)

$$2 \int \frac{(dp)}{(2\pi)^4} \pi |K(p)|^2 \delta\left(p^2+m^2\right) = \int \frac{(d\mathbf{p})}{(2\pi)^3} \frac{1}{2p^0} \left| K\left(p^0, \mathbf{p}\right) \right|^2 \tag{3.1.11}$$

and then,

$$|\langle 0_+ \mid 0_- \rangle|^2 = \exp\left\{ -\int d\omega_p |K(p)|^2 \right\} \tag{3.1.12}$$

where

$$d\omega_p = \frac{(d\mathbf{p})}{(2\pi)^3}\frac{1}{2p^0} \quad p^0 = +\left(\mathbf{p}^2 + m^2\right)^{1/2} \tag{3.1.13}$$

Equation (3.1.12) indicates that when the scalar source $K(x)$ is present, the probability of the vacuum state persisting is ≤ 1.

Next, will demonstrate the derivation of the field equation from the action W for the scalar field φ, (Pardy, 2002) where

$$\begin{aligned} W &= \frac{1}{2}\int K\Delta_+ K = \frac{1}{2}\int \varphi K = \frac{1}{2}\int \varphi\left(-\partial^2 + m^2\right)\varphi \\ &= \frac{1}{2}\int \left(\partial_\mu\varphi\partial^\mu\varphi + m^2\varphi^2\right) = 2W - W \\ &= \int \varphi K - \frac{1}{2}\left[(\partial\varphi)^2 + m^2\varphi^2\right] = \int (dx)[K(x)\varphi(x) + \mathcal{L}(\varphi(x))] \end{aligned} \tag{3.1.14}$$

with

$$\mathcal{L}(\varphi(x)) = -\frac{1}{2}\left[\partial_\mu\varphi\partial^\mu\varphi + m^2\varphi^2\right]. \tag{3.1.15}$$

By putting

$$\delta_\varphi W = 0, \tag{3.1.16}$$

or

$$\int \delta\varphi K - \left[\partial_\mu\varphi\partial^\mu\delta\varphi + m^2\varphi\delta\varphi\right] = 0. \tag{3.1.17}$$

After some modification will obtain (Pardy, 2002)

$$\int (dx)\left[K - \left(-\partial_\mu\partial^\mu\varphi + m^2\varphi\right)\right]\delta\varphi = 0 \tag{3.1.18}$$

As variable φ is an arbitrary one the last integral is 0 only if

$$\left(-\partial^2 + m^2\right)\varphi(x) = K(x), \tag{3.1.19}$$

where is the Klein-Gordon equation with source $K(x)$ on the right side of equation. Next, we will present the Proca equation for massive particles with spin 1 and generate the Maxwell equations for massive photons.

3.1.2 The Massive Spin 1 Fields

We present the natural construction of the field of the particles with spin 1. The derivation of the action for this massive spin 1 field is based on the modification of the derivation of spin 0 fields (Pardy, 2002). The relation

$$|\langle 0_+ \mid 0_- \rangle|^2 = \exp\{-2 \operatorname{Im} W\} \leq 1 \tag{3.1.20}$$

is postulated to be valid for all spin fields. Here, will show the construction of action and field equations concerning spin 1.

Scalar sources characterize spin 0 particles and fields, whereas a vector source, represented as $J^{\mu}(x)$, may serve as a potential descriptor for spin 1 particles and fields. Yet, a challenge arises due to the vector source $J^{\mu}(x)$ comprising four components, while spin 1 particles are limited to three distinct spin states. Despite this, it is worthwhile to explore, drawing parallels to spin 0 fields, a specific action form for unit spin fields:

$$W(J) = \frac{1}{2} \int (dx)\,(dx')\, J^{\mu}(x) \Delta_+ (x - x')\, J_{\mu}(x') \tag{3.1.21}$$

Then,

$$|\langle 0_+ \mid 0_- \rangle|^2 = e^{iW} e^{-iW^*} = \exp\left\{ - \int d\omega_p J^{*\mu}(p) J_{\mu}(p) \right\}. \tag{3.1.22}$$

However,

$$J^{*\mu}(p) J_{\mu}(p) = |\mathbf{J}(p)|^2 - \left|J^0(p)\right|^2 \leq 0 \text{ or } > 0 \tag{3.1.23}$$

and this implies that the value specified in Equation (3.1.21) should not be interpreted as the likelihood of vacuum stability.

To address the issue, one can substitute the initial expression $J^{*\mu}(x) J_{\mu}(x)$ with an alternative invariant form (Pardy, 2002):

$$J^{*\mu}(p) \left[g_{\mu\nu} + \frac{1}{m^2} p_{\mu} p_{v} \right] J^{v}(p) \tag{3.1.24}$$

which can be identified, considering its consistency, within the reference frame of the time-oriented vector p^{μ}, where $p^{\mu} = (m, 0, 0, 0)$ in the rest frame. By $g_{\alpha\alpha} =$

$(-1,1,1,1)$ and $g_{\mu\nu}=0$ for $\mu \neq v$, with

$$\bar{g}_{\mu\nu} = g_{\mu\nu} + \frac{1}{m^2} p_\mu p_v = \begin{cases} \delta_{kl}; & \mu = k; v = l \\ 0; & \mu = 0; v = 0 \\ 0; & \mu = k; v = 0 \end{cases} \tag{3.1.25}$$

and

$$J^{*\mu}(p)\bar{g}_{\mu\nu}J^{\nu}(p) \equiv |\mathbf{J}|^2 \tag{3.1.26}$$

now the quantity $|\langle 0_+ \mid 0_- \rangle|^2$ can interpreted as the vacuum persistence probability.

Subsequently, upon applying Equation (3.1.24), one can straightforwardly obtain the function $W(J)$ within the space-time framework through the application of a Fourier transform (Pardy, 2002):

$$\begin{aligned} W(J) =& \frac{1}{2}\int (dx)\,(dx')\,\{J_\mu(x)\Delta_+(x-x')\,J^\mu(x') \\ &+ \frac{1}{m^2}\partial_\mu J^\mu(x)\Delta_+(x-x')\,\partial'_v J^v(x')\Big\} \end{aligned} \tag{3.1.27}$$

The field associated with particles of spin 1 can be established through the definition of a test source, denoted as $\delta J^\mu(x)$, by employing a specific relational expression

$$\delta W(J) = \int (dx)\delta J^\mu(x)\varphi_\mu(x) \tag{3.1.28}$$

where φ_μ is the field consists of particles that possess a spin of 1. By varying formula (3.1.27) and equating it with equation (3.1.28), will get the equation for the spin 1 field as follows (Pardy, 2002):

$$\varphi_\mu(x) = \int (dx')\,\Delta_+(x-x')\,J_\mu(x') - \frac{1}{m^2}\partial_\mu \int (dx')\,\Delta_+(x-x')\,\partial'_v J^v(x')\,. \tag{3.1.29}$$

The divergence of the vector field $\varphi_\mu(x)$ is given by the relation

$$\begin{aligned} \partial_\mu\varphi^\mu(x) &= \int (dx')\,\Delta_+(x-x')\,\partial'_\mu J^\mu(x') - \frac{1}{m^2}\partial^2 \int (dx')\,\Delta_+(x-x')\,\partial'_v J^\nu(x') \\ &= \frac{1}{m^2}\partial_\mu J^\mu(x) \end{aligned} \tag{3.1.30}$$

as a consequence of Eq. (3.1.3) or

$$-\partial^2\Delta_+ = \delta(x-x') - m^2\Delta_+. \tag{3.1.31}$$

Further, after applying operator $(-\partial^2 + m^2\ )$ on Eq. (3.1.29) get the equations follows (Pardy, 2002):

$$\left(-\partial^2 + m^2\right)\varphi_\mu(x) = J_\mu(x) - \frac{1}{m^2}\partial_\mu\partial_\nu J^v(x) \tag{3.1.32}$$

$$\left(-\partial^2 + m^2\right)\varphi_\mu(x) + \partial_\mu\partial_\nu\varphi^\nu(x) = J_\mu(x) \tag{3.1.33}$$

as a consequence of Eq. (3.1.30).

The final equation can be readily reformulated as follows:

$$\partial^\nu G_{\mu\nu} + m^2\varphi_\mu = J_\mu, \tag{3.1.34}$$

where

$$G_{\mu\nu}(x) = -G_{\nu\mu}(x) = \partial_\mu\varphi_\nu - \partial_\nu\varphi_\mu. \tag{3.1.35}$$

By equating the tensor $G_{\mu\nu}$ to the electromagnetic field tensor $F_{\mu\nu}$, will get an alternative to equations (3.1.33) and (3.1.34), known as the Proca equation. This equation describes the electromagnetic field in the context of a photon that possesses mass or massive photon (Pardy, 2002):

$$\left(-\partial^2 + m^2\right)A_\mu(x) + \partial_\mu\partial_\nu A^\nu(x) = J_\mu(x), \tag{3.1.36}$$

$$\partial^\nu F_{\mu\nu} + m^2 A_\mu = J_\mu, \tag{3.1.37}$$

$$F_{\mu\nu}(x) = -F_{\nu\mu}(x) = \partial_\mu A_\nu - \partial_\nu A_\mu. \tag{3.1.38}$$

In the case $m^2 \neq 0$, set $\partial_\mu A^\mu = 0$ to obtain

$$\left(-\partial^2 + m^2\right)A_\mu(x) = 0, \quad \partial_\mu A^\mu = 0. \tag{3.1.39}$$

The solution of the system (3.1.39) is the plane wave

$$A_\mu = \varepsilon_\mu(\mathbf{k})e^{ikx}, \quad k^2 = -m^2, \tag{3.1.40}$$

the condition $k\varepsilon(\mathbf{k}) = 0$ accurately defines of a massive particle with spin 1.

Equation (3.1.34) can also be derived from the action (Pardy, 2002)

$$W = \int (dx) \left(J^{\mu}(x)\varphi_{\mu}(x) + \mathcal{L}(\varphi(x)) \right) \tag{3.1.41}$$

where

$$\mathcal{L} = -\frac{1}{2}\left(\frac{1}{2} \left(\partial^{\mu}\varphi^{\nu} - \partial^{\nu}\varphi^{\mu} \right) \left(\partial_{\mu}\varphi_{\nu} - \partial_{\nu}\varphi_{\mu} \right) + m^2 \varphi^{\mu}\varphi_{\mu} \right), \tag{3.1.42}$$

use the arrangement

$$\int (dx) \varphi^{\mu} \left(-\partial^2 \right) \varphi_{\mu} = \int (dx) \partial^{\nu}\varphi^{\mu}\partial_{\nu}\varphi_{\mu} \tag{3.1.43}$$

and

$$\int (dx) \varphi^{\mu}\partial_{\mu}\partial^{\nu}\varphi_{\nu} = -\int (dx) \varphi^{\nu}\partial^{\mu}\partial_{\mu}\varphi_{\nu} = -\int (dx) \varphi_{\mu}\partial^{\mu}\partial^{\nu}\varphi_{\nu} \tag{3.1.44}$$

The Lagrange function can be derived in its standard form by applying the last equation (3.1.44) (Pardy, 2002):

$$\mathcal{L} = -\frac{1}{2}\left(\partial^{\nu}\varphi^{\mu}\partial_{\nu}\varphi_{\mu} - \left(\partial_{\mu}\varphi^{\mu} \right)^2 + m^2 \varphi^{\mu}\varphi_{\mu} \right). \tag{3.1.45}$$

Utilize the A and F symbols, from equation (3.1.42) the Proca Lagrangian

$$\mathcal{L} = -\frac{1}{2}\left(\frac{1}{2} F^{\mu\nu}F_{\mu\nu} + m^2 A^{\mu}A_{\mu} \right) \tag{3.1.46}$$

or

$$\mathcal{L} = -\frac{1}{2}\left(\partial^{v}A^{\mu}\partial_{\nu}A_{\mu} - \left(\partial_{\mu}A^{\mu} \right)^2 + m^2 A^{\mu}A_{\mu} \right) \tag{3.1.47}$$

When adjust the associated Lagrangians for a massive field with spin 1, it naturally leads to the formulation of the massive Maxwell equations.

The absence of a zero mass limit is clear when $\partial_{\mu}J^{\mu}(x) \neq 0$. Consequently, there is a necessity to reevaluate the action $W(J)$. One potential approach is to consider an alternative definition (Pardy, 2002)

$$\partial_{\mu}J^{\mu}(x) = mK(x) \tag{3.1.48}$$

and identify $K(x)$ in the limit $m \to 0$ with the source of massless spin 0 particles. Since the zero mass particles with zero spin are experimentally unknown in any event, take $K(x) = 0$ and get (Pardy, 2002)

$$W_{[m=0]}(J) = \frac{1}{2} \int (dx)\,(dx')\, J_\mu(x) D_+ (x - x')\, J^\mu (x')\,, \tag{3.1.49}$$

where

$$\partial_\mu J^\mu(x) = 0 \tag{3.1.50}$$

and

$$D_+ (x - x') = \Delta_+ (x - x'; m = 0)\,. \tag{3.1.51}$$

When dealing with electrodynamics within a medium, it's essential to consider key parameters including the speed of light (denoted as c), magnetic permeability (μ), and dielectric constant (ϵ). The formulation of electromagnetic potential equations, which are consistent with Maxwell's equations, was detailed by Schwinger et al. (1976). These equations are crucial for understanding how electromagnetic fields behave in different mediums and conditions (Pardy, 2002):

$$\left(\Delta - \frac{\mu\epsilon}{c^2}\frac{\partial^2}{\partial t^2}\right) A^\mu = \frac{\mu}{c}\left(g^{\mu\nu} + \frac{n^2 - 1}{n^2}\eta^\mu\eta^\nu\right) J_v, \tag{3.1.52}$$

where the Lorentz gauge condition was specified by Schwinger et al. (1976) and is expressed as follows:

$$\partial_\mu A^\mu - (\mu\epsilon - 1)(\eta\partial)(\eta A) = 0, \tag{3.1.53}$$

where in the medium's rest frame, the unit timelike vector is represented as $\eta^\mu = (1, \mathbf{0})$. There are four potentials denoted by $A^\mu = (\phi, \mathbf{A})$, and similarly, the four currents are expressed as $J^\mu = (c\varrho, \mathbf{J})$. Additionally, the medium's index of refraction is indicated by n.

The Green function that corresponds to these variables in the x-representation is denoted by $D_+^{\mu\nu}$

$$D_+^{\mu\nu} (x - x') = \frac{\mu}{c}\left(g^{\mu\nu} + \frac{n^2 - 1}{n^2}\eta^\mu\eta^\nu\right) D_+ (x - x')\,. \tag{3.1.54}$$

where $D_+(x-x')$ was derived by Schwinger et al. 1976 as the following:

$$D_+(x-x') = \int \frac{(dk)}{(2\pi)^4} \frac{e^{ik(x-x')}}{|\mathbf{k}^2| - n^2 (k^0)^2 - i\varepsilon}, \tag{3.1.55}$$

or

$$D_+(x-x') = \frac{i}{c} \frac{1}{4\pi^2} \int_0^\infty d\omega \frac{\sin \frac{n\omega}{c} |\mathbf{x}-\mathbf{x}'|}{|\mathbf{x}-\mathbf{x}'|} e^{-i\omega|t-t'|} \tag{3.1.56}$$

3.1.3 The Massive Photon in Electrodynamics

Massive electrodynamics in a medium may be generated by applying massless electrodynamics to the situation of massive photons. In our situation, this means that we will replace simply Eq. (3.1.52) with the following (Pardy, 2002):

$$\left(\Delta - \frac{\mu\epsilon}{c^2}\frac{\partial^2}{\partial t^2} + \frac{m^2c^2}{\hbar^2}\right) A^\mu = \frac{\mu}{c}\left(g^{\mu\nu} + \frac{n^2-1}{n^2}\eta^\mu\eta^\nu\right) J_v \tag{3.1.57}$$

where m is mass of photon. The Lorentz gauge (3.1.53) is also conserved in the massive situation.

According to Pardy (1989; 1994; 1995) with the analogy of the massless photon propagator $D(k)$ in the momentum representation

$$D(k) = \frac{1}{|\mathbf{k}|^2 - n^2 (k^0)^2 - i\varepsilon} \tag{3.1.58}$$

we will get the massive photon propagator at finite temperature is of the form

$$D_T(k, m^2) = \frac{1}{|\mathbf{k}|^2 - n^2 (k^0)^2 + \frac{m^2c^2}{\hbar^2} - i\varepsilon} + \frac{2\pi \mathrm{i}}{\mathrm{e}^{E/k_BT} - 1} \delta\left(|\boldsymbol{k}|^2 - n^2 (k^0)^2\right), \tag{3.1.59}$$

where $E = \hbar\omega$ is the energy, k_B is boltzmann constant, and T is temperature in the meduim. This propagator is derived from an assumption that the photon energy equation is (Pardy, 2002)

$$|\mathbf{k}|^2 - n^2 (k^0)^2 = -\frac{m^2c^2}{\hbar^2}, \tag{3.1.60}$$

where n is the parameter of the medium and m is mass of photon in this medium.

From Eq. (3.1.60) the dispersion relation for the massive photons follows:

$$\omega = \frac{c}{n}\sqrt{k^2 + \frac{m^2c^2}{\hbar^2}} \tag{3.1.61}$$

The correctness of Eq.(3.1.60) may be proven using a very basic idea: for $n = 1$, the Einstein equation for mass and energy must be followed. Putting $\mathbf{p} = \hbar\mathbf{k}, \hbar k^0 = \hbar(\omega/c) = E/c$, will get the Einstein energy equation

$$E^2 = \mathbf{p}^2c^2 + m^2c^4. \tag{3.1.62}$$

The propagator for the massive photon at finite temperature is then derived as

$$D_{+T}\left(x - x', m^2\right) = \frac{i}{c}\frac{1}{4\pi^2}\int_0^\infty d\omega \frac{\sin\left[\frac{n^2\omega^2}{c^2} - \frac{m^2c^2}{\hbar^2}\right]^{1/2}|\mathbf{x} - \mathbf{x}'|}{|\mathbf{x} - \mathbf{x}'|}\frac{2}{\exp(\hbar\omega/k_BT) - 1}e^{-i\omega|t-t'|} \tag{3.1.63}$$

The function (3.1.63) differs from the the original function $D_+$by the factor

$$\frac{2}{\exp(\hbar\omega/k_BT) - 1}\left(\frac{\omega^2n^2}{c^2} - \frac{m^2c^2}{\hbar^2}\right)^{1/2} \tag{3.1.64}$$

3.2 Power Spectrum of Massive Photons at Finite Temperature

In the situation of a massive electromagnetic field in the medium at finite temperature, the action W can be calculated from the following (Pardy, 2002):

$$W = \frac{1}{2c^2}\int (dx)\,(dx')\,J^{\mu}(x)D^{\mu\nu}_{+T}\left(x-x',m^2\right)J^{v}\left(x'\right), \tag{3.2.1}$$

where

$$D^{\mu\nu}_{+T} = \frac{\mu}{c}\left[g^{\mu\nu}+\left(1-n^{-2}\right)\eta^{\mu}\eta^{\nu}\right]D_{+T}\left(x-x',m^2\right), \tag{3.2.2}$$

where $\eta^{\mu}\equiv(1,\mathbf{0})$, $J^{\mu}\equiv(c\varrho,\mathbf{J})$ is the conserved current, μ is the magnetic permeability of the medium, ϵ is the dielectric constant of the medium, and $n=\sqrt{\epsilon\mu}$ is the index of refraction of the medium.

The probability of the persistence of vacuum follows from the vacuum amplitude (3.1.2) in the form (Pardy, 2002):

$$|\langle 0_+ \mid 0_-\rangle|^2 = e^{-\frac{2}{\hbar}\operatorname{Im}W}, \tag{3.2.3}$$

where $\operatorname{Im}W$ is the foundation for the definition of the spectrum function $P(\omega,t)$:

$$-\frac{2}{\hbar}\operatorname{Im}W = -\int dtd\omega\frac{P(\omega,t)}{\hbar\omega}. \tag{3.2.4}$$

We insert Eq. (3.2.2) into Eq. (3.2.1), we will get after extracting $P_T(\omega,t)$ the following general expression for the spectrum formula:

$$\begin{aligned}P_T(\omega,t) =& \frac{2}{\exp(\hbar\omega/k_BT)-1}\\ &\times\frac{\omega}{4\pi^2}\frac{\mu}{n^2}\int d\mathbf{x}d\mathbf{x}'dt'\left[\frac{\sin\left[\frac{n^2\omega^2}{c^2}-\frac{m^2c^2}{\hbar^2}\right]^{1/2}|\mathbf{x}-\mathbf{x}'|}{|\mathbf{x}-\mathbf{x}'|}\right]\\ &\times\cos\left[\omega\left(t-t'\right)\right]\left[\varrho(\mathbf{x},t)\varrho\left(\mathbf{x}',t'\right)-\frac{n^2}{c^2}\mathbf{J}(\mathbf{x},t)\cdot\mathbf{J}\left(\mathbf{x}',t'\right)\right].\end{aligned} \tag{3.2.5}$$

The power spectrum at finite temperature is expressed through the following

$$\begin{aligned} P_{\mathrm{T}} =& P_{T=0} + P_{T\neq 0} \\ &= P_{T=0}\left(1 + \frac{2}{\exp(\hbar\omega/k_B T) - 1}\right) \\ &= P_{T=0} \times \coth(\hbar\omega/2k_B T) \end{aligned} \tag{3.2.6}$$

By using

$$1 + \frac{2}{\exp(x) - 1} = \coth\left(\frac{x}{2}\right)$$

$$\begin{aligned} P_{\mathrm{T}} =& \frac{\omega}{4\pi^2}\frac{\mu}{n^2}\coth(\hbar\omega/2k_B T)\int d\mathbf{x}d\mathbf{x}'dt' \left[\frac{\sin\left[\frac{n^2\omega^2}{c^2} - \frac{m^2c^2}{\hbar^2}\right]^{1/2}|\mathbf{x}-\mathbf{x}'|}{|\mathbf{x}-\mathbf{x}'|}\right] \\ &\times \cos\left[\omega\left(t-t'\right)\right]\left[\varrho(\mathbf{x},t)\varrho\left(\mathbf{x}',t'\right) - \frac{n^2}{c^2}\mathbf{J}(\mathbf{x},t)\cdot\mathbf{J}\left(\mathbf{x}',t'\right)\right]. \end{aligned} \tag{3.2.7}$$

Next, we apply the formula (3.2.7) in order to get the power spectrum of massive photons at finite temperature. The Cherenkov radiation is produced by charged particle of charge e moving at a constant velocity $\mathbf{v}$. Thus, we can write the charge density and the current density as

$$\varrho = e\delta(\mathbf{x} - \mathbf{v}t), \quad \mathbf{J} = e\mathbf{v}\delta(\mathbf{x} - \mathbf{v}t) \tag{3.2.8}$$

After insertion of Eq. (3.2.8) into Eq. (3.2.7), will get ($v = |\mathbf{v}|$)

$$\begin{aligned} P_{\mathrm{T}} =& \frac{e^2}{4\pi^2}\frac{v\mu\omega}{c^2}\left(1 - \frac{1}{n^2\beta^2}\right) \times \coth(\hbar\omega/2k_B T) \\ &\times \int_{\infty}^{\infty}\frac{d\tau}{\tau}\sin\left(\left[\frac{n^2\omega^2}{c^2} - \frac{m^2c^2}{\hbar^2}\right]^{1/2} v\tau\right)\cos\omega\tau, \end{aligned} \tag{3.2.9}$$

where $\tau = t' - t$ and $\beta = v/c$.

Consider the integral in equation (3.2.9): by using

$$\int_{-\infty}^{\infty} d\tau \frac{\sin X\tau}{\tau}\cos\omega\tau = \frac{1}{2}\pi\left(\frac{X-\omega}{\sqrt{(X-\omega)^2}} + \frac{X+\omega}{\sqrt{(X+\omega)^2}}\right) = \pi \tag{3.2.10}$$

so

$$\int_{-\infty}^{\infty}\frac{d\tau}{\tau}\sin\left(\left[\frac{n^2\omega^2}{c^2}-\frac{m^2c^2}{\hbar^2}\right]^{1/2}v\tau\right)\cos\omega\tau=\begin{cases}\pi, & 0<m^2<\frac{\omega^2\hbar^2}{c^2v^2}\left(n^2\beta^2-1\right)\\ 0, & m^2>\frac{\omega^2\hbar^2}{c^2v^2}\left(n^2\beta^2-1\right).\end{cases} \tag{3.2.11}$$

From Eq. (3.2.11) it immediately follows that $m^2>0$ implies that the Cherenkov threshold $n\beta>1$. From Eqs. (3.2.9) and (3.2.11) we get the spectrum formula of the Cherenkov radiation at finite temperature of massive photons in the form

$$P_{\mathrm{T}}=\frac{e^2}{4\pi}\frac{v\mu\omega}{c^2}\left(1-\frac{1}{n^2\beta^2}\right)\times\coth(\hbar\omega/2k_BT) \tag{3.2.12}$$

for

$$\omega>\frac{mcv}{\hbar}\frac{1}{\sqrt{n^2\beta^2-1}}>0$$

and $P_{\mathrm{total}}=0$ for

$$\omega<\frac{mcv}{\hbar}\frac{1}{\sqrt{n^2\beta^2-1}}.$$

Using the dispersion relation for the massive photons follows:

$$\omega=\frac{c}{n}\sqrt{k^2+\frac{m^2c^2}{\hbar^2}} \tag{3.2.13}$$

We can obtain the power spectrum of massive photons at finite temperatures as follows:

$$P_{\mathrm{T}}=\frac{e^2}{4\pi}\frac{v\mu}{nc}\sqrt{k^2+\frac{m^2c^2}{\hbar^2}}\left(1-\frac{1}{n^2\beta^2}\right)\times\coth\left(\frac{\hbar c}{2nk_BT}\sqrt{k^2+\frac{m^2c^2}{\hbar^2}}\right),\quad n\beta>1 \tag{3.2.14}$$

and

$$P_{\mathrm{T}}=0,\quad n\beta<1. \tag{3.2.15}$$

When we substitute $m = 0$ in equation (3.2.13) and (3.2.14), we get

$$\omega = \frac{ck}{n} \tag{3.2.16}$$

and

$$P_{\mathrm{T}} = \frac{e^2}{4\pi}\frac{v\mu\omega}{c^2}\left(1 - \frac{1}{n^2\beta^2}\right) \times \coth(\hbar\omega/2k_BT) \tag{3.2.17}$$

where $\beta = v/c$ and $E = \hbar\omega$, which corresponds to the power spectrum formula of the Cherenkov radiation at finite temperatures derived by Pardy (1989).

3.3 Numerical Calculation of Power Spectrum at Finite Temperature

For the numerical calculations, the result of the power spectrum of massive photons at finite temperatures is derived from the source theory. We take into account a charged electron moving through a water medium. In order to plot graphs in both 2D and 3D from equation (3.2.14), we utilize Wolfram Mathematica. Details of the numerical calculations and plot graph are in Appendix C.

3.2.1 The power spectrum of massive photons at temperature 0, 20, 50, 80, and 100 °C

To analyze the power spectrum at a finite temperature, we have plotted the first graph of the power spectrum at a temperature of T = 0, 20, 50, 80, and 100 °C as shown in Figure 7. The y-axis is the power spectrum in watts (W) and the x-axis is the velocity in meters per second (m/s). The green, blue dash, yellow, blue, and

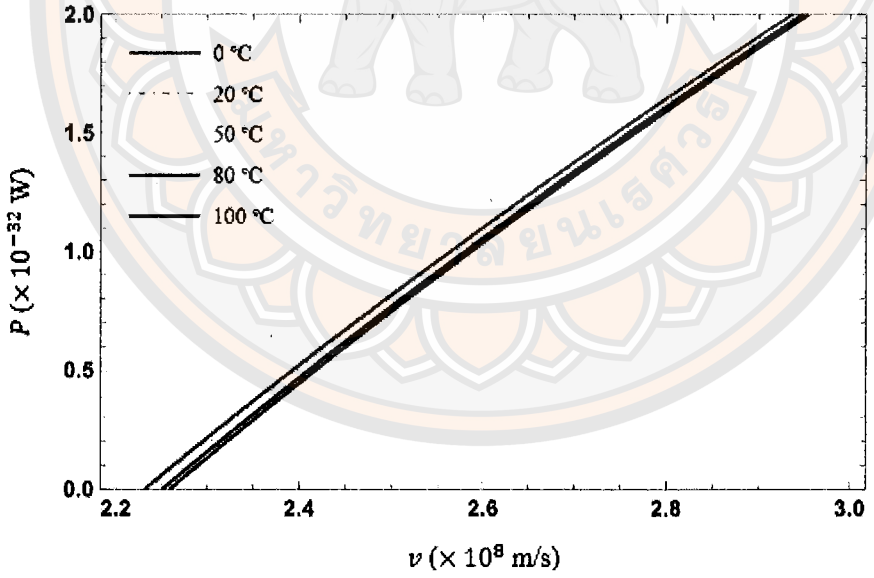

Figure 7 The power spectrum of massive photons at 0, 20, 50, 80, and 100 °C.

red lines represent the temperature cases of 0, 20, 50, 80, and 100 °C, respectively. From the graph, it was found that the power spectrum at temperatures 0 and 20

°C has almost no difference, while the power spectrum at temperatures 50, 80, and 100 °C decreased slightly. We also found that the minimum velocity that causes the power spectrum to be above zero at temperatures 0 and 20 °C is approximately 2.23×10^8 m/s, while at temperatures 100 °C it is more than 2.26×10^8 m/s. So, it can be inferred that the temperature and the velocity influence the power spectrum of Cherenkov radiation.

3.2.2 The power spectrum of massless and massive photons at temperature 20 °C

The second graph as displayed in Figure 8 is a 2D graph of the power spectrum of massless and massive photons at a temperatures of $T = 20$ °C. The y-axis is the power spectrum in watts (W) and the x-axis is the velocity in meters per second (m/s). The orange and blue lines represent the cases of massless and massive photons, respectively. We found that the power spectrum of massive photons is

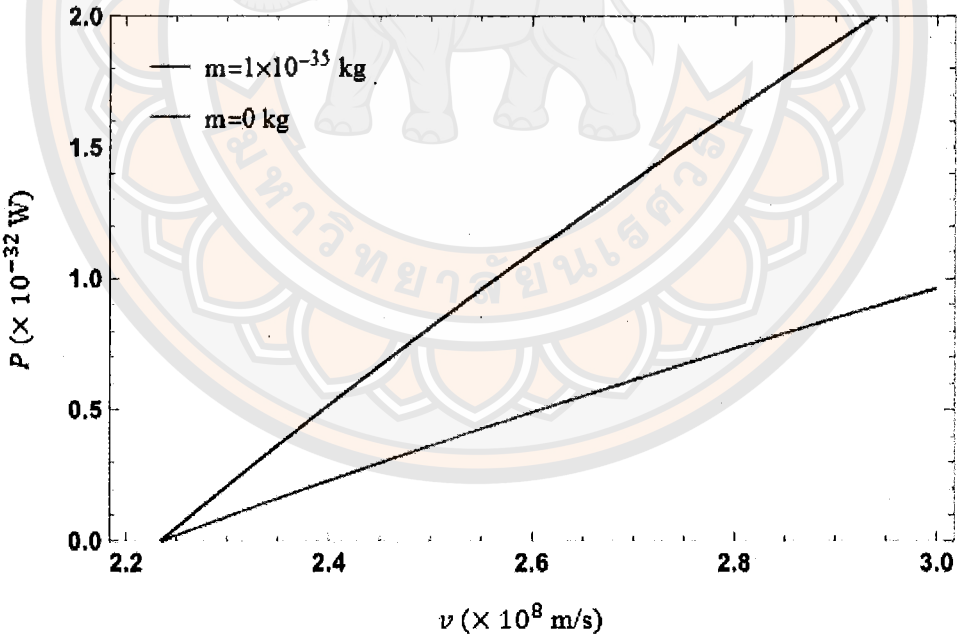

Figure 8 The power spectrum of massless and massive photons at 20 °C.

more than approximately two times of massless photons. We also found that the minimum velocity that causes the power spectrum of massless and massive photons to be above zero is about 2.23×10^8 m/s. Hence, the graph indicates that the mass

of photons and the velocity affect the power spectrum of Cherenkov radiation.

3.2.3 The power spectrum of massive photons at temperature 0, 20, and 100 °C

The third graph as demonstrated in Figure 9 is a 3D graph of the power spectrum of massive photons at a temperature of $T = 0$ °C, which is similar to the previous graph and adds a z-axis of the mass of photons in kilograms (kg). From

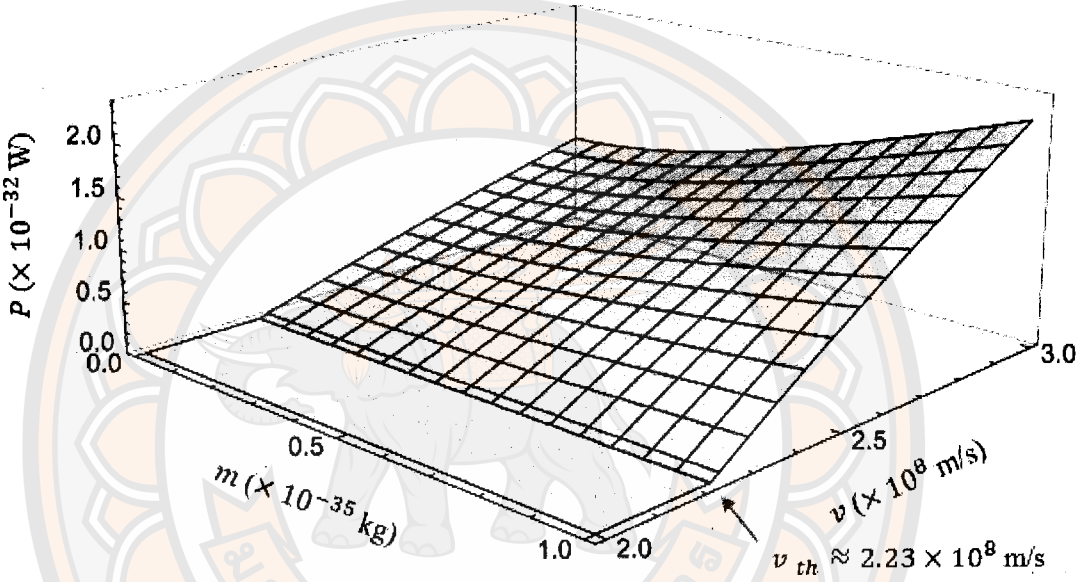

Figure 9 The power spectrum of massive photons at 0 °C.

the graph, we found that as in the previous graph, increasing the photon mass and the velocity increases the power spectrum. Additionally, we found that the power spectrum of massive photons above zero at the velocity is more than 2.23×10^8 m/s. Thus, the graph reveals that the photon mass and the velocity influence the power spectrum of Cherenkov radiation.

The fourth and fifth graphs as demonstrated in Figures 10 and 11 are a 3D graph of the power spectrum of massive photons at a temperatures of $T = 20$ and 100 °C. From the graph, we found that the power spectrum of massive photons at a temperature of 20 and 100 °C had similar results as the power spectrum at a temperature of 0 °C. We also found that the minimum velocity that causes the power spectrum to be above zero at a temperature of 20 °C is more than 2.23×10^8

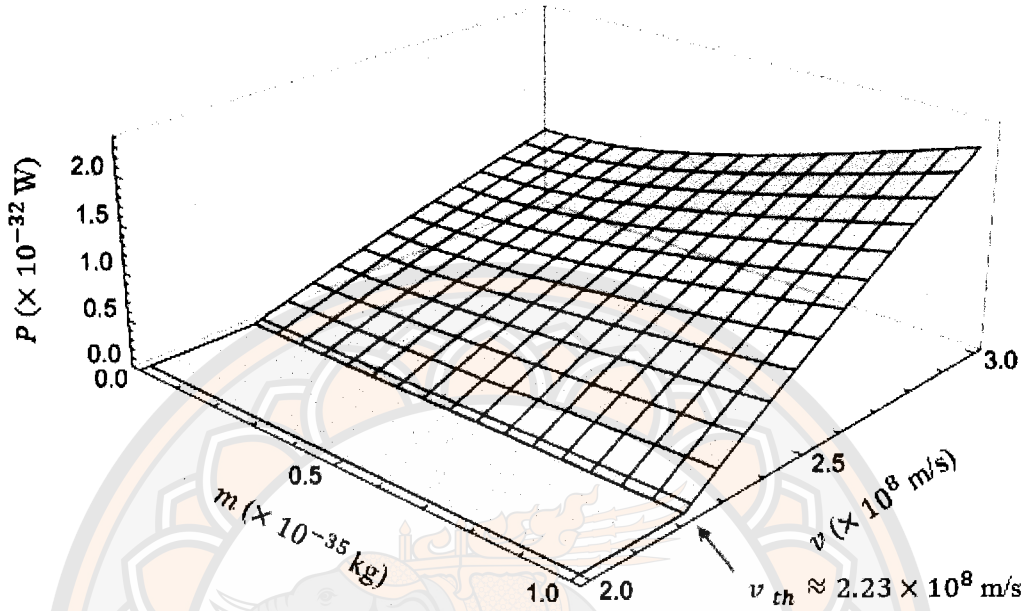

Figure 10 The power spectrum of massive photons at 20 °C.

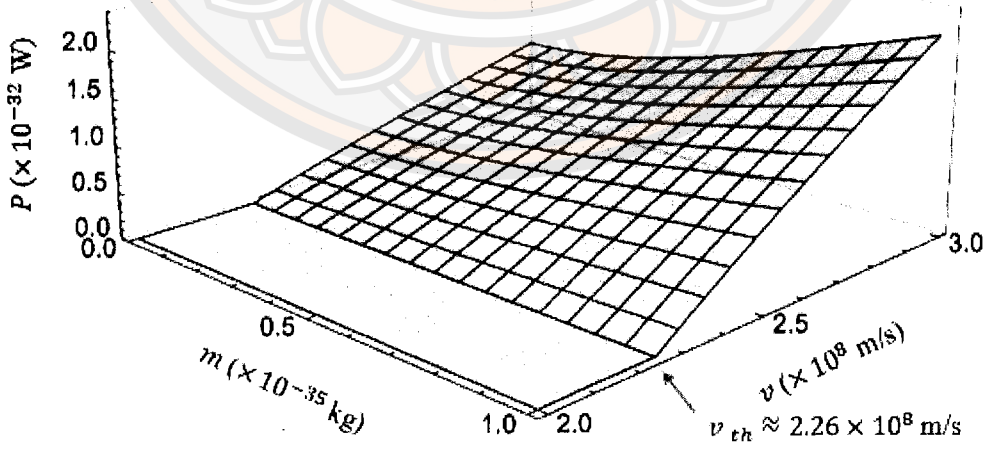

Figure 11 The power spectrum of massive photons at 100 °C.

m/s, while at a temperature of 100 °C it is more than 2.26×10^8 m/s. Therefore, these graphs indicate that the photon mass, the velocity, and the temperatures affect the power spectrum of Cherenkov radiation.

CHAPTER IV

CHERENKOV RADIATION OF MASSLESS AND MASSIVE PHOTON IN TWO CHARGE SYSTEM

This chapter we will use the same concepts of quantum theory as Chapter III in order to study Cherenkov radiation, which occurs from a two-charge electron system moving through a dielectric medium as show in Figure 12. We will utilize source theory to calculate the power spectrum of massless and massive photons from a two-charge electron system at a finite temperature moving through a dielectric medium. This chapter has three sections. Section 4.1 Power Spectrum of Massless Photons in Two Charge System, we will present steps to calculate the power spectrum of massless photons from a two-charge electron moving through a dielectric medium. Section 4.2 Power Spectrum of Massive Photons in Two Charge System, we will represent steps to calculate the power spectrum of massive photons from a two-charge electron moving through the medium. In section 4.3 Numerical Calculation of the Power Spectrum in Two Charge System, we will numerically calculate the results of the power spectrum obtained and display the results as a graph of massless and massive photons.

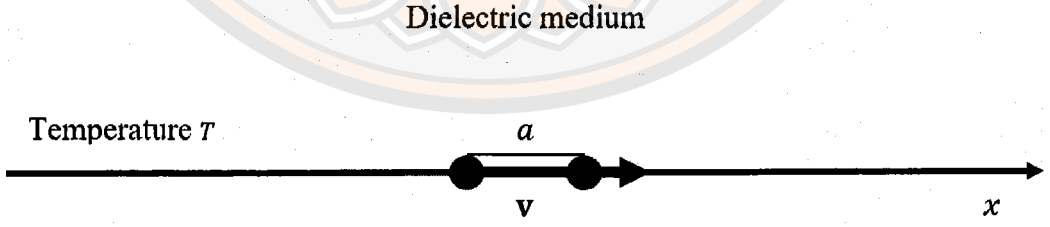

Figure 12 A system of two charges electron e moves through a dielectric medium with velocity v at finite temperatures T.

4.1 Power Spectrum of Massless Photons in Two Charge System

In source theory, the fundamental equation is the vacuum-to-vacuum amplitude (Schwinger et al., 1976)

$$\langle 0_+ \mid 0_- \rangle = e^{(i/\hbar)W(S)}, \tag{4.1.1}$$

where the minus and plus marks on the vacuum symbol are causal labels, indicating time before and after the space-time region where sources are altered. The exponential form assumes physically independent experimental configurations, resulting in multiplying probability amplitudes and adding W expressions (Schwinger et al., 1970).

The description of the electromagnetic field can be characterized by its amplitude, denoted as (4.1.1), in conjunction with associated the action

$$W(J) = \frac{1}{2c^2} \int (dx)\,(dx')\, J^{\mu}(x) D^{\mu\nu}_{+T}(x - x')\, J^{\nu}(x'), \tag{4.1.2}$$

where $W(J)$ denoted as the action. Here, J_{μ} represents the densities of charge and current. Meanwhile, $D^{\mu\nu}_{+T}(x - x')$ signifies the propagator of photon, whose precise structure is to be defined in subsequent analysis.

The probability of the persistence of vacuum can be found from the following formula (Schwinger et al., 1976):

$$|\langle 0_+ \mid 0_- \rangle|^2 = \exp\left\{-\frac{2}{\hbar} \operatorname{Im} W\right\} = \exp\left\{-\int dt d\omega \frac{P(\omega, t)}{\hbar\omega}\right\}, \tag{4.1.3}$$

where $P(\omega, t)$ is known as the power spectrum function. To derive the spectrum function from the imaginary part of $\operatorname{Im} W$, one must be acquainted with the precise structure of the propagator of photon, represented as $D^{\mu\nu}_{+T}(x - x')$.

The fourpotentials, denoted as $A^{\mu}(\phi, \mathbf{A})$, characterize the electromagnetic field, while the generation of this field stems from the four-current, represented by $J^{\mu}(c\varrho, \mathbf{J})$. These relationships are governed by a specific differential equation. This equation establishes how the four-current influences the electromagnetic field through the fourpotentials (Schwinger et al., 1976)

$$\left(\Delta - \frac{\mu\varepsilon}{c^2}\frac{\partial^2}{\partial t^2}\right) A^{\mu} = \frac{\mu}{c}\left(g^{\mu\nu} + \frac{n^2-1}{n^2}\eta^{\mu}\eta^{\nu}\right) J_{\nu} \tag{4.1.4}$$

wiht the corresponding Green's function $D_{+\mu\nu}$:

$$D_{+T}^{\mu\nu} = \frac{\mu}{c}\left(g^{\mu\nu} + \frac{n^2-1}{n^2}\eta^{\mu}\eta^{\nu}\right) D_{+T}\left(x - x'\right), \tag{4.1.5}$$

where $\eta^{\mu} \equiv (1, 0)$, the symbol μ represents the magnetic permeability of the dielectric medium with the dielectric constant ε. The symbol c stands for the speed of light in a vacuum. The term n refers to the refractive index of the medium. Additionally, the function $D_{+}(x - x')$ was derived by Schwingeret et al. (1976) in the following:

$$D_{+T}\left(x - x'\right) = \frac{i}{4\pi^2 c}\int_0^{\infty} d\omega \frac{\sin(n\omega/c)\left|\mathbf{x} - \mathbf{x}'\right|}{\left|\mathbf{x} - \mathbf{x}'\right|} \frac{2}{\exp(\hbar\omega/k_B T) - 1} e^{-i\omega|t-t'|}. \tag{4.1.6}$$

By applying equations (4.1.2), (4.1.3), (4.1.5), and (4.1.6), the resulting expression for the power spectrum can be derived as (Schwinger et al., 1976):

$$\begin{aligned} P_T(\omega, t) =& \frac{2}{\exp(\hbar\omega/k_B T) - 1} \frac{\omega}{4\pi^2} \frac{\mu}{n^2} \int d\mathbf{x} d\mathbf{x}' dt' \frac{\sin(n\omega/c)\left|\mathbf{x} - \mathbf{x}'\right|}{\left|\mathbf{x} - \mathbf{x}'\right|} \\ &\times \cos\left[\omega\left(t - t'\right)\right] \times \left\{\varrho(\mathbf{x}, t)\varrho\left(\mathbf{x}', t'\right) - \frac{n^2}{c^2}\mathbf{J}(\mathbf{x}, t) \cdot \mathbf{J}\left(\mathbf{x}', t'\right)\right\}. \end{aligned} \tag{4.1.7}$$

The power spectrum at finite temperature is expressed through the following

$$P_{\mathrm{T}} = P_{T=0} + P_{T\neq 0} \tag{4.1.8}$$

$$= P_{T=0}\left(1 + \frac{2}{\exp(\hbar\omega/k_B T) - 1}\right) \tag{4.1.9}$$

$$= P_{T=0} \times \coth(\hbar\omega/2k_B T) \tag{4.1.10}$$

By using

$$1 + \frac{2}{\exp(x) - 1} = \coth\left(\frac{x}{2}\right) \tag{4.1.11}$$

get

$$P_{\mathrm{T}}(\omega, t) = \coth(\hbar\omega/2k_B T)\frac{\omega}{4\pi^2}\frac{\mu}{n^2}\int d\mathbf{x}d\mathbf{x}'dt'\frac{\sin(n\omega/c)\,|\mathbf{x}-\mathbf{x}'|}{|\mathbf{x}-\mathbf{x}'|}$$
$$\times \cos\left[\omega\left(t-t'\right)\right] \times \left\{\varrho(\mathbf{x},t)\varrho\left(\mathbf{x}',t'\right) - \frac{n^2}{c^2}\mathbf{J}(\mathbf{x},t)\cdot\mathbf{J}\left(\mathbf{x}',t'\right)\right\}. \tag{4.1.12}$$

We are now ready to utilize the final equation for scenarios involving two identical charges traveling through a dielectric medium.

The common belief is that Cherenkov radiation within electrodynamics arises from a charge moving at a steady speed. This discussion, however, focuses on a pair of identical charges, denoted as e, which maintain a fixed separation, represented by $a = |\mathbf{a}|$, and travel at a velocity $\mathbf{v}$ through a dielectric medium. Under these conditions, the expressions for a charge and current densities of the configuration are specified by the following equations:

$$\varrho = e[\delta(\mathbf{x} - \mathbf{v}t) + \delta(\mathbf{x} - \mathbf{a} - \mathbf{v}t)] \tag{4.1.13}$$

$$\mathbf{J} = e\mathbf{v}[\delta(\mathbf{x} - \mathbf{v}t) + \delta(\mathbf{x} - \mathbf{a} - \mathbf{v}t)] \tag{4.1.14}$$

where in the system S, the vector $\mathbf{a}$ represents the directed distance from the left charge to the right charge, and the magnitude of this vector is denoted by $a = |\mathbf{a}|$.

Let us suppose that $\mathbf{v}\|\mathbf{a}\|\mathbf{x}$, and upon substituting equations (4.1.13) and (4.1.14) into equation (4.1.12), while defining $\tau = t' - t$, and $\beta = v/c$, where $v = |\mathbf{v}|$, we get instead of the formula (4.1.12) the following relation (Pardy, 1997):

$$P_{total}(\omega, t) = 2P_1(\omega, t) + P_2(\omega, t) + P_3(\omega, t), \tag{4.1.15}$$

where

$$P_1(\omega,t) = \frac{e^2}{4\pi^2}\frac{v\mu\omega}{c^2}\left(1-\frac{1}{n^2\beta^2}\right)\times\coth(\hbar\omega/2k_BT) \times\int_{-\infty}^{\infty}d\tau\frac{\sin n\omega\beta\tau}{\tau}\cos\omega\tau \tag{4.1.16}$$

$$P_2(\omega,t) = \frac{e^2}{4\pi^2}\frac{v\mu\omega}{c^2}\left(1-\frac{1}{n^2\beta^2}\right)\times\coth(\hbar\omega/2k_BT) \times\int_{-\infty}^{\infty}d\tau\frac{\sin n\omega\beta|a/v+\tau|}{|a/v+\tau|}\cos\omega\tau \tag{4.1.17}$$

$$P_3(\omega,t) = \frac{e^2}{4\pi^2}\frac{v\mu\omega}{c^2}\left(1-\frac{1}{n^2\beta^2}\right)\times\coth(\hbar\omega/2k_BT) \times\int_{-\infty}^{\infty}d\tau\frac{\sin n\omega\beta|a/v-\tau|}{|a/v-\tau|}\cos\omega\tau. \tag{4.1.18}$$

Consider the integral in equation (4.1.16):

$$\int_{-\infty}^{\infty}d\tau\frac{\sin n\omega\beta\tau}{\tau}\cos\omega\tau = \frac{1}{2}\pi\left(\frac{n\omega\beta-\omega}{\sqrt{(n\omega\beta-\omega)^2}}+\frac{n\omega\beta+\omega}{\sqrt{(n\omega\beta+\omega)^2}}\right) \tag{4.1.19}$$

$$= \frac{1}{2}\pi\left(\frac{\omega(n\beta-1)}{\omega\sqrt{(n\beta-1)^2}}+\frac{\omega(n\beta+1)}{\omega\sqrt{(n\beta+1)^2}}\right) = \pi \tag{4.1.20}$$

so

$$I_1 = \int_{-\infty}^{\infty}d\tau\frac{\sin n\omega\beta\tau}{\tau}\cos\omega\tau = \begin{cases}\pi; & n\beta>1\\ 0; & n\beta<1\end{cases}. \tag{4.1.21}$$

Consider the integral in equation (4.1.17) and (4.1.18):

$$I_2 = \int_{-\infty}^{\infty}d\tau\frac{\sin n\omega\beta|a/v+\tau|}{|a/v+\tau|}\cos\omega\tau \tag{4.1.22}$$

and

$$I_3 = \int_{-\infty}^{\infty}d\tau\frac{\sin n\omega\beta|a/v-\tau|}{|a/v-\tau|}\cos\omega\tau. \tag{4.1.23}$$

By applying integral (4.1.21), we obtain the power spectrum formula P_1:

$$P_1(\omega,t) = \frac{e^2}{4\pi}\frac{\mu\omega}{c^2}v\left(1-\frac{1}{n^2\beta^2}\right)\times\coth(\hbar\omega/2k_BT), \quad n\beta>1 \tag{4.1.24}$$

and

$$P_1(\omega,t) = 0, \quad n\beta<1. \tag{4.1.25}$$

Using transformations

$$\frac{a}{v}+\tau=T, \quad \frac{a}{v}-\tau=T \tag{4.1.26}$$

Upon evaluating the integrals denoted by I_2 and I_3, we get the power spectrum formula P_2, P_3 (Pardy, 1997):

$$P_2(\omega,t)=\frac{e^2}{4\pi}\frac{\mu\omega}{c^2}\cos\left(\frac{\omega a}{v}\right)v\left(1-\frac{1}{n^2\beta^2}\right)\times\coth(\hbar\omega/2k_BT)=P_3(\omega,t), \quad n\beta>1 \tag{4.1.27}$$

and

$$P_2(\omega,t)=P_3(\omega,t)=0, \quad n\beta<1. \tag{4.1.28}$$

The total power spectrum released by the Cherenkov radiation in a system with two charges is the sum result of the individual power spectrum:

$$P_{total}=2\left(P_1+P_2\right) \tag{4.1.29}$$

$$=2\left(1+\cos\left(\frac{\omega a}{v}\right)\right)\frac{e^2}{4\pi}\frac{\mu\omega}{c^2}v\left(1-\frac{1}{n^2\beta^2}\right)\times\coth(\hbar\omega/2k_BT) \tag{4.1.30}$$

$$=4\cos^2\left(\frac{a\omega}{2v}\right)\frac{e^2}{4\pi}\frac{\mu\omega}{c^2}v\left(1-\frac{1}{n^2\beta^2}\right)\times\coth(\hbar\omega/2k_BT) \tag{4.1.31}$$

$$=\frac{e^2}{\pi}\frac{\mu\omega}{c^2}v\left(1-\frac{1}{n^2\beta^2}\right)\cos^2\left(\frac{a\omega}{2v}\right)\times\coth(\hbar\omega/2k_BT), \quad n\beta>1 \tag{4.1.32}$$

By using

$$2(1+\cos(x))=4\cos^2\left(\frac{x}{2}\right) \tag{4.1.33}$$

We get the total power spectrum of massless photons in two charge systems at finite temperatures in the following:

$$P_{total}=\frac{e^2}{\pi}\frac{\mu\omega}{c^2}v\left(1-\frac{1}{n^2\beta^2}\right)\cos^2\left(\frac{a\omega}{2v}\right)\times\coth(\hbar\omega/2k_BT), \quad n\beta>1 \tag{4.1.34}$$

and

$$P_{total}=0, \quad n\beta<1. \tag{4.1.35}$$

4.2 Power Spectrum of Massive Photons in Two Charge System

For the calculation of the power spectrum of massive photons in the two-charge system, we will use the same method as in the previous section.

Rather than considering the Cherenkov radiation produced by a single moving charge, this study examines a pair of identical charges, denoted as e, maintaining a fixed separation distance $a = |\mathbf{a}|$ and traveling at a velocity $\mathbf{v}$ within a dielectric medium. Under these conditions, the expressions for a charge and current density on the system are described by the following equations:

$$\varrho = e[\delta(\mathbf{x} - \mathbf{v}t) + \delta(\mathbf{x} - \mathbf{a} - \mathbf{v}t)] \tag{4.2.1}$$

$$\mathbf{J} = e\mathbf{v}[\delta(\mathbf{x} - \mathbf{v}t) + \delta(\mathbf{x} - \mathbf{a} - \mathbf{v}t)]. \tag{4.2.2}$$

where the vector $\mathbf{a}$ represents the directed distance from the left charge to the right charge, and the magnitude of this vector is denoted by $a = |\mathbf{a}|$ in the system S.

Assuming that $\mathbf{v}\|\mathbf{a}\|\mathbf{x}$, we proceed by substituting equations (4.2.1) and (4.2.2) into equation (3.2.7), we define $\tau = t' - t$, and $\beta = v/c$, where $v = |\mathbf{v}|$, we obtain instead of the formula (3.2.7) the following relation (Pardy, 1997):

$$P_{total}(\omega, t) = 2P_1(\omega, t) + P_2(\omega, t) + P_3(\omega, t), \tag{4.2.3}$$

where

$$\begin{aligned} P_1(\omega, t) =& \frac{e^2}{4\pi^2}\frac{v\mu\omega}{c^2}\left(1 - \frac{1}{n^2\beta^2}\right) \times \coth(\hbar\omega/2k_BT) \\ & \times \int_{-\infty}^{\infty} d\tau \frac{\sin\left(\left[\frac{n^2\omega^2}{c^2} - \frac{m^2c^2}{\hbar^2}\right]^{1/2} v\tau\right)}{\tau} \cos\omega\tau \end{aligned} \tag{4.2.4}$$

$$\begin{aligned} P_2(\omega, t) =& \frac{e^2}{4\pi^2}\frac{v\mu\omega}{c^2}\left(1 - \frac{1}{n^2\beta^2}\right) \times \coth(\hbar\omega/2k_BT) \\ & \times \int_{-\infty}^{\infty} d\tau \frac{\sin\left(\left[\frac{n^2\omega^2}{c^2} - \frac{m^2c^2}{\hbar^2}\right]^{1/2} \left|\frac{a}{v} + \tau\right|\right)}{\left|\frac{a}{v} + \tau\right|} \cos\omega\tau \end{aligned} \tag{4.2.5}$$

$$P_3(\omega,t) = \frac{e^2}{4\pi^2}\frac{v\mu\omega}{c^2}\left(1-\frac{1}{n^2\beta^2}\right)\times\coth(\hbar\omega/2k_BT) \times\int_{-\infty}^{\infty}d\tau\frac{\sin\left(\left[\frac{n^2\omega^2}{c^2}-\frac{m^2c^2}{\hbar^2}\right]^{1/2}\left|\frac{a}{v}-\tau\right|\right)}{\left|\frac{a}{v}-\tau\right|}\cos\omega\tau \tag{4.2.6}$$

Consider the integral in equation (4.2.4): by using

$$\int_{-\infty}^{\infty}d\tau\frac{\sin X\tau}{\tau}\cos\omega\tau = \frac{1}{2}\pi\left(\frac{X-\omega}{\sqrt{(X-\omega)^2}}+\frac{X+\omega}{\sqrt{(X+\omega)^2}}\right)=\pi \tag{4.2.7}$$

so

$$I_1=\int_{-\infty}^{\infty}d\tau\frac{\sin\left(\left[\frac{n^2\omega^2}{c^2}-\frac{m^2c^2}{\hbar^2}\right]^{1/2}v\tau\right)}{\tau}\cos\omega\tau=\begin{cases}\pi; & n\beta>1\\ 0; & n\beta<1\end{cases}. \tag{4.2.8}$$

Consider the integral in equation (4.2.5) and (4.2.6):

$$I_2=\int_{-\infty}^{\infty}d\tau\frac{\left(\left[\frac{n^2w^2}{c^2}-\frac{m^2c^2}{\hbar^2}\right]^{1/2}\left|\frac{a}{v}+\tau\right|\right)}{\left|\frac{a}{v}+\tau\right|}\cos\omega\tau \tag{4.2.9}$$

and

$$I_3=\int_{-\infty}^{\infty}d\tau\frac{\left(\left[\frac{n^2\omega^2}{c^2}-\frac{m^2c^2}{\hbar^2}\right]^{1/2}\left|\frac{a}{v}-\tau\right|\right)}{\left|\frac{a}{v}-\tau\right|}\cos\omega\tau. \tag{4.2.10}$$

By applying the integral (4.2.8), we are able to derive the power spectrum formula P_1:

$$P_1(\omega,t)=\frac{e^2}{4\pi}\frac{\mu\omega}{c^2}v\left(1-\frac{1}{n^2\beta^2}\right)\times\coth(\hbar\omega/2k_BT);\quad n\beta>1 \tag{4.2.11}$$

and

$$P_1(\omega,t)=0;\quad n\beta<1. \tag{4.2.12}$$

Using transformations

$$\frac{a}{v}+\tau=T, \quad \frac{a}{v}-\tau=T, \tag{4.2.13}$$

Following the evaluation of the relevant integrals, we obtain the results I_2, I_3, the corresponding the power spectrum formula P_2, P_3 (Pardy, 1997):

$$P_2(\omega,t)=\frac{e^2}{4\pi}\frac{\mu\omega}{c^2}\cos\left(\frac{\omega a}{v}\right)v\left(1-\frac{1}{n^2\beta^2}\right)\times\coth(\hbar\omega/2k_BT)=P_3(\omega,t); \quad n\beta>1 \tag{4.2.14}$$

and

$$P_2(\omega,t)=P_3(\omega,t)=0; \quad n\beta<1. \tag{4.2.15}$$

The total power spectrum released by the Cherenkov radiation in a system with two charges is the sum result of the individual power spectrum:

$$P_{total}=2\left(P_1+P_2\right) \tag{4.2.16}$$

$$=2\left(1+\cos\left(\frac{\omega a}{v}\right)\right)\frac{e^2}{4\pi}\frac{\mu\omega}{c^2}v\left(1-\frac{1}{n^2\beta^2}\right)\times\coth(\hbar\omega/2k_BT) \tag{4.2.17}$$

$$=4\cos^2\left(\frac{a\omega}{2v}\right)\frac{e^2}{4\pi}\frac{\mu\omega}{c^2}v\left(1-\frac{1}{n^2\beta^2}\right)\times\coth(\hbar\omega/2k_BT), n\beta>1 \tag{4.2.18}$$

Using the dispersion relation for the massive photons follows:

$$\omega=\frac{c}{n}\sqrt{k^2+\frac{m^2c^2}{\hbar^2}} \tag{4.2.19}$$

Finally, we obtain the total power spectrum of massive photons in two charge systems at finite temperatures in the following form:

$$P_{total}=2\left(P_1+P_2\right) \tag{4.2.20}$$

$$=\frac{e^2}{\pi}\frac{\mu v}{cn}\sqrt{k^2+\frac{m^2c^2}{\hbar^2}}\left(1-\frac{1}{n^2\beta^2}\right)\cos^2\left(\frac{ac}{2vn}\sqrt{k^2+\frac{m^2c^2}{\hbar^2}}\right)$$

$$\times\coth\left(\frac{\hbar c}{2nk_BT}\sqrt{k^2+\frac{m^2c^2}{\hbar^2}}\right); \quad n\beta>1 \tag{4.2.21}$$

and

$$P_{total}=0; \quad n\beta<1 \tag{4.2.22}$$

4.3 Numerical Calculation of Power Spectrum in Two Charge System at Finite Temperature

For the numerical calculations, the result of the power spectrum of massless and massive photons in two charge systems at finite temperatures comes from the source theory. We consider a two-electron move through a water medium. To plot graphs in both 2D and 3D from equations (4.1.34) and (4.2.21), we utilize Wolfram Mathematica. The details of numerical calculations and plot graphs are in Appendix D.

4.3.1 The power spectrum of massless photons in two charge system at temperature 0, 20, 50, 80, and 100 °C

To investigate the power spectrum of Cherenkov radiation produced by two-charge electron systems at a temperature of $T = 0$, 20, 50, 80, and 100 °C. We have plotted the first 2D graph of the power spectrum of massless photons in two-charge systems, as shown in Figure 13. The y-axis is the power spectrum in watts (W) and the x-axis is the distance between two charges in meters (m). The green, blue dash, yellow, blue, and red lines represent the temperature cases of 0, 20, 50, 80, and 100 °C, respectively. From the graph, we found that the power spectrum of two-charge systems is in the form of the function $\cos^2\left(\frac{a\omega}{2v}\right)$, where $a = 0$ m there is constructive interference, and at $a = 1.8 \times 10^{-7}$ m there is destructive interference. We also found that the power spectrum at temperatures 0 and 20 °C has almost no difference, while the power spectrum at temperatures 50, 80, and 100 °C has decreased slightly, respectively. The graph of the power spectrum for two-charge systems shows that the distance between two charges and the temperatures affect the value of the power spectrum, in which the distance between two charges a is related to the position of constructive and destructive interference in the power spectrum of Cherenkov radiation.

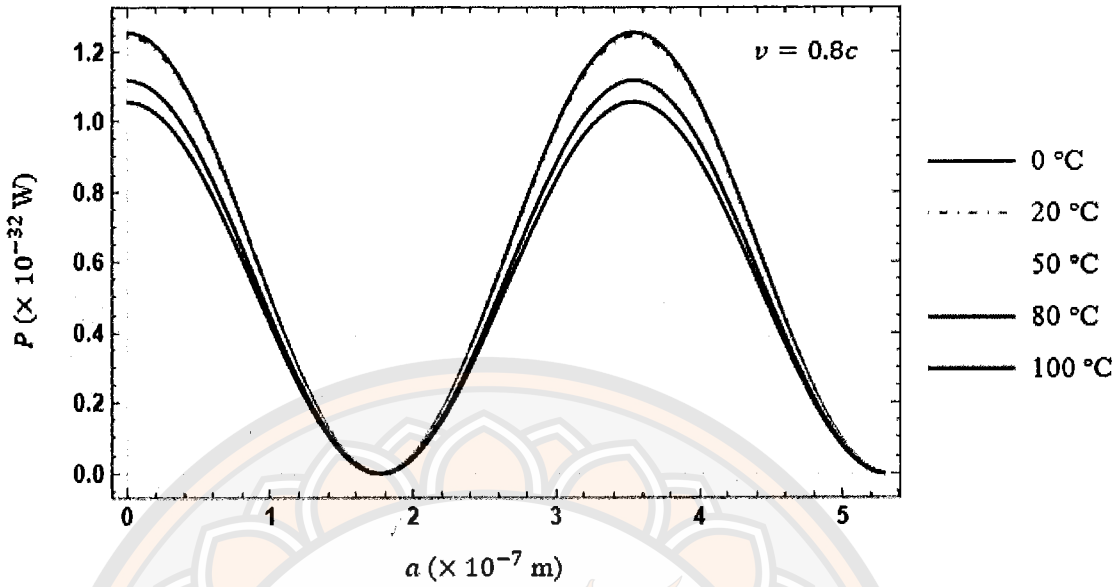

Figure 13 The power spectrum of massless photons in two charge system at 0, 20, 50, 80, and 100 °C.

4.3.2 The power spectrum of massless photons in two charge system at temperature 20 °C

The second graph is a 3D graph of the power spectrum of massless photons in two-charge electron systems at a finite temperature of $T = 20$ °C, which is similar to the previous graph and adds a z-axis of the velocity in meters per second (m/s) as in Figure 14. From the graph, it is found that the power spectrum is in the form of the function $\cos^2\left(\frac{a\omega}{2v}\right)$ as in the previous graph, and at higher velocities it affects interference of the power spectrum. However, at a velocity less than 2.2×10^8 m/s, there is weak interference of the power spectrum, and at a velocity greater than 2.2×10^8 m/s, there is more strong interference of the power spectrum. The graph indicate that the distance between two charges and the velocity affects interference in the power spectrum.

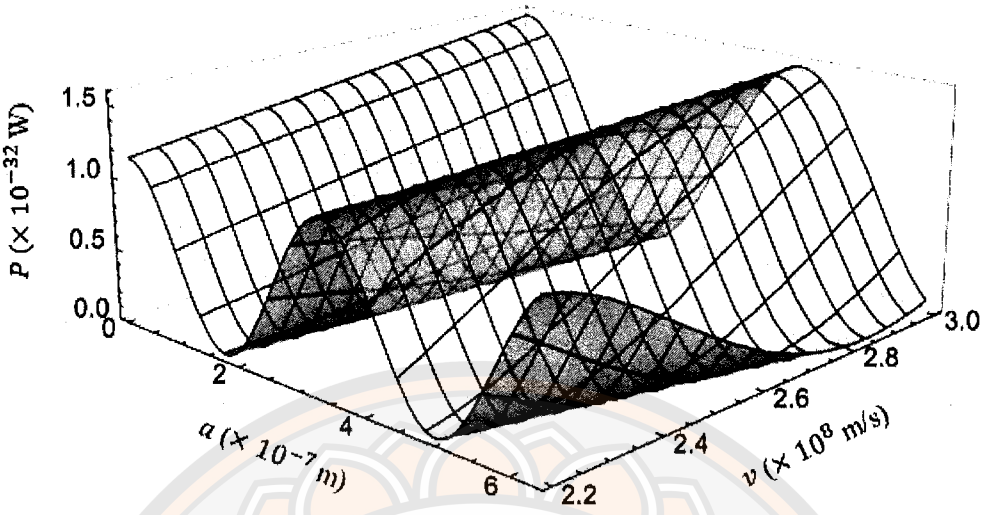

Figure 14 The power spectrum of massless photons in two charge system at 20 °C.

4.3.3 The power spectrum of massive photons in two charge system at temperature 0, 20, 50, 80, and 100 °C

The third graph as displayed in Figure 15 is a 2D graph of the power spectrum of massive photons in two charge systems at a temperature of $T = 0$, 20, 50, 80, and 100 °C. The y-axis is the power spectrum in watts (W) and the x-axis is the distance between two charges in meters (m). The green, blue dash, yellow, blue, and red lines represent the temperature cases of 0, 20, 50, 80, and 100 °C, respectively. From the graph, we found that the power spectrum of two-charge systems is in the form of the function $\cos^2\left(\frac{ac}{2vn}\sqrt{k^2+\frac{m^2c^2}{\hbar^2}}\right)$, where $a = 0$ m there is constructive interference, and at $a = 1.1 \times 10^{-7}$ m there is destructive interference. We also found that the power spectrum at temperatures 0 and 20 °C had no difference, while the power spectrum at temperatures 50, 80, and 100 °C decreased a little. The graph shows that the distance between two charges and the temperatures affect the power spectrum.

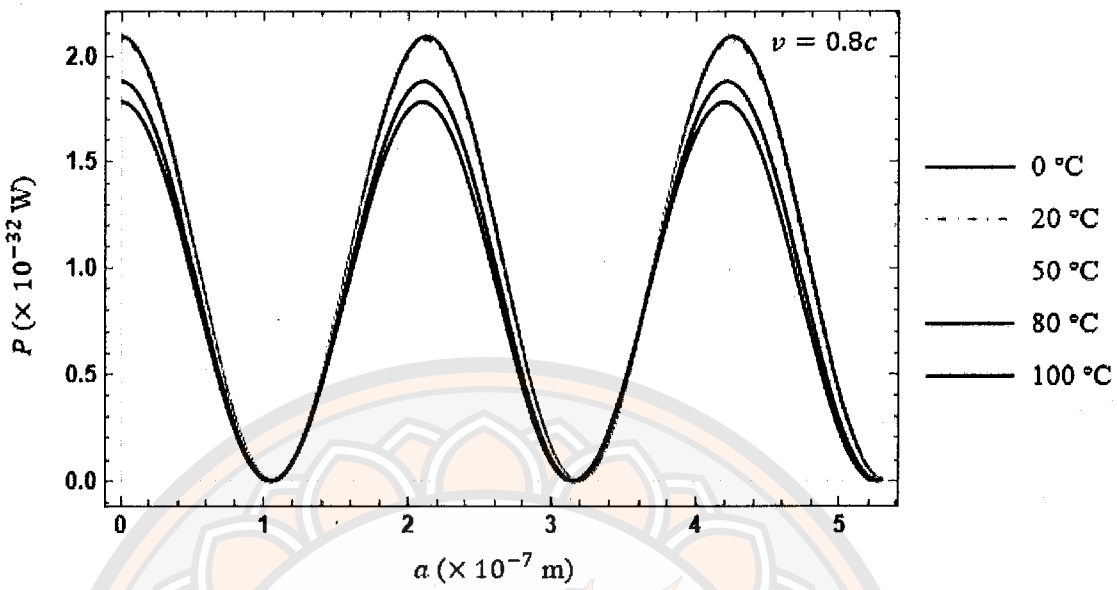

Figure 15 The power spectrum of massive photons in two charge system at 0, 20, 50, 80, and 100 °C.

4.3.4 The power spectrum of massive photons in two charge system at temperature 20 °C

The last graph as demonstrated in Figure 16 is a 3D graph of the power spectrum of massive photons in two charge systems at a temperature of $T = 20$ °C, which is similar to the previous graph in Figure 15 and adds a z-axis of the velocity in meters per second (m/s). From the graph, it is found that the power spectrum is in the form of the function $\cos^2\left(\frac{ac}{2vn}\sqrt{k^2+\frac{m^2c^2}{\hbar^2}}\right)$ as in the previous graph, and at higher velocities it affects the interference of the power spectrum as well. We also found that the minimum threshold velocity that causes the power spectrum of massive photons in water at a temperature of 20 °C is approximately 2.23×10^8 m/s. However, at a velocity less than 2.23×10^8 m/s, there is no interference with the power spectrum, and at a velocity greater than 2.23×10^8 m/s, there is beginning to be interference with the power spectrum. The graph indicates that the distance between two charges and the velocity influence the interference of the power spectrum. Therefore, we can infer that the distance between two charges

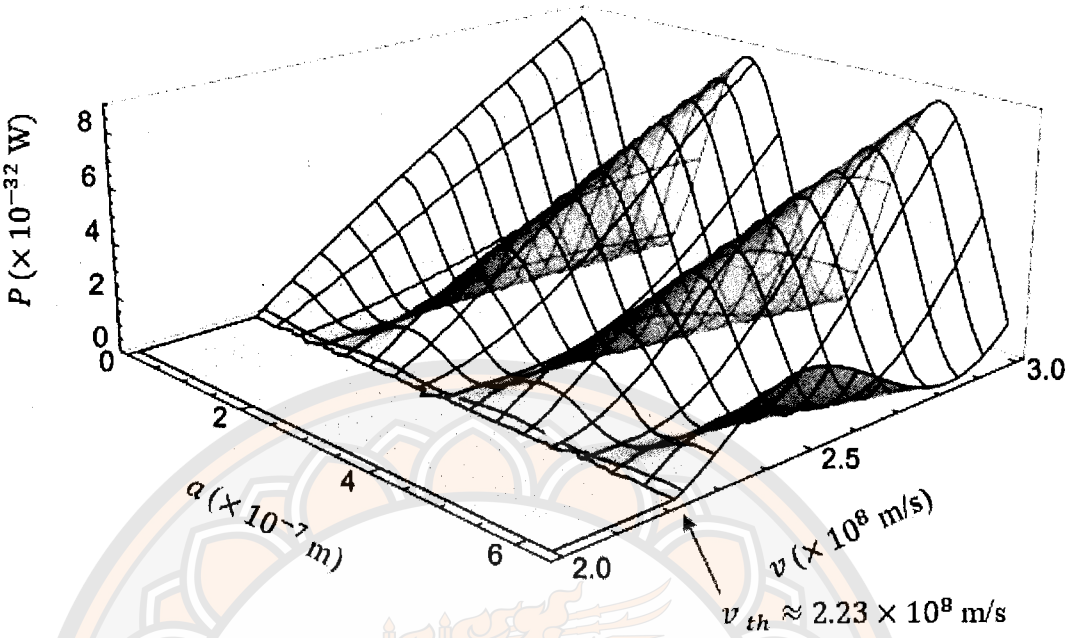

Figure 16 The power spectrum of massive photons in two charge system at 20 °C.

and the velocity affect the constructive and destructive interference of the power spectrum of Cherenkov radiation.

CHAPTER V

CONCLUSION AND DISCUSSION

The current theoretical study of the power spectrum of Cherenkov radiation is mostly based on classical electrodynamics theory. Nevertheless, quantum theory has been slightly applied in the Cherenkov radiation investigation, especially the source theory. In the study of Cherenkov radiation, we believe that quantum theory is powerful in calculating the properties of Cherenkov radiation. Therefore, this dissertation aims to apply the quantum theory focus on the source theory to calculate the power spectrum of Cherenkov radiation in two cases. The first case is to calculate the power spectrum of massive photons at a finite temperature from a charged electron moving through a dielectric medium. In the second case, to calculate the power spectrum of massless and massive photons at a finite temperature from a two-charge electron system moving through a dielectric medium. In addition, to prove the validity of the result, we also did numerical calculations of the power spectrum in each case.

5.1 Conclusion

5.1.1 Power Spectrum of Massive Photons at Finite Temperature

In order to calculate the power spectrum of the massive photon at a finite temperature, we start with the calculation of the propagator of massive photons at finite temperatures in the medium by applying the calculation of the massless photon propagator. Then, we calculate the action of the massive electromagnetic field from the propagator of massive photons at finite temperatures. Finally, we can derive the power spectrum of the massive photon at a finite temperature from the action as follows

$$P_{\mathrm{T}} = \frac{e^2}{4\pi}\frac{v\mu}{nc}\sqrt{k^2+\frac{m^2c^2}{\hbar^2}}\left(1-\frac{1}{n^2\beta^2}\right)\times\coth\left(\frac{\hbar c}{2nk_BT}\sqrt{k^2+\frac{m^2c^2}{\hbar^2}}\right) \quad (5.1.1)$$

In addition, to validate the power spectrum calculation at a finite temperature derived from the source theory above, we apply the numerical calculation method with conditions to present trends and the probability of the power spectrum changing by the graph. Firstly, we plotted the 2D graph of the power spectrum at a temperature of 0, 20, 50, 80, and 100 °C, it was found that the power spectrum at 0 and 20 °C has almost no difference, while the power spectrum at 50, 80, and 100 °C has decreased slightly. In addition, we also found that the minimum velocity that causes the power spectrum to be above zero at temperatures 0 and 20 °C is approximately 2.23×10^8 m/s, however, at temperature 100 °C the velocity is more than 2.26×10^8 m/s. So, it can be inferred that temperature and velocity influence the power spectrum of Cherenkov radiation. Secondly, the comparison of massless and massive photons at a temperature of 20 °C, displays that the power spectrum of massive photons is more than approximately two times of the massless photons. We also found that the minimum velocity that causes the power spectrum of massless and massive photons to be above zero is about 2.23×10^8 m/s. It concludes that the mass of photons and the velocity affect the power spectrum of Cherenkov radiation. Thirdly, the graph shows the power spectrum of massive photons at a temperature of 20 °C in the 3D graph, we also found that the results are the same as in the previous graph which shows that increasing the photon mass and velocity influence the power spectrum of Cherenkov radiation.

5.1.2 Power Spectrum of Massless and Massive Photons in Two Charge System

To calculate the total power spectrum of the massless photon in two charge systems at a finite temperature, we start with the calculation of the propagator of massless photons at finite temperatures in the medium. After that, we calculate the action of the massless electromagnetic field from the propagator of massless

photons at finite temperatures. Then, we calculate the power spectrum of the massive photon at a finite temperature from the action. Lastly, we sum the power spectrum of two charged systems and will get the total power spectrum of the massless photon in two charged systems at a finite temperature the following:

$$P_{\text{total}} = \frac{e^2}{\pi}\frac{\mu\omega}{c^2}v\left(1-\frac{1}{n^2\beta^2}\right)\cos^2\left(\frac{a\omega}{2v}\right)\times\coth(\hbar\omega/2k_BT) \tag{5.1.2}$$

For the case of the total power spectrum of the massive photon in two charge systems at finite temperatures, the calculation method is similar to the previous one. We can calculate the total power spectrum of the massive photon in two charged systems at a finite temperature from the summation of the power spectrum of the massive photon at a finite temperature of two charged systems. Eventually, we get the total power spectrum of the massive photon in two charge systems at finite temperatures as the following:

$$\begin{aligned} P_{\text{total}} = &\frac{e^2}{\pi}\frac{\mu v}{cn}\sqrt{k^2+\frac{m^2c^2}{\hbar^2}}\left(1-\frac{1}{n^2\beta^2}\right)\cos^2\left(\frac{ac}{2vn}\sqrt{k^2+\frac{m^2c^2}{\hbar^2}}\right) \\ &\times\coth\left(\frac{\hbar c}{2nk_BT}\sqrt{k^2+\frac{m^2c^2}{\hbar^2}}\right) \end{aligned} \tag{5.1.3}$$

For the numerical verification, we plot 2D and 3D graphs with circumstances that fit with the power spectrum calculation above. Firstly, the power spectrum of massless photons in two charge systems at temperatures 0, 20, 50, 80, and 100 °C, concludes that the power spectrum at 0 and 20 °C has almost no difference, in turn, the power spectrum at 50, 80, and 100 °C has decreased slightly. The distance between two charges and temperatures affects the value of the power spectrum, in which the distance between two charges a, is related to the position of constructive and destructive interference in the power spectrum of Cherenkov radiation. Secondly, when plotting the 3D graph of the power spectrum of massless photons in two charge systems at a temperature of 20 °C, the result revealed the change in the power spectrum is the same as the 2D graph plotting, which is the distance between two charges and the velocity affects the interference of the power spectrum. Thirdly, the 2D graph plotting the power spectrum of massive photons

in two charge systems at temperatures 0, 20, 50, 80, and 100 °C, concludes that the power spectrum at 0 and 20 °C had no difference, however, the power spectrum at 50, 80, and 100 °C has decreased a tiny. Also, the distance between two charges and the temperature affects the power spectrum of Cherenkov radiation. Lastly, the graph shows the power spectrum of massive photons in two charge systems at a temperature of 20 °C in the 3D graph. We found that the results are the same as the previous graph, which shows the distance between two charges and how temperatures affect the power spectrum of Cherenkov radiation. We also found that the minimum threshold velocity that causes the power spectrum of massive photons in water at a temperature of 20 °C is approximately 2.23×10^8 m/s.

5.2 Discussion

This study indicates a correlation between the temperature of the medium and the power spectrum of Cherenkov radiation. As the temperature rises, there is a slight decrease in the power spectrum. This is because of the change in the refractive index of the medium (n) with temperature (T) (Bashkatov and Genina, 2003; Tan, 2021). The refractive index is crucial because it determines the phase speed of light in the medium. A higher temperature leads to a lower refractive index, which in turn increases the phase speed of light ($v_p = c/n$). The phase speed of light affects the threshold of Cherenkov radiation generated. Therefore, when the temperature increases, it influences the power spectrum of Cherenkov radiation. The result is consistent with Pardy (1989), which studies the power spectrum of Cherenkov radiation at finite temperatures. This study contributes to a deeper understanding of the relation of light-medium interactions at various temperatures for the occurrence of Cherenkov radiation.

In the case of massive photons, the study found that a mass of photons greater than zero results in an increase in the power spectrum of Cerenkov radiation. This is because the dispersion relation for massive photons indicates that the frequency (ω) and refractive index of light (n) depend on the photon mass (m)

(Pardy, 2002). Consequently, when we consider photon mass greater than zero, this would lead to an increase in the power spectrum of Cerenkov radiation. The results of this study correspond to the power spectrum formula of massive photons derived from Pardy (2002). The concept of massive photons, though not widely accepted in the standard model of particle physics, presents interesting possibilities in the realm of theoretical research.

Cherenkov radiation, a phenomenon where charged particles emit light as they travel through a dielectric medium faster than the phase velocity of light in that medium, is well-known for the case of single particles (Schwinger et al., 1976). However, in the case of two charged particles, the radiation emitted is an output of the superposition of the electromagnetic waves produced by each particle. If the particles move in parallel and at the same velocity, the wavefronts may cause constructive interference, potentially intensifying the power spectrum of Cerenkov radiation. Conversely, if their paths or velocities differ, the interference could be destructive, reducing the power spectrum of the radiation. The distance between two charged systems affects the interference in the power spectrum, which is consistent with Pardy's (1999) formula for the power spectrum in two charged systems. Additionally, the geometry of the radiation emitted may alter, forming a more complex pattern than the classic conical shape seen with a single particle. Understanding these variations is crucial for applications in particle physics experiments and medical imaging, where precise measurements of Cherenkov radiation are used to analyze high-speed particles and diagnose medical.

REFERENCES

REFERENCES

Agarwal, N. S. (2016). New Quantum Theory Explains All the Mysterious Quantum Phenomena. *Journal of Modern Physics, 7*(15), 2135-2154.

Alfimov, M. (2010). Cherenkov radiation in moving medium. *International Journal of Theoretical Physics, 49*, 2215-2229.

Bashkatov, A. N., & Genina, E. A. (2003). Water refractive index in dependence on temperature and wavelength: a simple approximation. In *Saratov Fall Meeting: Optical Technologies in Biophysics and Medicine IV* (p. 393-395).

Bolotovskii, B. M. (2009). Vavilov–Cherenkov radiation: its discovery and application. *Physics-Uspekhi, 52*(11), 1099.

Cerenkov, P. A. (1934). Visible luminescence of pure liquids under action of gamma radiation. *Doklady Akad Nauk (USSR)*, (2), 451-454.

Cerenkov, P.A. (1936). The effect of a magnetic field on the visible glow of liquids caused by gamma rays. *Dokl. Akad. Nauk, SSSR, 3*(9), 413-416.

Cerenkov, P.A. (1937). Visible radiation of pure liquids under the action of fast electrons. *Byull. Akad. Nauk, SSSR,* (4-5), 455-492.

Cerenkov, P.A. (1938). Spatial distribution of visible radiation produced by fast electrons. *Dokl. Akad. Nauk, SSSR, 21*(7), 319-321.

Chamberlain, O., Segre, E., Wiegand, C., & Ypsilantis, T. (1955). Observation of antiprotons. *Physical Review, 100*(3), 947.

Ciarrocchi, E., & Belcari, N. (2017). Cerenkov luminescence imaging: physics principles and potential applications in biomedical sciences. *EJNMMI physics, 4*, 1-31.

Curie, E., Barres, P., & de Sales, R. D. R. (Eds.). (1941). *They speak for a nation: Letters from France.* New York: Doubleday.

DeRaad Jr, L. L., Tsai, W. Y., & Erber, T. (1978). Interference between transition and Cerenkov radiation. *Physical Review D, 18*(6), 2152.

Drimal, J. (1984). Contribution to interference between transition and Cerenkov radiation. *Czechoslovak Journal of Physics B, 34*(4), 280-284.

Feynman, R. P., Leighton, R. B., & Sands, M. L. (2010). *The Feynman Lectures on Physics, Vol. III: The New Millenium Edition: Quantum Mechanics.* New York: Basic Books.

Feynman, R. P., Leighton, R. B., & Sands, M. (2011). *The Feynman lectures on physics, Vol. I: The new millennium edition: mainly mechanics, radiation, and heat.* New York: Basic Books.

Frank, I.M., & Tamm, I.G. (1937). Coherent visible radiation of fast electrons passing through matter. *Dokl. Akad. Nauk, SSSR, 14*, 109.

Garibian, G. M. (1958). Contribution to the theory of transition radiation. *Sov. Phys. JETP, 6*(6), 1079.

Ginzburg, V. L. (1940). Quantum theory of radiation of electron uniformly moving in medium. *Zh. Eksp. Teor. Fiz, 10*, 589.

Ginzburg, V. L., & Frank, I. M. (1945). Radiation of a uniformly moving electron due to its transition from one medium into another. *Journal of Physics (USSR), 9*, 353-362.

Ginzburg, V. L., & Tsytovich, V. N. (1979). Several problems of the theory of transition radiation and transition scattering. *Physics Reports, 49*(1), 1-89.

Ginzburg, V. L. (1982). Transition radiation and transition scattering. *Physica Scripta, 1982*(T2A), 182.

Ginzburg, V. L. (1996). Radiation by uniformly moving sources. *Physics-Uspekhi, 39*(10), 973.

Ginzburg, V. L. (2005). Radiation from uniformly moving sources (Vavilov-Cherenkov effect, transition radiation, and some other phenomena). *Acoustical Physics, 51*(1), 11-23.

Griffiths, D. J. (2013). *Introduction to electrodynamics.* New York: Cambridge University Press.

Hamming, R. (2012). *Numerical methods for scientists and engineers.* New York: Courier Corporation.

Helbig, K. (2015). *Foundations of Anisotropy for Exploration Seismics: Section I.* Seismic Exploration. N.P.: Elsevier.

Jackson, J. D. (1999). *Classical electrodynamics.* New York: John Wiley and Sons.

Jelley, J. V. (1959). *Cerenkov Radiation, and Its Applications.* Published for the United Kingdom Energy Authority by Pergamon Press

Kheirandish, F., & Amooghorban, E. (2010). Finite-temperature Cherenkov radiation in the presence of a magnetodielectric medium. *Physical Review A, 82*(4), 042901.

Kobzev, A. P. (2010). The mechanism of Vavilov-Cherenkov radiation. *Physics of Particles and Nuclei, 41*, 452-470.

Kobzev, A. P. (2014). On the radiation mechanism of a uniformly moving charge. *Physics of Particles and Nuclei, 45*, 628-653.

Koshiba, M. (2003). Nobel Lecture: Birth of neutrino astrophysics. *Reviews of Modern Physics, 75*(3), 1011.

L'Annunziata, M. F., Grahek, Z., & Todorovic, N. (2020). *Cherenkov counting. In Handbook of Radioactivity Analysis* (p. 393-530). London: Academic Press.

Lifshitz, E.M., & Pitaevskii, L.P. (1984). *Statistical Physics, Part2.* Oxford: Pergamon Press.

Macleod, A. J., Noble, A., & Jaroszynski, D. A. (2019). Cherenkov radiation from the quantum vacuum. *Physical review letters, 122*(16), 161601.

Mallet, L. (1926). Spectral research of luminescence of water and other media with gamma radiation. *Comptes Rendus, 187*, 222.

Mallet, L., (1928). Spectral study of the luminescence of water and carbon disulfide under gamma radiation. *Compt. Rend. Acad. Sci. Paris, 187*, 222-223.

Mallet, L., (1929). The ultra-violet radiation of substances subjected to grays. *Compt. Rend. Acad. Sci. Paris, 188*, 445-447.

Manoukian, E. B. (2012). *Modern concepts and theorems of mathematical statistics.* New York: Springer Science and Business Media.

Manoukian, E. B. (2015). Vacuum-to-vacuum transition probability and radiation in a medium. *Radiation Physics and Chemistry, 112*, 104-107.

Mirzoyan, R. (2022). Technological Novelties of Ground-Based Very High Energy Gamma-Ray Astrophysics with the Imaging Atmospheric Cherenkov Telescopes. *Universe, 8*(4), 219.

Pardy, M. (1989). Finite-temperature Cerenkov radiation. *Physics Letters A, 134* (6), 357-359.

Pardy, M. (1994). The Cerenkov effect with radiative corrections. *Physics Letters B, 325*(3-4), 517-520.

Pardy, M. (1995). Finite-temperature gravitational Cerenkov radiation. *International Journal of Theoretical Physics, 34*, 951-959.

Pardy, M. (1997). Cerenkov effect and the Lorentz contraction. *Physical Review A, 55*(3), 1647.

Pardy, M. (1999). The Cerenkov effect with massive photons. *arXiv*:hep-ph/9912544

Pardy, M. (2002). Cerenkov effect with massive photons. *International Journal of Theoretical Physics, 41*, 887-901.

Pardy, M. (2015). The two-dimensional Vavilov–Cerenkov radiation in LED. *Results in Physics, 5*, 69-71.

Pardy, M. (2022). The 3D and 2D Cerenkov effect with massive photons. *viXra*:2205.0103

Pardy, M. (2023). The Cerenkov Radiation from Dipole and the Lorentz Contraction. *viXra*:2305.0092

Roques-Carmes, C., Rivera, N., Joannopoulos, J. D., Soljacic, M., & Kaminer, I. (2018). Quantum Verenkov radiation in weakly and strongly-coupled regimes. In CLEO: QELS Fundamental Science. *Optica Publishing Group.*

Schwinger, J. (1970). *Particles, Sources and Fields; Vol.I.* Redwood: Addison-Wesley.

Schwinger, J., Tsai, W. Y., & Erber, T. (2000). Classical and Quantum Theory of Synergic Synchrotron–Cerenkov Radiation. *Annals of Physics, 281* (1-2), 1019-1048.

Schwinger, J., DeRaad Jr, L. L., Milton, K., & Tsai, W. Y. (2019). *Classical electrodynamics.* Boca Raton: CRC Press.

Tan, C. Z. (2021). Dependence of the refractive index on density, temperature, and the wavelength of the incident light. *The European Physical Journal B, 94*(7), 139.

Tanha, K., Pashazadeh, A. M., & Pogue, B. W. (2015). Review of biomedical Cerenkov luminescence imaging applications. *Biomedical optics express, 6*(8), 3053-3065.

Tuchin, K. (2018). Chiral Cherenkov and chiral transition radiation in anisotropic matter. *Physical Review D, 98*(11), 114026.

Vavilov, Y. N., Pugachova, G. I., & Fedorov, V. M. (1963). Muon groups near the axis of an extensive air shower. *Soviet Physics JETP, 17*(2).

Wang, X., Li, L., Li, J., Wang, P., Lang, J., & Yang, Y. (2022). Cherenkov luminescence in tumor diagnosis and treatment: a review. *Photonics, 9,* (6), 390.

APPENDICES

APPENDIX A List of Some Symbols and Physical Constants

The constants listed here are the values of some physical constants expressed in SI units. We use these constants for the numerical calculations of the power spectrum in each case.

c = Speed of light in vacuum, which is $299792458 \approx 3 \times 10^8$ m / s

$\hbar$ = Reduced Planck constant, which is $1.054571817 \times 10^{-34}$ J.s

e = Electron charge, which is $1.60217663 \times 10^{-19}$ C

k_B = Boltzmann constant, which is 1.380649×10^{-23} J / K

f = The frequency of photon

ω = The angular frequency of photons

n = The refractive index of the medium

T = The temperature of the medium

P = The power spectrum

APPENDIX B Photon Constants and Refractive Index

Table 4 True mass of photons for various wavelengths and frequencies.

Radiation Type	Wavelength (Nanometer)	Energy (Joule)	Frequency (f) (Cycles/second)	True Mass of Photon (af) (Kg)
Gamma Rays	0.001	$1.9864458 \times 10^{-13}$	$2.99792458 \times 10^{20}$	$4.420438115 \times 10^{-30}$
X Rays	1.0	$1.9864458 \times 10^{-16}$	$2.99792458 \times 10^{17}$	$4.420438115 \times 10^{-33}$
Ultra Violet	100	$1.9864458 \times 10^{-18}$	$2.99792458 \times 10^{15}$	$4.420438115 \times 10^{-35}$
Dark Blue	442	$4.4942213 \times 10^{-19}$	$6.78263479 \times 10^{14}$	$1.000099121 \times 10^{-35}$
Green	531	$3.7409525 \times 10^{-19}$	$5.64580900 \times 10^{14}$	$8.324742213 \times 10^{-36}$
Red	633	$6.6260700 \times 10^{-19}$	$4.73605778 \times 10^{14}$	$6.983314558 \times 10^{-36}$
Infra Red	1000	$1.9864458 \times 10^{-19}$	$2.99792458 \times 10^{14}$	$4.420438115 \times 10^{-36}$

Note: Data from the article titled New Quantum Theory Explains All the Mysterious Quantum Phenomena in the Journal of Modern Physics.

Table 5 Refractive index of water depends on temperature and wavelength.

Temperature, ^0C	*Wavelength*				
	226.5 *nm*	361.05 *nm*	404.41 *nm*	589 *nm*	632.8 *nm*
0	1.3945	1.34896	1.34415	1.33432	1.33306
10	1.39422	1.3487	1.34389	1.33408	1.33282
20	1.39336	1.34795	1.34315	1.33336	1.33211
30	1.39208	1.34682	1.34205	1.3323	1.33105
40	1.39046	1.3454	1.34065	1.33095	1.32972
50	1.38854	1.34373	1.33901	1.32937	1.32814
60	1.38636	1.34184	1.33714	1.32757	1.32636
70	1.38395	1.33974	1.33508	1.32559	1.32438
80	1.38132	1.33746	1.33284	1.32342	1.32223
90	1.37849	1.33501	1.33042	1.32109	1.31991
100	1.37547	1.33239	1.32784	1.31861	1.31744

Source: Index of refraction of water in Handbook of Chemistry and Physics, Eds. Lide D.R., CRC Press, 2000-2001.

APPENDIX C Numerical Calculation of Power Spectrum at Finite Temperature

The numerical calculations, the result of the power spectrum of massive photons at finite temperatures is derived from the source theory. We plot graphs in both 2D and 3D from equation (3.2.14). Details of the numerical calculations and plot graph are following.

$$P_T = \frac{e^2}{4\pi}\frac{v}{nc}\sqrt{k^2+\frac{m^2c^2}{\hbar^2}}\left(1-\frac{1}{n^2\beta^2}\right)\times\coth\left[\frac{\hbar c}{2nk_BT}\sqrt{k^2+\frac{m^2c^2}{\hbar^2}}\right];$$

$$m = 0\ \text{kg}, k^2 = \frac{(2\pi)^2}{\lambda^2}, \lambda = 442 * 10\text{^} - 9\ \text{m}$$

$$n = 1.34415\,(0°\text{C})\,, n = 1.34315\,(20°\text{C})\,, n = 1.32784\,(100°\text{C})$$

$$T = 0°\text{C}(273.15\ \text{K}), T = 20°\text{C}(293.15\ \text{K}), T = 100°\text{C}(373.15\ \text{K})$$

$$\text{ln}[1] := P_{T=20} = \frac{(1.60217663\times 10\text{^} - 19)\text{^}\,2}{4\pi}$$
$$\times\frac{v}{(1.34315)*(3*10\text{^}8)}\sqrt{\frac{(2\pi)^2}{(442*10\text{^} - 9)^2}}\left(1-\frac{1}{(1.34315)^2\left(\frac{v}{3*10\text{^}8}\right)^2}\right)$$
$$\times\coth\left[\frac{1.054571817\times 10\text{^} - 34*(3*10\text{^}8)}{2*(1.34315)*1.380649\times 10\text{^} - 23*293.15}\sqrt{\frac{(2\pi)^2}{(442*10\text{^} - 9)^2}}\right]$$

$$\text{Out}\ [1] = 7.20647\times 10^{-41}\left(1-\frac{4.98877\times 10^{16}}{v^2}\right)v$$

$$P_T = \frac{e^2}{4\pi}\frac{v}{nc}\sqrt{k^2+\frac{m^2c^2}{\bar{h}^2}}\left(1-\frac{1}{n^2\beta^2}\right)\times \mathrm{Coth}\left[\frac{\bar{h}c}{2nk_BT}\sqrt{k^2+\frac{m^2c^2}{\bar{h}^2}}\right];$$

$$m = 1.000099121\times 10\text{^}-35\ \mathrm{kg}, \mathrm{k}^2 = \frac{(2\pi)^2}{\lambda^2}, \lambda = 442*10\text{^}-9\ \mathrm{m}$$

$$\mathrm{T} = 0°\mathrm{C}(273.15\ \mathrm{K}), \mathrm{T} = 20°\mathrm{C}(293.15\ \mathrm{K}), \mathrm{T} = 100°\mathrm{C}(373.15\ \mathrm{K})$$

$$\mathrm{In}[2] := P_{T=0} = \frac{(1.60217663\times 10\text{^}-19)\text{^}2}{4\pi}\frac{v}{(1.34415)*(3*10\text{^}8)}$$
$$\times\sqrt{\frac{(2\pi)^2}{(442*10\text{^}-9)^2}+\frac{(1.000099121\times 10\text{^}-35)^2*(3*10\text{^}8)^2}{(1.054571817\times 10\text{^}-34)^2}}$$
$$\times\left(1-\frac{1}{(1.34415)^2\left(\frac{v}{3*10\text{^}8}\right)^2}\right)\times\coth\left[\frac{1.054571817\times 10\text{^}-34*(3*10\text{^}8)}{2*(1.34415)*1.380649\times 10\text{^}-23*273.15}\right.$$
$$\left.\times\sqrt{\frac{(2\pi)^2}{(442*10\text{^}-9)^2}+\frac{(1.000099121\times 10\text{^}-35)^2*(3*10\text{^}8)^2}{(1.054571817\times 10\text{^}-34)^2}}\right]$$

$$\mathrm{Out}[2] = 1.61111\times 10^{-40}\left(1-\frac{4.98135\times 10^{16}}{v^2}\right)v$$

$$\mathrm{In}[3] := P_{T=20} = \frac{(1.60217663\times 10\text{^}-19)\text{^}2}{4\pi}\frac{v}{(1.34315)*(3*10\text{^}8)}$$
$$\times\sqrt{\frac{(2\pi)^2}{(442*10\text{^}-9)^2}+\frac{(1.000099121\times 10\text{^}-35)^2*(3*10\text{^}8)^2}{(1.054571817\times 10\text{^}-34)^2}}$$
$$\times\left(1-\frac{1}{(1.34315)^2\left(\frac{v}{3*10\text{^}8}\right)^2}\right)\times\coth\left[\frac{1.054571817\times 10\text{^}-34*(3*10\text{^}8)}{2*(1.34315)*1.380649\times 10\text{^}-23*293.15}\right.$$
$$\left.\times\sqrt{\frac{(2\pi)^2}{(442*10\text{^}-9)^2}+\frac{(1.000099121\times 10\text{^}-35)^2*(3*10\text{^}8)^2}{(1.054571817\times 10\text{^}-34)^2}}\right]$$

$$\mathrm{Out}[3] = 1.61231\times 10^{-40}\left(1-\frac{4.98877\times 10^{16}}{v^2}\right)v$$

$$\ln[4] := P_{T=50} = \frac{(1.60217663 \times 10\text{^} - 19)\text{^}2}{4\pi} \frac{v}{(1.33901) * (3 * 10\text{^}8)}$$
$$\sqrt{\frac{(2\pi)^2}{(442 * 10\text{^} - 9)^2} + \frac{(1.000099121 \times 10\text{^} - 35)^2 * (3 * 10\text{^}8)^2}{(1.054571817 \times 10\text{^} - 34)^2}}$$
$$\left(1 - \frac{1}{(1.33901)^2 \left(\frac{v}{3*10\text{^}8}\right)^2}\right) \times \text{Coth}\left[\frac{1.054571817 \times 10\text{^} - 34 * (3 * 10\text{^}8)}{2 * (1.33901) * 1.380649 \times 10\text{^} - 23 * 323.15}\right.$$
$$\left.\sqrt{\frac{(2\pi)^2}{(442 * 10\text{^} - 9)^2} + \frac{(1.000099121 \times 10\text{^} - 35)^2 * (3 * 10\text{^}8)^2}{(1.054571817 \times 10\text{^} - 34)^2}}\right]$$
$$\text{Out}[4]= 1.61729 \times 10^{-40} \left(1 - \frac{5.01967 \times 10^{16}}{v^2}\right) v$$

$$\ln[5] := P_{T=80} = \frac{(1.60217663 \times 10\text{^} - 19)\text{^}2}{4\pi} \frac{v}{(1.33284) * (3 * 10\text{^}8)}$$
$$\sqrt{\frac{(2\pi)^2}{(442 * 10\text{^} - 9)^2} + \frac{(1.000099121 \times 10\text{^} - 35)^2 * (3 * 10\text{^}8)^2}{(1.054571817 \times 10\text{^} - 34)^2}}$$
$$\left(1 - \frac{1}{(1.33284)^2 \left(\frac{v}{3*10\text{^}8}\right)^2}\right) \times \text{Coth}\left[\frac{1.054571817 \times 10\text{^} - 34 * (3 * 10\text{^}8)}{2 * (1.33284) * 1.380649 \times 10\text{^} - 23 * 353.15}\right.$$
$$\left.\sqrt{\frac{(2\pi)^2}{(442 * 10\text{^} - 9)^2} + \frac{(1.000099121 \times 10\text{^} - 35)^2 * (3 * 10\text{^}8)^2}{(1.054571817 \times 10\text{^} - 34)^2}}\right]$$
$$\text{Out}[5]= 1.62478 \times 10^{-40} \left(1 - \frac{5.06625 \times 10^{16}}{v^2}\right) v$$

$$\ln[6] := P_{T=100} = \frac{(1.60217663 \times 10\text{^} - 19)\text{^}2}{4\pi} \frac{v}{(1.32784) * (3 * 10\text{^}8)}$$
$$\sqrt{\frac{(2\pi)^2}{(442 * 10\text{^} - 9)^2} + \frac{(1.000099121 \times 10\text{^} - 35)^2 * (3 * 10\text{^}8)^2}{(1.054571817 \times 10\text{^} - 34)^2}}$$
$$\left(1 - \frac{1}{(1.32784)^2 \left(\frac{v}{3*10\text{^}8}\right)^2}\right) \times \text{Coth}\left[\frac{1.054571817 \times 10\text{^} - 34 * (3 * 10\text{^}8)}{2 * (1.32784) * 1.380649 \times 10\text{^} - 23 * 373.15}\right.$$
$$\left.\sqrt{\frac{(2\pi)^2}{(442 * 10\text{^} - 9)^2} + \frac{(1.000099121 \times 10\text{^} - 35)^2 * (3 * 10\text{^}8)^2}{(1.054571817 \times 10\text{^} - 34)^2}}\right]$$
$$\text{Out}[6]= 1.6309 \times 10^{-40} \left(1 - \frac{5.10447 \times 10^{16}}{v^2}\right) v$$

$$\text{In[7]} := \text{Plot}\left[\left\{1.6111 \times 10^{-40}\left(1 - \frac{4.9813 \times 10^{16}}{\text{v}^2}\right)\text{v}\ ,\right.\right.$$

$$1.6123 \times 10^{-40}\left(1 - \frac{4.9888 \times 10^{16}}{v^2}\right)v, 1.61729 \times 10^{-40}\left(1 - \frac{5.01967 \times 10^{16}}{v^2}\right)v,$$

$$\left.\left.1.62478 \times 10^{-40}\left(1 - \frac{5.06625 \times 10^{16}}{v^2}\right)v, 1.6309 \times 10^{-40}\left(1 - \frac{5.1045 \times 10^{16}}{v^2}\right)v\right\},\right.$$

$$\{v, 2.2 \times 10^8, 3 \times 10^8\},\ \text{PlotRange} \rightarrow \{0, 2 \times 10^{-32}\},$$

$$\text{PlotLegends} \rightarrow \{\ 0°\text{C}, 20°\text{C}, 50°\text{C}, 80°\text{C}, 100°\text{C}\},$$

$$\text{PlotStyle} \rightarrow \{Green, DotDashed, Yellow, Blue, Red\}]$$

Out[7]=

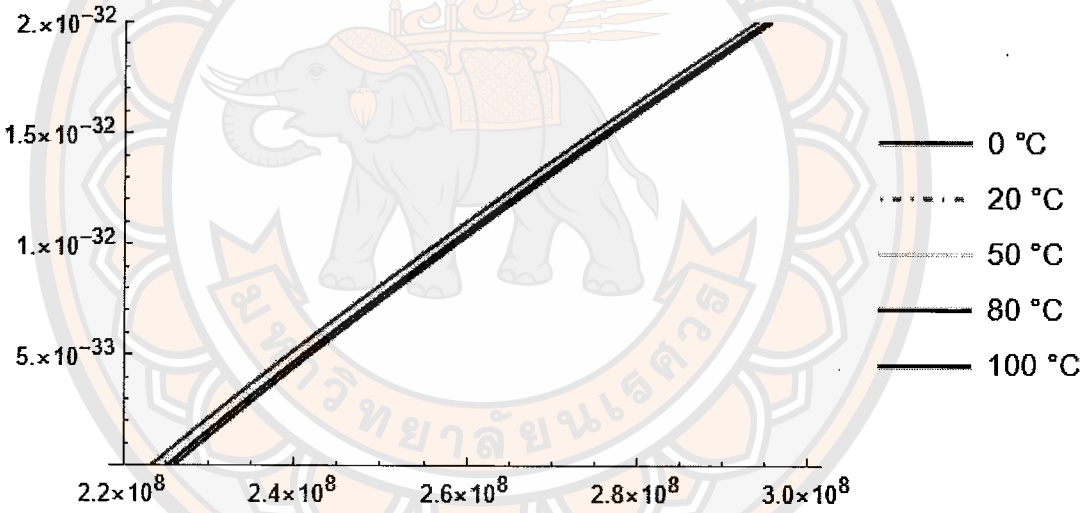

Figure 17 Plot the power spectrum of massive photons at 0, 20, and 100 °C.

$$\text{In[8]} := \text{Plot}\left[\left\{1.6123087853709085 \times 10^{-40}\left(1 - \frac{4.9887699393530056 \times 10^{16}}{v^2}\right)v\right.\right.$$

$$\left.\left.7.206472756429646 \times 10^{-41}\left(1 - \frac{4.9887699393530056 \times 10^{16}}{v^2}\right)v\right\}, \{v, 2.2 \times 10^8, 3 \times 10^8\}\right.$$

$$\text{PlotRange} \rightarrow \{0, 2 \times 10^{-32}\},\ \text{PlotLegends} \rightarrow \{\text{m} = 1 \times 10^{-35}\ \text{kg},\ \text{m} = 0\ \text{kg}\}]$$

Out[8]=

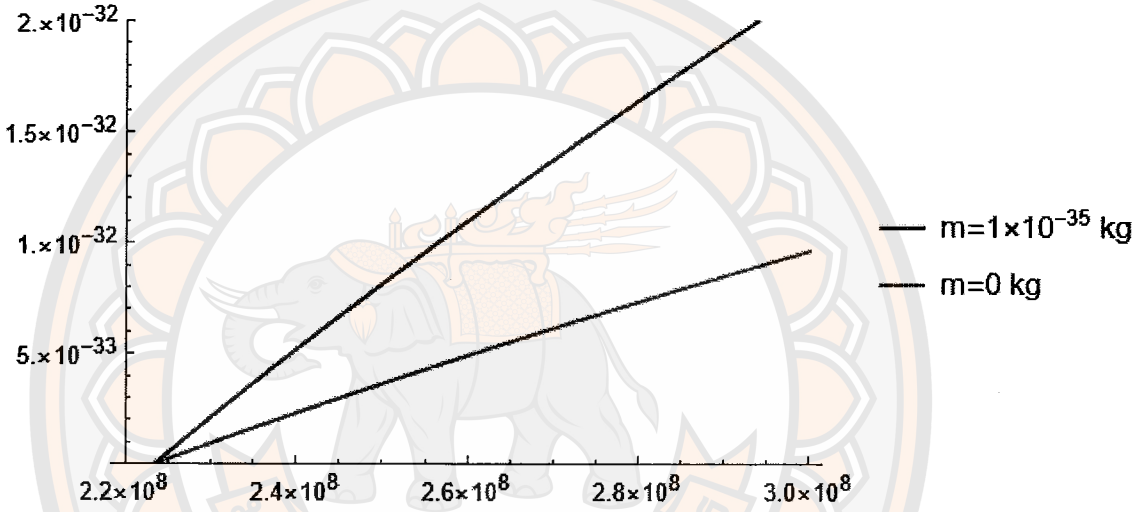

Figure 18 Plot the power spectrum of massless and massive photons at 20 °C.

$$\text{In[9]} := \text{Plot3D}\left[5.06573 \times 10^{-48}\sqrt{8.09264 \times 10^{84}m^2 + \frac{10^{18}\pi^2}{48841}}\left(1 - \frac{4.98135 \times 10^{16}}{v^2}\right)v\right.$$

$$\sqrt{8.092639376356166 \times 10^{84}\ \text{m}^2 + \frac{10^{18}\pi^2}{48841}}\left(1 - \frac{4.9887699393530056 \times 10^{16}}{v^2}\right)v$$

$$\left.\text{Coth}\left[3.12058 \times 10^{-6}\sqrt{8.092639376356166 \times 10^{84}\ \text{m}^2 + \frac{10^{18}\pi^2}{48841}}\right],\right.$$

$$\left.\{m, 0, 1 \times 10^{-35}\}, \{v, 2 \times 10^8, 3 \times 10^8\},\ \text{PlotRange} \to \{0, 2.4 \times 10^{-32}\}\right]$$

Out[9]=

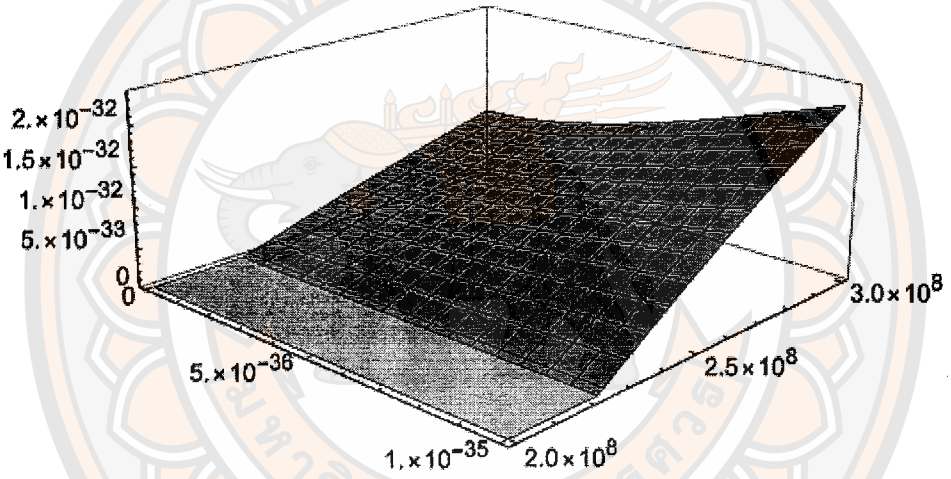

Figure 19 Plot the power spectrum of massive photons at 0 °C.

$$\text{In[10]} := \text{Plot3D}\left[5.0695 \times 10^{-48}\sqrt{8.09264 \times 10^{84}m^2 + \frac{10^{18}\pi^2}{48841}}\left(1 - \frac{4.98877 \times 10^{16}}{v^2}\right)v\right.$$

$$\sqrt{8.092639376356166 \times 10^{84}\ \text{m}^2 + \frac{10^{18}\pi^2}{48841}}\left(1 - \frac{4.9887699393530056 \times 10^{16}}{v^2}\right)v$$

$$\left.\text{Coth}\left[2.9098441048689325 \times 10^{-6}\sqrt{8.092639376356166 \times 10^{84}\ \text{m}^2 + \frac{10^{18}\pi^2}{48841}}\right],\right.$$

$$\left.\{m, 0, 1 \times 10^{-35}\}, \{v, 2 \times 10^8, 3 \times 10^8\},\ \text{PlotRange} \to \{0, 2.4 \times 10^{-32}\}\right]$$

Out[10]=

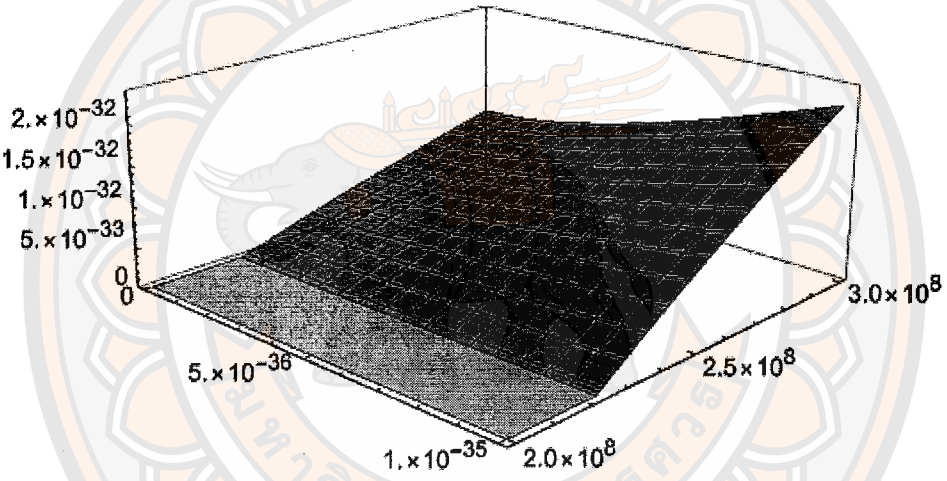

Figure 20 Plot the power spectrum of massive photons at 20 °C.

$$\text{In[11]} := \text{Plot3D}\left[5.12795 \times 10^{-48}\sqrt{8.09264 \times 10^{84}m^2 + \frac{10^{18}\pi^2}{48841}}\left(1 - \frac{5.10447 \times 10^{16}}{v^2}\right)v\right.$$

$$\sqrt{8.092639376356166 \times 10^{84}\ \text{m}^2 + \frac{10^{18}\pi^2}{48841}}\left(1 - \frac{4.9887699393530056 \times 10^{16}}{v^2}\right)v$$

$$\text{Coth}\left[2.31236 \times 10^{-6}\sqrt{8.092639376356166 \times 10^{84}\ \text{m}^2 + \frac{10^{18}\pi^2}{48841}}\right],$$

$$\left.\{m, 0, 1 \times 10^{-35}\}, \{v, 2 \times 10^8, 3 \times 10^8\},\ \text{PlotRange} \rightarrow \{0, 2.4 \times 10^{-32}\}\right]$$

Out[11]=

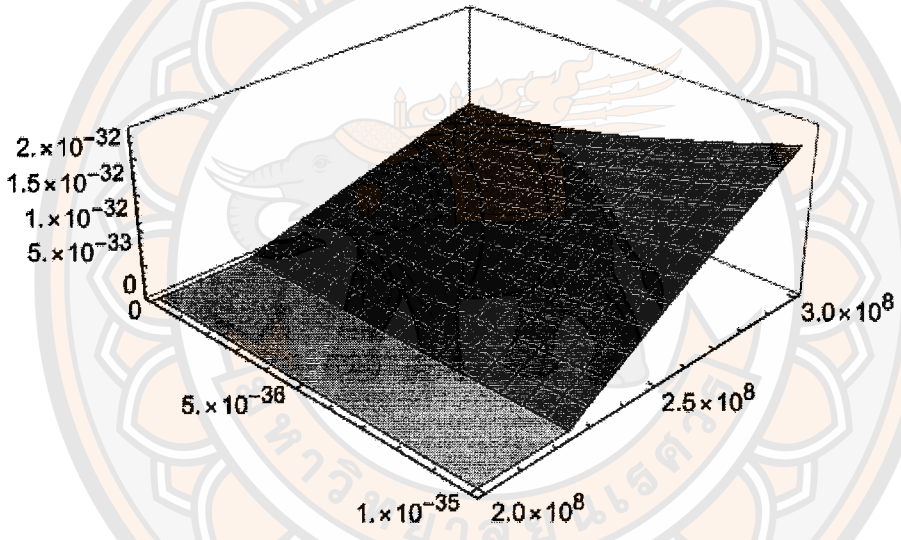

Figure 21 Plot the power spectrum of massive photons at 100 °C.

APPENDIX D Numerical Calculation of Power Spectrum in Two Charge System at Finite Temperature

The numerical calculations, the result of the power spectrum of massive photons at finite temperatures is derived from the source theory. We plot graphs in both 2D and 3D from equation (4.1.34) and (4.2.21). Details of the numerical calculations and plot graph are shown as follows.

$$P_T(a) = \frac{e^2}{\pi}\frac{v\omega}{c^2}\left(1-\frac{1}{n^2\beta^2}\right)\cos^2\left[\frac{a\omega}{2v}\right]\times\coth\left[\frac{\hbar\omega}{2k_BT}\right]$$

m = 0 kg, T = 0°C(273.15 K), T = 20°C(293.15 K), T = 100°C(373.15 K),

$n = 1.34415\,(0°\mathrm{C})\,, n = 1.34315\,(20°\mathrm{C})\,, n = 1.32784\,(100°\mathrm{C})\,,$ v = 0.8C

$$\ln[1] := P_{T=0} = \frac{(1.60217663\times 10\text{\^{}}-19)\text{\^{}}2\,0.8*3*10\text{\^{}}8*4.26165512564931*10\text{\^{}}15}{\pi\,(3*10\text{\^{}}8)\text{\^{}}2}$$
$$\times\left(1-\frac{1}{(1.34415)^2(0.8)^2}\right)\left(\cos\left[\frac{a*4.26165512564931\text{\^{}}*10\text{\^{}}15}{2*0.8*3*10\text{\^{}}8}\right]\right)^2$$
$$\times\,\mathrm{Coth}\left[\frac{1.054571817\times 10\text{\^{}}-34*4.26165512564931*10\text{\^{}}15}{2*1.380649\times 10\text{\^{}}-23*273.15}\right]$$

$$\mathrm{Out}[1] = 1.25527\times 10^{-32}\mathrm{Cos}[\times 8.87845\times 10^6 a]^2$$

$$\ln[2] := P_{T=20} = \frac{(1.60217663\times 10\text{\^{}}-19)\text{\^{}}2\,0.8*3*10\text{\^{}}8*4.26165512564931*10\text{\^{}}15}{\pi\,(3*10\text{\^{}}8)\text{\^{}}2}$$
$$\times\left(1-\frac{1}{(1.34315)^2(0.8)^2}\right)\left(\cos\left[\frac{a*4.26165512564931\text{\^{}}*10\text{\^{}}15}{2*0.8*3*10\text{\^{}}8}\right]\right)^2$$
$$\times\,\mathrm{Coth}\left[\frac{1.054571817\times 10\text{\^{}}-34*4.26165512564931*10\text{\^{}}15}{2*1.380649\times 10\text{\^{}}-23*293.15}\right]$$

$$\mathrm{Out}[2] = 1.24331\times 10^{-32}\mathrm{Cos}[\times 8.87845\times 10^6 a]^2$$

$$\ln[3] := P_{T=50} = \frac{(1.60217663 \times 10\text{^} - 19)\text{^}2\, 0.8 * 3 * 10\text{^}8 * 4.26165512564931 * 10\text{^}15}{\pi\, (3 * 10\text{^}8)\text{^}2}$$
$$\times \left(1 - \frac{1}{(1.33901)^2 (0.8)^2}\right) \left(\cos\left[\frac{a * 4.26165512564931\text{^} * 10\text{^}15}{2 * 0.8 * 3 * 10\text{^}8}\right]\right)^2$$
$$\times \text{Coth}\left[\frac{1.054571817 \times 10\text{^} - 34 * 4.26165512564931 * 10\text{^}15}{2 * 1.380649 \times 10\text{^} - 23 * 323.15}\right]$$

$$\text{Out}[3] = 1.1935 \times 10^{-32} \text{Cos}[\times 8.87845 \times 10^6 a]^2$$

$$\ln[4] := P_{T=80} = \frac{(1.60217663 \times 10\text{^} - 19)\text{^}2\, 0.8 * 3 * 10\text{^}8 * 4.26165512564931 * 10\text{^}15}{\pi\, (3 * 10\text{^}8)\text{^}2}$$
$$\times \left(1 - \frac{1}{(1.33284)^2 (0.8)^2}\right) \left(\cos\left[\frac{a * 4.26165512564931\text{^} * 10\text{^}15}{2 * 0.8 * 3 * 10\text{^}8}\right]\right)^2$$
$$\times \text{Coth}\left[\frac{1.054571817 \times 10\text{^} - 34 * 4.26165512564931 * 10\text{^}15}{2 * 1.380649 \times 10\text{^} - 23 * 353.15}\right]$$

$$\text{Out}[4] = 1.11841 \times 10^{-32} \text{Cos}[\times 8.87845 \times 10^6 a]^2$$

$$\ln[5] := P_{T=100} = \frac{(1.60217663 \times 10\text{^} - 19)\text{^}2\, 0.8 * 3 * 10\text{^}8 * 4.26165512564931 * 10\text{^}15}{\pi\, (3 * 10\text{^}8)\text{^}2}$$
$$\times \left(1 - \frac{1}{(1.32784)^2 (0.8)^2}\right) \left(\cos\left[\frac{a * 4.26165512564931\text{^} * 10\text{^}15}{2 * 0.8 * 3 * 10\text{^}8}\right]\right)^2$$
$$\times \text{Coth}\left[\frac{1.054571817 \times 10\text{^} - 34 * 4.26165512564931 * 10\text{^}15}{2 * 1.380649 \times 10\text{^} - 23 * 373.15}\right]$$

$$\text{Out}[5] = 1.05678 \times 10^{-32} \text{Cos}[\times 8.87845 \times 10^6 a]^2$$

$$\text{In[6]} := \text{Plot}\left[\left\{1.25527 \times 10^{-32}\text{Cos}[\times 8.87845 \times 10^{6} a]^2\right.\right. , 1.24331 \times 10^{-32}\text{Cos}[\times 8.87845 \times 10^{6} a]^2,$$

$$1.1935 \times 10^{-32}\text{Cos}[\times 8.87845 \times 10^{6} a]^2, 1.11841 \times 10^{-32}\text{Cos}[\times 8.87845 \times 10^{6} a]^2$$

$$\left.\left. 1.0567815865201587 \times 10^{-32}\,\text{Cos}\left[8.878448178436063 \times 10^{6} a\right]^2\right\}, \{a, 0, 5.3 \times 10^{-7}\}\right],$$

$$\text{PlotLegends} \rightarrow \{\,0°\text{C}, 20°\text{C}, 50°\text{C}, 80°\text{C}, 100°\text{C}\},$$

$$\text{PlotStyle} \rightarrow \{Green, DotDashed, Yellow, Blue, Red\}]$$

Out[6] =

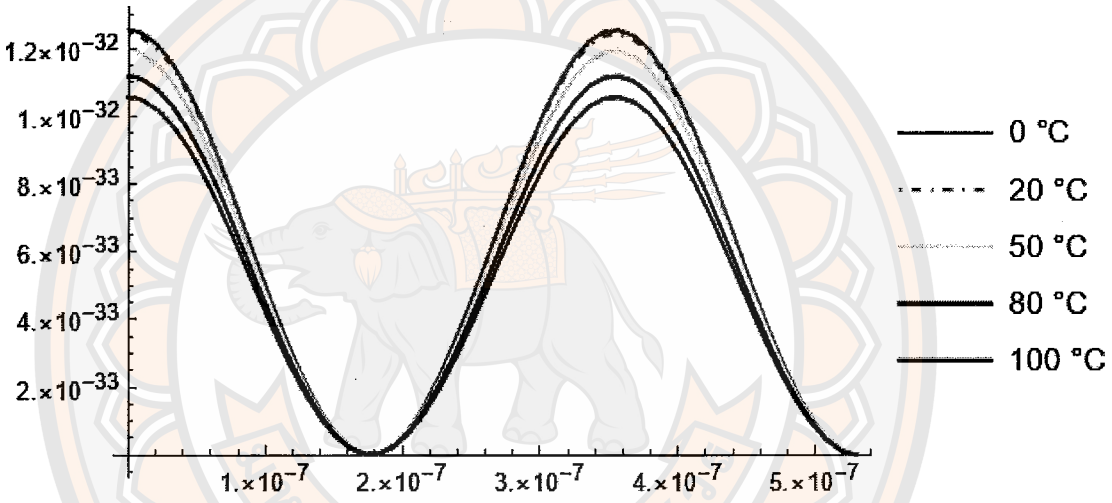

Figure 22 Plot the power spectrum of massless photons in two charge system at 0, 20, 50, 80, and 100 °C.

$$P_T(a) = \frac{e^2}{\pi}\frac{v\omega}{c^2}\left(1 - \frac{1}{n^2\beta^2}\right)\cos^2\left[\frac{a\omega}{2v}\right] \times \text{Coth}\left[\frac{\hbar\omega}{2k_B T}\right]; m = 0kg, T = 20C$$

$$\text{In[7]} := \text{P}_{\text{T=20}} = \frac{(1.60217663 \times 10\text{\^{}} - 19)\text{\^{}}2\,\text{V} * 4.26165512564931\text{\^{}} * 10\text{\^{}}15}{\pi}$$

$$\times \left(1 - \frac{1}{(1.34315)^2(0.8)^2}\right)\left(\cos\left[\frac{a * 4.26165512564931\text{\^{}} * 10\text{\^{}}15}{2 * v}\right]\right)^2$$

$$\times \text{Coth}\left[\frac{1.054571817 \times 10\text{\^{}} - 34 * 4.26165512564931\text{`} * 10\text{\^{}}15}{2 * 1.380649 \times 10\text{\^{}} - 23 * 293.15}\right]$$

$$\text{Out[7]} = 5.18046 \times 10^{-41} v\,\text{Cos}\left[\frac{2.13083 \times 10^{15} a}{v}\right]^2$$

$$\text{In[8]} := \text{Plot3D}\left[5.18046 \times 10^{-41} v \,\text{Cos}\left[\frac{2.13083 \times 10^{15} a}{v}\right]^2,\right.$$

$$\left.\{a, 0, 6.3 \times 10^{-7}\}, \{v, 2.2 \times 10^{8}, 3 \times 10^{8}\}, \text{PlotRange} \rightarrow \{0, 1.6 \times 10^{-32}\}\right]$$

Out[8]=

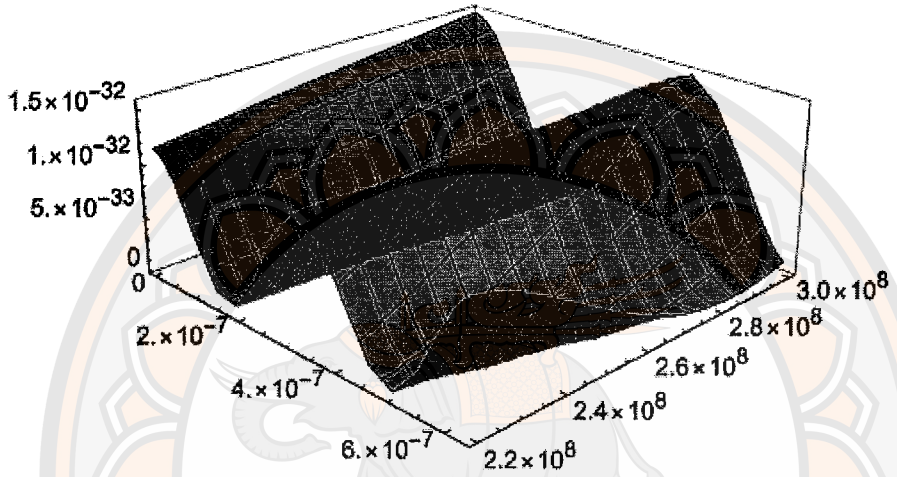

Figure 23 Plot the power spectrum of massless photons in two charge system at 20 °C.

$$P_T(a) = \frac{e^2}{\pi}\frac{v}{nc}\sqrt{k^2+\frac{m^2c^2}{\hbar^2}}\left(1-\frac{1}{n^2\beta^2}\right)\cos^2\left[\frac{ac}{2vn}\sqrt{k^2+\frac{m^2c^2}{\hbar^2}}\right]\times\coth\left[\frac{\hbar c}{2nk_BT}\sqrt{k^2+\frac{m^2c^2}{\hbar^2}}\right];$$

$$m = 1.000099121\times 10\text{\^{}}-35\ \text{kg}, k^2 = \frac{(2\pi)^2}{\lambda^2}, \lambda = 442*10\text{\^{}}-9\ \text{m}, v = 0.8\text{c}$$

$$\text{ln}[9] := P_{T=\theta} = \frac{(1.60217663\times 10\text{\^{}}-19)\text{\^{}}2}{\pi}\frac{0.8*3*10\text{\^{}}8}{(1.34415)(3*10\text{\^{}}8)}$$

$$\sqrt{\frac{(2\pi)^2}{(442*10\text{\^{}}-9)^2}+\frac{(1.000099121\times 10\text{\^{}}-35)^2*(3*10\text{\^{}}8)^2}{(1.054571817\times 10\text{\^{}}-34)^2}}\left(1-\frac{1}{(1.34415)^2(0.8)^2}\right)(\cos[$$

$$\frac{a*3*10\text{\^{}}8}{2*0.8*3*10\text{\^{}}8*1.34415}\sqrt{\frac{(2\pi)^2}{(442*10\text{\^{}}-9)^2}+\frac{(1.000099121\times 10\text{\^{}}-35)^2*(3*10\text{\^{}}8)^2}{(1.054571817\times 10\text{\^{}}-34)^2}}\Bigg]\Bigg)^2$$

$$\coth\left[\frac{1.05457\times 10\text{\^{}}-34*(3*10\text{\^{}}8)}{2*(1.34)*1.38\times 10\text{\^{}}-23*273.15}\sqrt{\frac{(2\pi)^2}{(442*10\text{\^{}}-9)^2}+\frac{(1\times 10\text{\^{}}-35)^2*(3*10\text{\^{}}8)^2}{(1.05457\times 10\text{\^{}}-34)^2}}\right]$$

$$\text{Out}[9]=2.09082\times 10^{-32}\,\text{Cos}\left[1.47882\times 10^7\text{a}\right]^2$$

$$\text{ln}[10] := P_{T=20} = \frac{(1.60217663\times 10\text{\^{}}-19)\text{\^{}}2}{\pi}\frac{0.8*3*10\text{\^{}}8}{(1.34315)(3*10\text{\^{}}8)}$$

$$\sqrt{\frac{(2\pi)^2}{(442*10\text{\^{}}-9)^2}+\frac{(1.000099121\times 10\text{\^{}}-35)^2*(3*10\text{\^{}}8)^2}{(1.054571817\times 10\text{\^{}}-34)^2}}\left(1-\frac{1}{(1.34315)^2(0.8)^2}\right)(\cos[$$

$$\frac{a*3*10\text{\^{}}8}{2*0.8*3*10\text{\^{}}8*1.34315}\sqrt{\frac{(2\pi)^2}{(442*10\text{\^{}}-9)^2}+\frac{(1.000099121\times 10\text{\^{}}-35)^2*(3*10\text{\^{}}8)^2}{(1.054571817\times 10\text{\^{}}-34)^2}}\Bigg]\Bigg)^2$$

$$\text{Coth}\left[\frac{1.054571817\times 10\text{\^{}}-34*(3*10\text{\^{}}8)}{2*(1.34315)*1.380649\times 10\text{\^{}}-23*293.15}\right.$$

$$\left.\sqrt{\frac{(2\pi)^2}{(442*10\text{\^{}}-9)^2}+\frac{(1.000099121\times 10\text{\^{}}-35)^2*(3*10\text{\^{}}8)^2}{(1.054571817\times 10\text{\^{}}-34)^2}}\right]$$

$$\text{Out}[10]= 2.07244\times 10^{-32}\,\text{Cos}\left[1.47992\times 10^7\text{a}\right]^2$$

$$\ln[11] := P_{T=50} = \frac{(1.60217663 \times 10\text{^} - 19)\text{^}2}{\pi} \frac{0.8 * 3 * 10\text{^}8}{(1.33901)(3 * 10\text{^}8)}$$

$$\sqrt{\frac{(2\pi)^2}{(442 * 10\text{^} - 9)^2} + \frac{(1.000099121 \times 10\text{^} - 35)^2 * (3 * 10\text{^}8)^2}{(1.054571817 \times 10\text{^} - 34)^2}} \left(1 - \frac{1}{(1.33901)^2(0.8)^2}\right) (\cos[$$

$$\frac{a * 3 * 10\text{^}8}{2 * 0.8 * 3 * 10\text{^}8 * 1.33901} \sqrt{\frac{(2\pi)^2}{(442 * 10\text{^} - 9)^2} + \frac{(1.000099121 \times 10\text{^} - 35)^2 * (3 * 10\text{^}8)^2}{(1.054571817 \times 10\text{^} - 34)^2}}\Bigg]\Bigg)^2$$

$$\text{Coth}\left[\frac{1.05457 \times 10\text{^} - 34 * (3 * 10\text{^}8)}{2 * (1.34) * 1.38 \times 10\text{^} - 23 * 323.15} \sqrt{\frac{(2\pi)^2}{(442 * 10\text{^} - 9)^2} + \frac{(1 \times 10\text{^} - 35)^2 * (3 * 10\text{^}8)^2}{(1 \times 10\text{^} - 34)^2}}\right]$$

$$\text{Out}[11]= 1.99556 \times 10^{-32} \text{Cos}\left[1.4845 \times 10^7 \text{a}\right]^2$$

$$\ln[12] := P_{T=80} = \frac{(1.60217663 \times 10\text{^} - 19)\text{^}2}{\pi} \frac{0.8 * 3 * 10\text{^}8}{(1.33901)(3 * 10\text{^}8)}$$

$$\sqrt{\frac{(2\pi)^2}{(442 * 10\text{^} - 9)^2} + \frac{(1.000099121 \times 10\text{^} - 35)^2 * (3 * 10\text{^}8)^2}{(1.054571817 \times 10\text{^} - 34)^2}} \left(1 - \frac{1}{(1.33284)^2(0.8)^2}\right) (\cos[$$

$$\frac{a * 3 * 10\text{^}8}{2 * 0.8 * 3 * 10\text{^}8 * 1.33284} \sqrt{\frac{(2\pi)^2}{(442 * 10\text{^} - 9)^2} + \frac{(1.000099121 \times 10\text{^} - 35)^2 * (3 * 10\text{^}8)^2}{(1.054571817 \times 10\text{^} - 34)^2}}\Bigg]\Bigg)^2$$

$$\text{Coth}\left[\frac{1.05457 \times 10\text{^} - 34 * (3 * 10\text{^}8)}{2 * (1.33) * 1.38 \times 10\text{^} - 23 * 353.15} \sqrt{\frac{(2\pi)^2}{(442 * 10\text{^} - 9)^2} + \frac{(1 \times 10\text{^} - 35)^2 * (3 * 10\text{^}8)^2}{(1 \times 10\text{^} - 34)^2}}\right]$$

$$\text{Out}[12]= 1.87866 \times 10^{-32} \text{Cos}\left[1.49137 \times 10^7 \text{a}\right]^2$$

$$\ln[13] := P_{T=100} = \frac{(1.60217663 \times 10\text{^} - 19)\text{^}2}{\pi} \frac{0.8 * 3 * 10\text{^}8}{(1.32784)(3 * 10\text{^}8)}$$

$$\sqrt{\frac{(2\pi)^2}{(442 * 10\text{^} - 9)^2} + \frac{(1.000099121 \times 10\text{^} - 35)^2 * (3 * 10\text{^}8)^2}{(1.054571817 \times 10\text{^} - 34)^2}} \left(1 - \frac{1}{(1.32784)^2(0.8)^2}\right) (\text{Cos}[$$

$$\frac{a * 3 * 10\text{^}8}{2 * 0.8 * 3 * 10\text{^}8 * 1.32784} \sqrt{\frac{(2\pi)^2}{(442 * 10\text{^} - 9)^2} + \frac{(1.000099121 \times 10\text{^} - 35)^2 * (3 * 10\text{^}8)^2}{(1.054571817 \times 10\text{^} - 34)^2}}\Bigg]\Bigg)^2$$

$$\text{Coth}\left[\frac{1.05457 \times 10\text{^} - 34 * (3 * 10\text{^}8)}{2 * (1.33) * 1.38 \times 10\text{^} - 23 * 373.15} \sqrt{\frac{(2\pi)^2}{(442 * 10\text{^} - 9)^2} + \frac{(1 \times 10\text{^} - 35)^2 * (3 * 10\text{^}8)^2}{(1 \times 10\text{^} - 34)^2}}\right]$$

$$\text{Out}[13]= 1.78183 \times 10^{-32} \text{Cos}\left[1.49698 \times 10^7 a\right]^2$$

$$\text{ln}[14] := \text{Plot}\left[\left\{2.09082 \times 10^{-32}\,\text{Cos}\left[1.47882 \times 10^{7}\text{a}\right]^{2}, 2.07244 \times 10^{-32}\,\text{Cos}\left[1.47992 \times 10^{7}\text{a}\right]^{2},\right.\right.$$

$$1.99556 \times 10^{-32}\,\text{Cos}\left[1.4845 \times 10^{7}\text{a}\right]^{2}, 1.87866 \times 10^{-32}\,\text{Cos}\left[1.49137 \times 10^{7}\text{a}\right]^{2}$$

$$\left.\left.1.7818269105990336 \times 10^{-32}\,\text{Cos}\left[1.4969846267655965 \times 10^{7}a\right]^{2}\right\}, \{a, 0, 5.3 * 10\text{\^{}} - 7\}\right],$$

$$\text{PlotLegends} \rightarrow \{\,0°\text{C}, 20°\text{C}, 50°\text{C}, 80°\text{C}, 100°\text{C}\},$$

$$\text{PlotStyle} \rightarrow \{Green, DotDashed, Yellow, Blue, Red\}]$$

Out[14]=

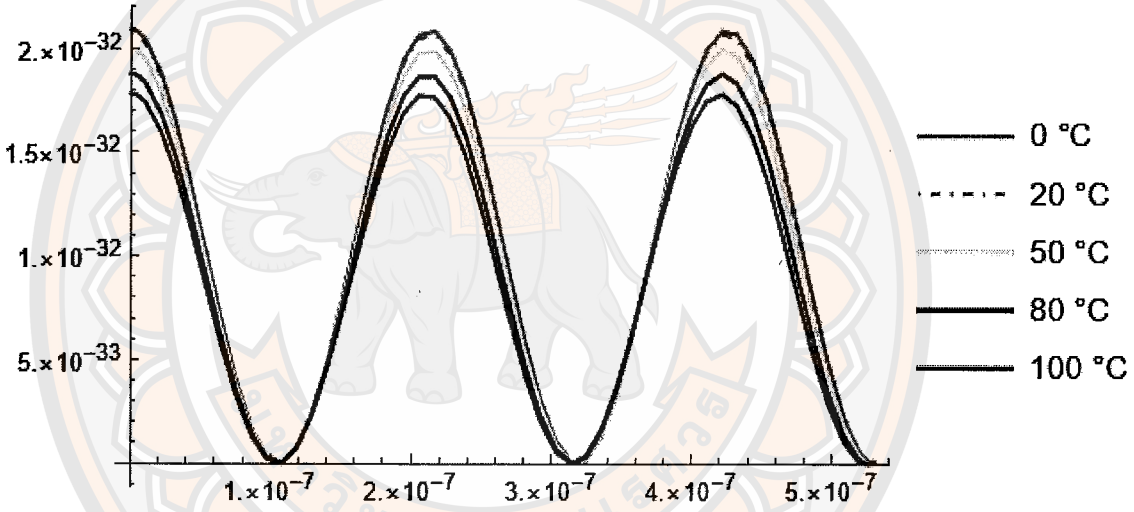

Figure 24 Plot the power spectrum of two charge systems with massive photons at 0, 20, 50, 80, and 100 °C.

$$\text{In[15]} := P_{T=20} = \frac{(1.60217663\times10\text{^}-19)\text{^}2}{\pi}\frac{V}{(1.34315)(3*10\text{^}8)}$$
$$\sqrt{\frac{(2\pi)^2}{(442*10\text{^}-9)^2}+\frac{(1.000099121\times10\text{^}-35)^2*(3*10\text{^}8)^2}{(1.054571817\times10\text{^}-34)^2}}\left(1-\frac{1}{(1.34315)^2\left(\frac{v}{3*10\text{^}8}\right)^2}\right)$$
$$\left(\cos\left[\frac{a*3*10\text{^}8}{2*v*1.34315}\sqrt{\frac{(2\pi)^2}{(442*10\text{^}-9)^2}+\frac{(1.000099121\times10\text{^}-35)^2*(3*10\text{^}8)^2}{(1.05457181710\text{^}-34)^2}}\right]\right)^2$$
$$\coth\left[\frac{1.054571817\times10\text{^}-34*(3*10\text{^}8)}{2*(1.34315)*1.380649\times10\text{^}-23*293.15}\sqrt{\frac{(2\pi)^2}{(442*10\text{^}-9)^2}+\frac{(1.000099121\times10\text{^}-35)^2*(3*10\text{^}8)^2}{(1.054571817\times10\text{^}-34)^2}}\right]$$
$$\text{Out[15]}=6.44924\times10^{-40}\left(1-\frac{4.98877\times10^{16}}{v^2}\right)v\cos\left[\frac{3.55181\times10^{15}a}{v}\right]^2$$

$$\text{In[16]} := \text{Plot3D}\left[6.44924\times10^{-40}\left(1-\frac{4.98877\times10^{16}}{v^2}\right)v\cos\left[\frac{3.55181\times10^{15}a}{v}\right]^2,\right.$$
$$\left.\{a,0,6.3\times10^{-7}\},\{v,2\times10^8,3\times10^8\},\ \text{PlotRange}\rightarrow\{0,9\times10^{-32}\}\right]$$

Out[16]=

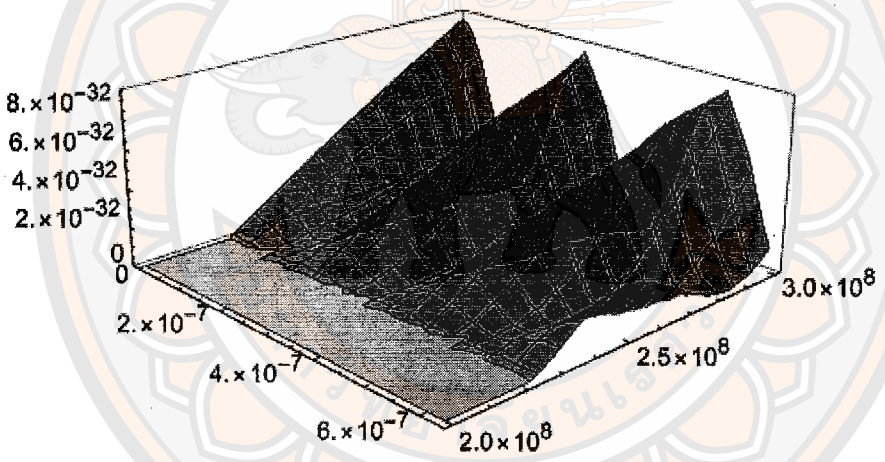

Figure 25 Plot the power spectrum of two charge systems with massive photons at temperature 20 °C.